

NAVAL POSTGRADUATE SCHOOL

Monterey, California



THESIS

CONSTRUCTION AND TESTING OF A MODERN ACOUSTIC IMPEDANCE TUBE

by

Sean P. O'Malley

June 2001

Thesis Advisor:
Second Reader:

Steven Baker
Thomas Hofler

Approved for public release; distribution is unlimited

20010905 142

REPORT DOCUMENTATION PAGE			<i>Form Approved OMB No. 0704-0188</i>	
Public reporting burden for this collection of information is estimated to average 1 hour per response, including the time for reviewing instruction, searching existing data sources, gathering and maintaining the data needed, and completing and reviewing the collection of information. Send comments regarding this burden estimate or any other aspect of this collection of information, including suggestions for reducing this burden, to Washington headquarters Services, Directorate for Information Operations and Reports, 1215 Jefferson Davis Highway, Suite 1204, Arlington, VA 22202-4302, and to the Office of Management and Budget, Paperwork Reduction Project (0704-0188) Washington DC 20503.				
1. AGENCY USE ONLY (Leave blank)		2. REPORT DATE June 2001	3. REPORT TYPE AND DATES COVERED Master's Thesis	
4. TITLE AND SUBTITLE: Title (Mix case letters) Construction and Testing of a Modern Acoustic Impedance Tube			5. FUNDING NUMBERS	
6. AUTHOR(S) O'Malley, Sean P.				
7. PERFORMING ORGANIZATION NAME(S) AND ADDRESS(ES) Naval Postgraduate School Monterey, CA 93943-5000			8. PERFORMING ORGANIZATION REPORT NUMBER	
9. SPONSORING / MONITORING AGENCY NAME(S) AND ADDRESS(ES) N/A			10. SPONSORING / MONITORING AGENCY REPORT NUMBER	
11. SUPPLEMENTARY NOTES The views expressed in this thesis are those of the author and do not reflect the official policy or position of the Department of Defense or the U.S. Government.				
12a. DISTRIBUTION / AVAILABILITY STATEMENT Approved for public release; distribution is unlimited.			12b. DISTRIBUTION CODE	
13. ABSTRACT (maximum 200 words) <p>The acoustic impedance of a material describes its reflective and absorptive properties. Acoustic impedance may be measured in a wide variety of ways. This thesis describes the construction and testing of an acoustic impedance measurement tube which employs modern Fourier Transform techniques. Two methods are employed for acoustic impedance measurement using this apparatus. One technique uses a two-microphone continuous excitation method and the other uses a single microphone transient excitation method. Simple acoustic theory is used to derive equations for both methods. MATLAB computer programs are developed using these equations, to provide graphical results of acoustic impedance measurements over a frequency range for a given material, from raw data. A procedure is subsequently developed for using this apparatus using to make acoustic impedance measurements. The performance of this device is evaluated by making measurements utilizing both methods on three sample materials and also with the end of the tube open to the atmosphere (referred to as an open tube measurement). The open tube measurements are compared with theoretical values. The results using both approaches compared favorably with the open tube theoretical values. Additionally both approaches agreed reasonably well with each other for the three sample materials. Performance at frequencies below 500 Hz, however, yielded deficient results, indicating a need for development of a filter for better accuracy.</p>				
14. SUBJECT TERMS Acoustic Impedance Measurement, Acoustic Impedance Tube, Reflection			15. NUMBER OF PAGES 157	
			16. PRICE CODE	
17. SECURITY CLASSIFICATION OF REPORT Unclassified	18. SECURITY CLASSIFICATION OF THIS PAGE Unclassified	19. SECURITY CLASSIFICATION OF ABSTRACT Unclassified	20. LIMITATION OF ABSTRACT UL	

THIS PAGE INTENTIONALLY LEFT BLANK

Approved for public release; distribution is unlimited.

**CONSTRUCTION AND TESTING OF A MODERN ACOUSTIC IMPEDANCE
TUBE**

Sean P. O'Malley
Lieutenant Commander, United States Navy
B.S., United States Naval Academy, 1989

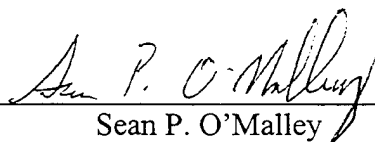
Submitted in partial fulfillment of the
requirements for the degree of

MASTER OF SCIENCE IN APPLIED PHYSICS

from the

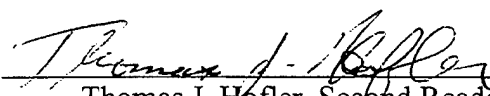
**NAVAL POSTGRADUATE SCHOOL
June 2001**


Author:


Sean P. O'Malley

Approved by:


Steven R. Baker, Thesis Advisor


Thomas J. Hofler, Second Reader


William B. Maier II, Chairman
Department of Physics

THIS PAGE INTENTIONALLY LEFT BLANK

ABSTRACT

The acoustic impedance of a material describes its reflective and absorptive properties. Acoustic impedance may be measured in a wide variety of ways. This thesis describes the construction and testing of an acoustic impedance measurement tube which employs modern Fourier Transform techniques. Two methods are employed for acoustic impedance measurement using this apparatus. One technique uses a two-microphone continuous excitation method and the other uses a single microphone transient excitation method. Simple acoustic theory is used in the derivation of equations for both methods. MATLAB computer programs are developed using these equations, to provide graphical results of acoustic impedance measurements over a frequency range for a given material, from raw data. A procedure is subsequently developed for using this apparatus to make acoustic impedance measurements. The performance of this device is evaluated by making measurements utilizing both methods on three sample materials and also with the end of the tube open to the atmosphere (referred to as an open tube measurement). The open tube measurements are compared with theoretical values. The results using both approaches compared favorably with the open tube theoretical values. Additionally both approaches agreed reasonably well with each other for the three sample materials. Performance at frequencies below 500 Hz, however, yielded deficient results, indicating a need for development of a filter for better accuracy.

THIS PAGE INTENTIONALLY LEFT BLANK

TABLE OF CONTENTS

I.	INTRODUCTION.....	1
A.	PURPOSE.....	1
B.	DEFINITION OF ACOUSTIC IMPEDANCE	3
1.	What Acoustic Impedance Is Used For.....	3
C.	HOW ACOUSTIC IMPEDANCE IS MEASURED.....	4
1.	Classical Standing Wave Ratio (SWR) Method.....	4
2.	Modern Acoustic Impedance Measurement Methods.....	4
D.	SCOPE OF THESIS	5
II.	ACOUSTIC IMPEDANCE MEASUREMENT THEORY	7
A.	BACKGROUND	7
1.	Classical Standing Wave Ratio (SWR) Method.....	7
a.	<i>Advantages and Disadvantages of Classical SWR Method.....</i>	9
2.	Modern Acoustic Impedance Measurement Methods.....	9
a.	<i>Comparison of the Advantages and Disadvantages of Modern Acoustic Impedance Measurement Methods.....</i>	9
B.	FREQUENCY LIMITS OF THE IMPEDANCE TUBES.....	11
C.	IMPEDANCE MEASUREMENT THEORY USING TWO MICROPHONES (CONTINUOUS EXCITATION)	12
1.	Simplest approximation	12
a.	<i>Using the Basic Approach in a Computer Program.....</i>	15
2.	The Exact Approach	15
a.	<i>Using the Exact Approach in a Computer Program</i>	17
3.	The Low Frequency Approximation	18
a.	<i>Using the Low Frequency Approximation in a Computer Program.....</i>	19
D.	IMPEDANCE MEASUREMENT THEORY USING ONE MICROPHONE	19
1.	Measurement of Reflectivity	19
2.	Measurement of Acoustic Impedance	22
3.	Using One Microphone Impedance Measurement Theory in a Computer Program.....	23
III.	DEVELOPMENT OF THE APPARATUS.....	25
A.	ACOUSTIC IMPEDANCE MEASUREMENT TUBE DESCRIPTION.....	25
B.	SELECTED COMPONENTS OF THE ACOUSTIC IMPEDANCE MEASUREMENT TUBE.....	26
1.	Microphone.....	26
a.	<i>Second Harmonic Distortion.....</i>	28
2.	Microphone Power Supply Assembly	31
3.	Driver (Speaker).....	32

a.	<i>Drivers That Were Tested</i>	33
b.	<i>How the Drivers Were Tested</i>	33
c.	<i>Driver Test Results</i>	35
C.	PROCEDURES	37
1.	Computing Speed of Sound and "Absorption of the Day"	37
2.	How the Samples Are Mounted	38
3.	Two-Microphone Continuous Excitation Acoustic Impedance Measurement	39
a.	<i>Microphone Calibration Procedure</i>	40
b.	<i>Sample Data Taking Procedure</i>	43
c.	<i>Processing the Sample Data Using MATLAB</i>	45
4.	One-Microphone Transient Acoustic Impedance Measurement ..	51
a.	<i>Absorption Compensation Procedure</i>	52
b.	<i>Sample Data Taking Procedure</i>	55
c.	<i>Processing the Sample Data Using MATLAB</i>	55
IV.	EXPERIMENTAL RESULTS	63
A.	TEST CASE: THE OPEN TUBE	63
1.	Expected Open Tube Results Based On Theory	63
2.	Open Tube Experimental Results	64
B.	RESULTS USING SAMPLE MATERIALS	68
1.	Speckled Ceiling Tile Sample	69
2.	Insulation Sample	71
3.	Ceiling Tile Sample (With Hole Perforations)	73
V.	SUMMARY	77
A.	CONCLUSIONS	77
B.	RECOMMENDATIONS	78
APPENDIX A:	MOUSER ELECTRONICS 25LM045 SPECIFICATIONS	81
APPENDIX B:	LIST OF PARTS FOR ACOUSTIC IMPEDANCE TUBE	83
APPENDIX C:	ANALYSIS OF SELENIUM DH200E DRIVER	85
APPENDIX D:	SELENIUM DH200E DRIVER SPECIFICATIONS	87
APPENDIX E:	ANALYSIS OF UNIVERSITY SOUND 1828R DRIVER	89
APPENDIX F:	UNIVERSITY SOUND 1828R DRIVER SPECIFICATIONS	91
APPENDIX G:	"REIM.78S" AND "REFLWTIM.78S" SETTINGS	93
APPENDIX H:	IMPEDANCE MEASUREMENT TUBE DRAWINGS	103
APPENDIX I:	COMPUTER PROGRAMS USED FOR IMPEDANCE TUBE ..	113
APPENDIX J:	LABORATORY TEST PROCEDURE	125
	LIST OF REFERENCES	133
	INITIAL DISTRIBUTION LIST	135

LIST OF FIGURES

Figure 1.	Older model acoustic impedance tube manufactured by Bruel and Kjaer. This will be replaced by the newer tube shown in Figure 2.	1
Figure 2.	The new acoustic impedance measurement tube is shown with the Stanford Research Systems SR-785 dynamic signal analyzer, the Philips PM-3384 oscilloscope, and the Techron 5507 power amplifier (below the impedance tube).	2
Figure 3.	Schematic for the acoustic impedance tube utilizing the SWR method.	8
Figure 4.	These are the microphone positions in the impedance tube during an impedance measurement.	13
Figure 5.	Acoustic impedance tube alignment for reflectivity measurement.	20
Figure 6.	Shown above is the acoustic impedance measurement tube.	25
Figure 7.	End cap blank is featured along with the retention ring.	25
Figure 8.	The acoustic impedance tube assembly is shown along with the dynamic signal analyzer in the foreground under the oscilloscope. The speaker/driver is installed on the tube on the right hand side. The sample cup is installed on the left hand side. Amplifier is shown under the impedance tube. The two junctions boxes are on top of the tube.	26
Figure 9.	Front-end view of Mouser Electronics microphone pair.	27
Figure 10.	Reverse view of Mouser Electronics microphone pair.	27
Figure 11.	Voltage required to excite one percent or -40dB second harmonic distortion plotted as function of frequency.	30
Figure 12.	External close up view of microphone power supply junction box.	32
Figure 13.	Internal view of junction box assembly including 9-volt battery.	32
Figure 14.	This is the set up for driver testing in the anechoic chamber.	34
Figure 15.	This is the Selenium DH200E driver.	36
Figure 16.	Microphones are installed in their sample measurement position. The end cup sample holder and the retention ring are featured in the foreground prior to installation.	39
Figure 17.	Acoustic impedance tube and associated equipment are set up in this configuration for an impedance measurement using the two-microphone continuous excitation method.	40
Figure 18.	Microphone cup holder with test microphone inserted.	41
Figure 19.	Microphones are aligned for calibration. Notice junction box has been advanced to support this alignment.	43
Figure 20.	Microphones and junction box are returned to their normal sample measurement position. The sample cup and retention ring are removed.	44
Figure 21.	Real part of ratio of the microphone's output voltages is shown where microphones are in the calibration position.	46

Figure 22.	Imaginary part of ratio of the microphone's output voltages is shown where microphones are in the calibration position.	47
Figure 23.	Real part of ratio of the microphone's output voltages is shown where microphones are in their normal position at top end of tube with sample installed.	48
Figure 24.	Imaginary part of ratio of the microphone's output voltages is shown where microphones are in their normal position at top end of tube with sample installed.	48
Figure 25.	Real part of the acoustic impedance is plotted against the frequency for the speckled ceiling tile sample.	49
Figure 26.	Imaginary part of the acoustic impedance is plotted against the frequency for the speckled ceiling tile sample.	50
Figure 27.	Real and imaginary parts of the acoustic impedance are plotted against the frequency for the speckled ceiling tile sample.	50
Figure 28.	Real versus imaginary parts of the acoustic impedance is plotted for the speckled ceiling tile sample.	51
Figure 29.	Acoustic impedance tube and associated equipment are set up in this configuration for an impedance measurement using the one microphone transient method.	52
Figure 30.	Rigid impedance tube boundary is shown with its retention ring.	53
Figure 31.	Above is pulsed transient signal and below is its frequency spectrum.	53
Figure 32.	This is the window display on the SR-785 showing incident and reflected pulses over time.	54
Figure 33.	Real part of microphone reflected voltage over incident voltage with rigid boundary installed.	57
Figure 34.	Imaginary part of microphone reflected voltage over incident voltage with rigid boundary installed.	57
Figure 35.	Real part of microphone reflected voltage over incident voltage with sample boundary installed.	58
Figure 36.	Imaginary part of microphone reflected voltage over incident voltage with sample boundary installed.	59
Figure 37.	Real part of the reflectivity versus the frequency is shown for a speckled ceiling tile.	60
Figure 38.	Imaginary part of the reflectivity versus the frequency is shown for a speckled ceiling tile.	60
Figure 39.	Real part of the acoustic impedance versus the frequency is shown for a speckled ceiling tile.	61
Figure 40.	Imaginary part of the acoustic impedance versus the frequency is shown for a speckled ceiling tile.	61
Figure 41.	Open pipe impedance circuit is presented above.	63
Figure 42.	Real part of acoustic impedance versus frequency for an open tube using a Selenium driver.	65
Figure 43.	Imaginary part of acoustic impedance versus frequency for an open tube using a Selenium driver.	65

Figure 44.	Real part of acoustic impedance versus frequency for an open tube using a University Sound driver.....	67
Figure 45.	Imaginary part of acoustic impedance versus frequency for open tube using a University Sound driver.	67
Figure 46.	Shown from left to right are the three samples measured: an insulation sample, a ceiling tile sample with perforated holes (in sample cup), and a speckled ceiling tile sample (in sample cup).	69
Figure 47.	Real part of acoustic impedance versus frequency for a speckled ceiling tile sample using the Selenium driver.....	70
Figure 48.	Imaginary part of acoustic impedance versus frequency for a speckled ceiling tile sample using the Selenium driver.	70
Figure 49.	Real part of acoustic impedance versus frequency for an insulation sample using the Selenium driver.	72
Figure 50.	Imaginary part of acoustic impedance versus frequency for an insulation sample using the Selenium driver.....	72
Figure 51.	Real part of acoustic impedance versus frequency for a ceiling tile sample using the Selenium driver and a 50 mV signal.	74
Figure 52.	Imaginary part of acoustic impedance versus frequency for ceiling tile sample using the Selenium driver with a 50 mV signal applied.....	74
Figure 53.	Mouser microphone data specifications.....	81
Figure 54.	Selenium driver pulse-excitation time response on the HP-35665.....	85
Figure 55.	Selenium driver pulse-excitation narrow band frequency response on the HP-35665 (FFT mode).....	86
Figure 56.	Selenium driver pulse-excitation narrow band frequency response on the HP-35665 (Swept Sine mode).	86
Figure 57.	Specifications for Selenium DH-200E driver.	87
Figure 58.	University Sound driver pulse-excitation time response on HP-35665.....	89
Figure 59.	University Sound driver pulse-excitation narrow band frequency response on the HP-35665 (FFT mode).....	89
Figure 60.	University Sound driver pulse-excitation narrow band frequency response on the HP-35665 (Swept Sine mode).....	90
Figure 61.	University Sound Driver product specifications.....	91
Figure 62.	University Sound performance specifications.	92
Figure 63.	Microphone calibration cup drawing.	103
Figure 64.	Calibration microphone end fitting drawing.....	104
Figure 65.	Calibration microphone retainer drawing.	105
Figure 66.	End cap modification drawing.	106
Figure 67.	Microphone holder plate drawing.....	107
Figure 68.	Microphone blank cover plate drawing.	108
Figure 69.	Microphone holder plate drawing.....	109
Figure 70.	End tube sample holder with microphone access port drawing.....	110
Figure 71.	End tube blank plate drawing.	111
Figure 72.	Acoustic impedance measurement tube drawing.....	112

THIS PAGE INTENTIONALLY LEFT BLANK

LIST OF TABLES

Table 1.	Measured driving voltages required to produce second harmonic distortion to a level of one percent.....	29
Table 2.	List of Parts For Microphone Junction Box Assembly.....	84

THIS PAGE INTENTIONALLY LEFT BLANK

ACKNOWLEDGMENTS

I would like to thank Professor Steven Baker for his advice and mentorship during the course of completing this research. Thanks also goes to Professor Thomas Hofler for his help as my co-advisor.

A special thanks goes to Jay Adeff for developing the drawings for the apparatus and to George Jaksha for machining the parts and assembly of the apparatus.

THIS PAGE INTENTIONALLY LEFT BLANK

I. INTRODUCTION

A. PURPOSE

The purpose of this thesis is to describe the construction and testing of a modern "impedance tube" apparatus to measure the acoustic impedance of any material placed in the cup holder at the end of the tube. This device will measure the complex acoustic impedances of a variety of materials over a frequency range (typically from 0 to 4 kHz). This acoustic impedance tube will replace the older acoustic impedance tube apparatus used in the Naval Postgraduate School Physics Department Acoustics Teaching Laboratory. A new laboratory experiment was developed using this new acoustic impedance tube. The older acoustic impedance tube and new acoustic impedance tube are shown below in Figures 1 and 2 respectively.

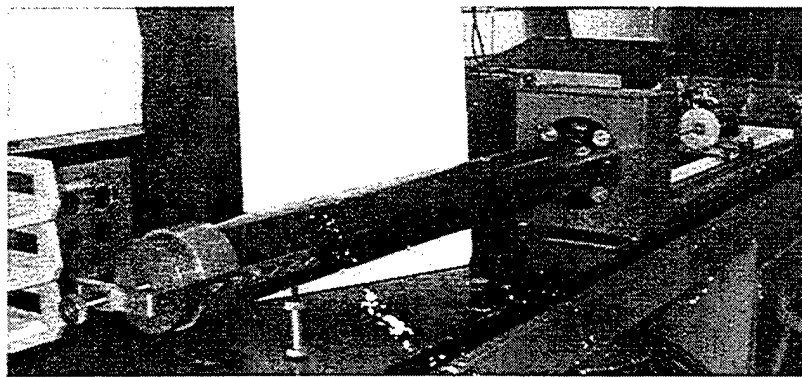


Figure 1. Older model acoustic impedance tube manufactured by Bruel and Kjaer. This will be replaced by the newer tube shown in Figure 2.

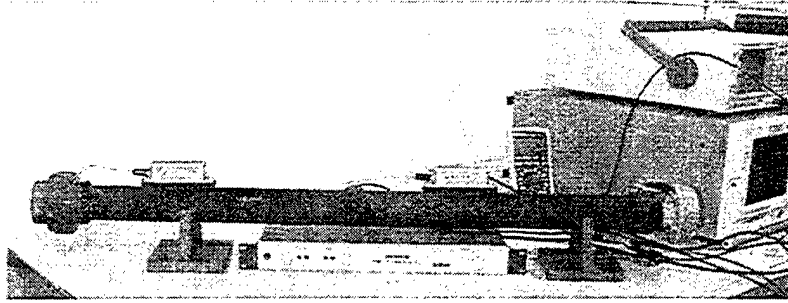


Figure 2. The new acoustic impedance measurement tube is shown with the Stanford Research Systems SR-785 dynamic signal analyzer, the Philips PM-3384 oscilloscope, and the Techron 5507 power amplifier (below the impedance tube).

Although the older acoustic impedance tube yields accurate results, the parts for this device are no longer in production, making repairs difficult and future longevity uncertain. The newer acoustic impedance tube has the primary advantages of making measurements much more rapidly and automatically, and uses modern computer software to show results graphically in very little time. It is also very inexpensive, being mostly made of plastic plumbing pipes. Measurements will be made using both devices, and the results will be compared, in Chapter IV.

The new acoustic impedance tube is used with a dynamic signal analyzer to measure the acoustic impedance of materials using the techniques described in detail in the next chapter. The most significant differences between the old and new measurement techniques are that the old technique requires a series of single-frequency measurements using a movable probe tube microphone, whereas the new techniques use stationary microphones, and employ broadband signals which are processed using FFT analysis. The new techniques do not offer any inherent improvement in accuracy over the old probe tube technique; they are just simpler and faster to perform.

The dynamic signal analyzer does not directly make the acoustic impedance measurement, but records Fourier transformed acoustic pressure data, which are saved on a floppy disk. These are subsequently loaded into a MATLAB computer program that does the actual calculations and presents the results in graphical format in only a few seconds. The results will be presented in Chapter IV.

B. DEFINITION OF ACOUSTIC IMPEDANCE

Throughout this thesis, by the term acoustic impedance will be meant specific acoustic impedance. The specific acoustic impedance, \tilde{z} , at a point in a sound field is the quotient of the complex acoustic pressure, \tilde{p} , and the complex acoustic velocity, \tilde{u} , at that point (Reference 1):

$$\tilde{z} = \frac{\tilde{p}}{\tilde{u}} \quad (\text{Equation 1})$$

For a plane progressive sound wave in a fluid, the specific acoustic impedance equals $\rho_0 c$, where ρ_0 is the fluid mass density and c is the speed of sound. The quantity $\rho_0 c$ is called the characteristic impedance of the fluid. For air, $\rho_0 c \approx 415 \text{ Pa-s/m}$; for water, $\rho_0 c = 1.5 \times 10^6 \text{ Pa-s/m}$ at normal temperature and pressure.

1. What Acoustic Impedance Is Used For

The specific acoustic impedance at a boundary between a fluid and a material is a property of the material. For sound waves in a fluid, normally-incident upon a planar boundary, the pressure reflection coefficient, \tilde{R} , is given by:

$$\tilde{R} = \frac{\tilde{z}_{bdy} - \rho_0 c}{\tilde{z}_{bdy} + \rho_0 c} \quad (\text{Equation 2})$$

where \tilde{z}_{bdy} is the boundary (normal) specific acoustic impedance and $\rho_0 c$ is the characteristic impedance of the fluid.

C. HOW ACOUSTIC IMPEDANCE IS MEASURED

Acoustic impedance may be measured by a variety of methods. These methods shall be discussed in detail in Chapter II and are briefly introduced here.

1. Classical Standing Wave Ratio (SWR) Method

This technique, as mentioned earlier, is the oldest method used for determining the acoustic impedance of a material. By generating acoustic planar pressure waves in a tube at various frequencies, the maxima and minima of the resulting standing waves are measured with one mobile probe tube microphone. The ratio of these values (the standing wave ratio or SWR) and their locations are subsequently used to calculate the acoustic impedance. (Reference 1)

2. Modern Acoustic Impedance Measurement Methods

Due to advances in technology (particularly in computers), many subsequent methods have been developed for acoustic impedance measurement. Some of these methods are: the two-microphone method (TMM), the single microphone method (SMM), and the multi-point method (MPM). Certainly other techniques exist, but only these methods will be briefly explored in Chapter II.

What makes these methods different from the SWR method is their use of stationary microphones, and their use of simultaneous, multiple frequencies. Although planar waves must be generated in a tube, as in the SWR method, these techniques employ more complex data processing to extract impedance. They do not use the standing wave ratio to determine the acoustic impedance. Since they do not employ a

moving microphone, these methods are considerably faster than the SWR method. The accuracies vary considerably, however, so there are clearly trade offs that will be involved.

D. SCOPE OF THESIS

Having provided a brief introduction to acoustic impedance measurement, the thesis outline is briefly presented. Chapter II will focus on the theory used by the acoustic impedance measurement apparatus. It will provide a background of several methods used to determine the acoustic impedance of a material, including their advantages and disadvantages. Next it will specifically explore the theory for acoustic impedance determination using two fixed microphones. Three equations will be derived for subsequent analysis: a basic equation, an exact equation, and a low frequency approximation equation. Additionally, a transient analysis technique, employing only one microphone, is presented. This analysis leads to the development of a formula for the (pressure) reflection coefficient of the material. From this, acoustic impedance can also be determined. MATLAB computer programs are developed for each of these approaches.

Chapter III will focus on the development of the apparatus and the procedures used. This will include a discussion of the microphone, power supply assembly, and compression horn drivers used. It will also explain in detail the procedures developed from the theories for this apparatus. One procedure makes a continuous-wave measurement with two microphones while the other makes a transient measurement with one microphone.

Chapter IV applies the procedures developed in the previous chapter to make acoustic impedance measurements for three sample materials using two compression horn drivers. It also describes the results of measurements made using an "open" tube (where the end cap is removed and the tube is open to the atmosphere). The "open" tube establishes a standard for which the effectiveness of the apparatus may be evaluated, since an approximate theory exists for the results in this case. The following approaches are compared: the two-microphone measurement (continuous) using both the exact and low frequency approximate equations and the one-microphone measurement (transient). The performances of two different drivers are compared as well.

Chapter V provides a brief summary of the conclusions developed during the experiments conducted using this acoustic impedance tube apparatus.

II. ACOUSTIC IMPEDANCE MEASUREMENT THEORY

A. BACKGROUND

1. Classical Standing Wave Ratio (SWR) Method

A great deal of research has been done in the past on acoustic impedance measurement tubes. The standing wave method (which the old impedance tube in Figure 1 incorporates) was the primary technique for measuring acoustic impedance over the last 80 years. This process requires location and amplitude measurement of the amplitude maxima and minima of the planar acoustic pressure waves in the tube using a mobile probe tube microphone, and, from these, computing the standing wave ratio (SWR). Figure 3 illustrates the basic set up for this process. Planar waves are generated by the speaker at the left end of the tube. (Reference 1)

The phase interference between the transmitted (incident) and reflected waves in a terminated pipe results in a standing wave pattern. The properties of the standing wave may be used to determine the boundary acoustic impedance. (Reference 1) We denote the complex amplitudes of these waves at the reflection boundary by the following:

Incident: $A = A$ Reflected: $B = Be^{j\theta}$ where $\theta \equiv$ phase angle (Equation 3)

Adapting from Kinsler et. al (Reference 1), the boundary specific acoustic impedance may be determined from the following equation:

$$\frac{\tilde{z}}{\rho_0 c} = \frac{1 + \left(\frac{B}{A}\right)e^{j\theta}}{1 - \left(\frac{B}{A}\right)e^{j\theta}} \quad (\text{Equation 4})$$

where ρ_0 and c are the density of air and speed of sound in air, respectively.

Again from Kinsler et. al (Reference 1), the amplitude at a pressure maximum is $A+B$, and the amplitude at a pressure minimum is $A-B$. The ratio of a pressure at a maximum to that at a minimum is:

$$SWR = \frac{A+B}{A-B} \quad (\text{Equation 5})$$

which may be rewritten as:

$$\frac{B}{A} = \frac{SWR - 1}{SWR + 1} \quad (\text{Equation 6})$$

From Figure 3, the SWR measurement may be obtained by probing the pressure field in the tube with a microphone and noting the amplitude at the first maximum and at the first minimum from the end where the sample material is located. (Reference 1) Equation 5 yields the B over A ratio. The phase angle, θ , may be determined by the distance of the first minimum from the sample end, x , shown in the following equation:

$$\theta = 2kx - \pi \quad (\text{Equation 7})$$

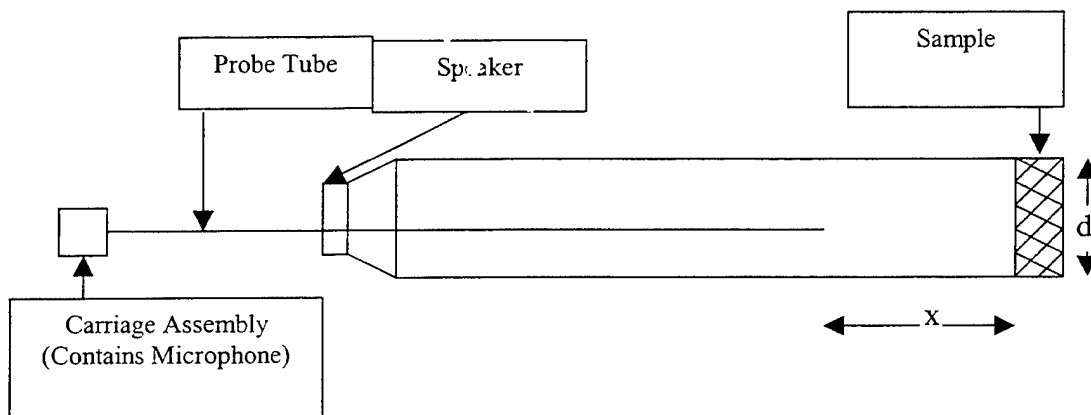


Figure 3. Schematic for the acoustic impedance tube utilizing the SWR method.

Therefore, by simply measuring the *SWR* and distance, x , Equations 4, 6, and 7 are used to calculate the acoustic impedance of any material placed at the end of the tube.

a. *Advantages and Disadvantages of Classical SWR Method*

This process exhibits good accuracy over the 0.1 to 10pc impedance range, and modern techniques have automated the process using SWR and null searching computer codes. It has the added benefit of being able to directly measure the standing wave parameters. (Reference 3) Despite these advantages, it is inherently time consuming (even with automation) and limited to frequencies below the cut on frequency of higher order propagating modes in the tube (as are the other methods). It additionally has accuracy limitations by SWR and null location resolution. (Reference 3) This is further discussed later in this chapter in part B.

2. Modern Acoustic Impedance Measurement Methods

With the development over the last 20 years of fast Fourier transform algorithms that can be performed on modern computers and dynamic signal analyzers, new impedance measurement techniques have emerged, employing stationary microphones, making point type measurements in a standing wave field. Some of these methods include the two-microphone method (TMM), the multipoint method (MPM), and even a single microphone method (SMM). (Reference 3)

a. *Comparison of the Advantages and Disadvantages of Modern Acoustic Impedance Measurement Methods*

The acoustic impedance tube analyzed in this discussion and shown in Figure 2 uses the TMM. The theory of operation and apparatus will be covered rigorously in part C later in this chapter. The primary advantages of the TMM are the significant time saving mentioned earlier, no required moving parts, and its excellent

suitability for quick screening tests with a random noise source. The disadvantages to this method are that its accuracy significantly degrades at large wavelengths (low frequencies) and at microphone separations near one-half wavelength (high frequencies). The TMM has the added problems of requiring highly accurate (relative) microphone calibrations and uses a 1-D wave propagation model. (Reference 3) The MPM, on the other hand, is very accurate (when using a least squares data fitting), has an enhanced frequency range, and has no restriction on microphone separation relative to wavelength. The drawbacks of the MPM are its complexity, required moving parts, and longer amount of time needed to make a measurement compared to the TMM. (Reference 3) It additionally needs all microphones to be calibrated with a high degree of accuracy.

The research of Patricia Stiede and Michael Jones, contained in Reference 3, explores the techniques described above (SWR method excepted) using different signal sources and compares their results. They found the MPM with a single discrete frequency to be the most accurate but also the most time consuming method in use. From their results, Stiede and Jones further note that the relative merits of each of the other methods were shown to depend upon a trade-off between the amount of time available and the accuracy necessary. (Reference 3) Interestingly, they note the TMM exhibited minimal loss of accuracy using a pseudo-random noise source (at frequencies under 2.5 kHz). The TMM analyzed in this thesis uses a band-limited, pseudo-random noise source, and thus will be expected to yield similar accuracy.

It is also important to note that all of these modern methods are also limited to frequencies below which non-planar wave propagation begins. This is discussed further in the following section.

B. FREQUENCY LIMITS OF THE IMPEDANCE TUBES

One of the first important steps in using an impedance measurement tube is knowledge of the range of frequencies for which it will yield accurate results. The old impedance tube (mentioned in Chapter I) uses the standing wave ratio method of computation for acoustic impedance. This technique was discussed previously in part A. The lower frequency limit of this impedance tube is determined by the requirement that there be two pressure nodes available for measurement. The upper limit is set by the cut-off frequency of the first non-planar standing wave.

In the case of the new acoustic impedance measurement tube, the upper frequency limit is also determined by the cut-off frequency of the first non-planar wave. This frequency can readily be determined from the relationship:

$$ka = 1.84 \qquad \qquad \qquad \text{(Equation 8)}$$

In this case " k " is the wave number and " a " is the radius of the impedance tube. Using the fact that the diameter of the new impedance tube is approximately 2 inches (5.08 cm) and applying appropriate conversion factors, the cut-off frequency of the first non-planar wave is approximately 4 kHz. By comparison, the old acoustic impedance tube has a diameter of 10 centimeters, and so the first non-planar wave is excited at approximately 2 kHz. This cut-off will limit the frequency range over which the old and new acoustic impedance tube measured impedances may be compared, as will be seen when the results are discussed in Chapter IV.

C. IMPEDANCE MEASUREMENT THEORY USING TWO MICROPHONES (CONTINUOUS EXCITATION)

The basic components of the apparatus used to measure acoustic impedance by the two-microphone method are schematized in Figure 4. A driver/loudspeaker at one end excites plane waves in the tube, which reflect off the sample, located at the other end. Two microphones are placed near the sample end of the tube. The specific acoustic impedance at the reflecting surface is given by:

$$\tilde{z}_{bdy} = \frac{\tilde{\delta p}}{\tilde{\delta u}} \Big|_{bdy} \quad (\text{Equation 9})$$

where $\tilde{\delta p}$ and $\tilde{\delta u}$ are the acoustic pressure and velocity, respectively, at the reflecting surface.

The following subsections describe three approximation methods that were investigated to estimate the right hand side of Equation 9 from microphone measurements made at two fixed locations near a reflection boundary.

1. Simplest approximation

Simple estimates for the complex pressure, $\tilde{\delta p}_{bdy}$, and complex velocity, $\tilde{\delta u}_{bdy}$, to be used in Equation 9 are:

$$\tilde{\delta p}_{bdy} \approx \tilde{\delta p}(x_1) \quad (\text{Equation 10})$$

$$\tilde{\delta u}_{bdy} \approx \frac{1}{j\omega\rho_0} \times \frac{(\delta p(x_2) - \delta p(x_1))}{(x_2 - x_1)} \quad (\text{Equation 11})$$

where $\tilde{\delta p}(x_1)$ and $\tilde{\delta p}(x_2)$ are the measured acoustic pressures at distances x_1 and x_2 from the end of the acoustic impedance measurement tube, respectively, as shown below in Figure 4. Additionally ρ_0 is the density of air and ω is the radial frequency (defined as

the product of 2π and the temporal frequency, measured in Hz). In this approximation, we estimate the pressure at the reflection boundary as the pressure at the closest microphone, and we estimate the velocity at the boundary as the velocity estimated at the location midway between the microphones, using simple linear interpolation of the pressure field.

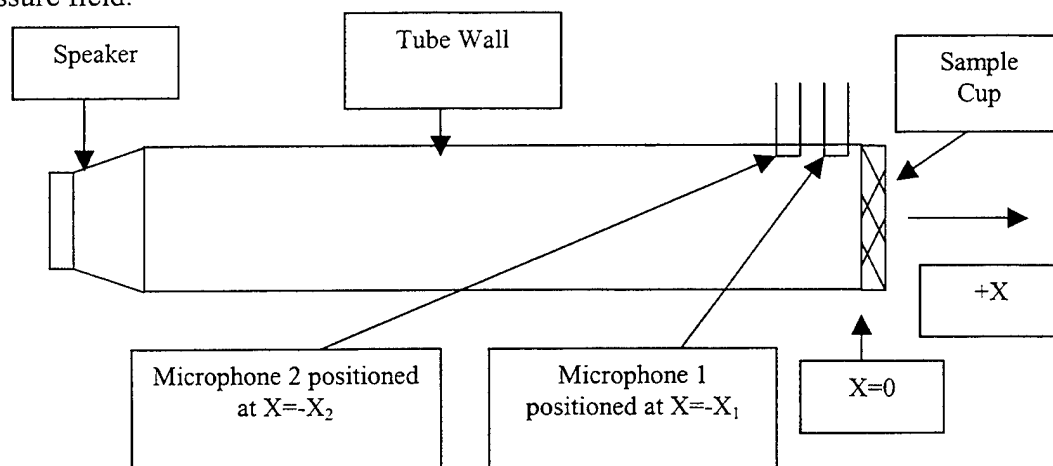


Figure 4. These are the microphone positions in the impedance tube during an impedance measurement.

Combining Equations 9, 10, and 11, the acoustic impedance of the sample surface is estimated as:

$$\tilde{z}_{bdy} \cong \frac{j\omega\rho_0 \times (\lambda_2 - x_1)}{\left(\frac{\tilde{\delta p}_2}{\tilde{\delta p}_1} - 1\right)} \quad (\text{Equation 12})$$

where using simplified notation: $\tilde{\delta p}_1 = \tilde{\delta p}(x_1)$ and $\tilde{\delta p}_2 = \tilde{\delta p}(x_2)$.

As one can see, complex pressure measurements are required at the two points, x_1 and x_2 . The measured microphone voltages are proportional to the acoustic pressures in the acoustic impedance measurement tube:

$$\delta\tilde{v}_1 = \tilde{C}_1(\omega) \times \delta\tilde{p}_1 \quad (\text{Equation 13})$$

$$\delta\tilde{v}_2 = \tilde{C}_2(\omega) \times \delta\tilde{p}_2 \quad (\text{Equation 14})$$

where $\delta\tilde{v}_1$ and $\delta\tilde{v}_2$ are the measured complex voltages, and \tilde{C}_1 and \tilde{C}_2 are complex microphone voltage sensitivities that are a function of frequency. It follows that the ratio of complex pressures is:

$$\frac{\delta\tilde{p}_2}{\delta\tilde{p}_1} = \frac{\tilde{C}_1}{\tilde{C}_2} \times \frac{\delta\tilde{v}_2}{\delta\tilde{v}_1} \quad (\text{Equation 15})$$

From Equation 15, if the ratio of the complex microphone sensitivities is known, the ratio of the complex pressures can readily be determined from the measured ratio of complex microphone voltages. In practice, the ratio of sensitivities is obtained from a measurement of the ratio of microphone output voltages with both microphones exposed to the same acoustic pressure:

$$\frac{\tilde{C}_2}{\tilde{C}_1} = \left. \frac{\delta\tilde{v}_2}{\delta\tilde{v}_1} \right|_{\delta\tilde{p}_1 = \delta\tilde{p}_2} = F\tilde{R}1 \quad (\text{Equation 16})$$

This is just the frequency response (designated as complex term $F\tilde{R}1$) of the signals from microphones. For this measurement, the microphones are flush-mounted in a rigid termination at the sample end of the tube. Notice that if two frequency response measurements are made, the first as described above, with both microphones flush at the end of the tube, and the second with a sample in place and with the microphones in their usual positions, the acoustic impedance as a function of frequency may readily be determined.

$$\text{Let: } \tilde{FR}2 = \left. \frac{\delta \tilde{v}_2}{\delta \tilde{v}_1} \right|_{\text{sample}} \quad (\text{Equation 17})$$

be the ratio of microphone output voltages with a sample in place.

The complex acoustic impedance is then determined by the equation:

$$\tilde{z} \approx \frac{j\omega\rho_0 \times (x_2 - x_1)}{\left(\frac{\tilde{FR}2}{\tilde{FR}1} - 1\right)} \quad (\text{Equation 18 – the Basic Equation})$$

In the new impedance tube apparatus, the spacing $x_2 - x_1$ is 0.0144m.

a. Using the Basic Approach in a Computer Program

A procedure was developed to obtain the two frequency response functions, $\tilde{FR}1$ and $\tilde{FR}2$, using a dynamic signal analyzer. These are stored to floppy disk, and transferred to a MATLAB program, which employs Equation 18 to calculate and plot acoustic impedance. These are described more fully in the following chapter and in the appendices.

2. The Exact Approach

Although the method described above in II.C.1 provides a simple, albeit rather crude approximation for estimating the acoustic impedance measurement, there is a more exact approach to calculating the complex value of the acoustic impedance. By referring to Figure 4 again, begin by representing the complex pressure at any given point in the tube as:

$$\tilde{\delta p}(x,t) = \tilde{A}e^{j\omega t} [e^{-j\tilde{k}x} + \tilde{R}e^{j\tilde{k}x}] \quad (\text{Equation 19})$$

$$\tilde{k} \equiv k + j\alpha \quad (\text{Equation 20})$$

$$\tilde{R} \equiv \frac{\tilde{z}_{rel} - 1}{\tilde{z}_{rel} + 1} \quad (\text{Equation 21})$$

$$\tilde{z}_{rel} \equiv \frac{\tilde{z}_{bdy}}{\rho_0 c} \quad (\text{Equation 21a})$$

Here, \tilde{A} is the complex wave amplitude, and \tilde{k} is the complex wave number.

Also: $k=2\pi/\lambda$ is the real wave number; α is the attenuation coefficient; \tilde{R} is the pressure reflection coefficient; \tilde{z}_{bdy} is the boundary specific acoustic impedance; and $\rho_0 c$ is the characteristic impedance of air. It can easily be shown from Equation 21 that:

$$\tilde{z}_{rel} = \frac{1 + \tilde{R}}{1 - \tilde{R}} \quad (\text{Equation 22})$$

The complex velocity at any given point in the tube is:

$$\tilde{u}(x, t) = \frac{-1}{j\omega\rho_0} \times \frac{\partial \tilde{p}(x, t)}{\partial x} = \frac{\tilde{A}}{\rho_0 c} e^{j\omega t} [e^{-j\tilde{k}x} - \tilde{R}e^{j\tilde{k}x}] \quad (\text{Equation 23})$$

Using Equation 19, define the complex pressures at x_1 and x_2 :

$$\tilde{p}(-x_1, t) = \tilde{A}e^{j\omega t} [e^{-j\tilde{k}x_1} + \tilde{R}e^{j\tilde{k}x_1}] \equiv \tilde{p}_1 e^{j\omega t} \quad (\text{Equation 24})$$

$$\tilde{p}(-x_2, t) = \tilde{A}e^{j\omega t} [e^{-j\tilde{k}x_2} + \tilde{R}e^{j\tilde{k}x_2}] \equiv \tilde{p}_2 e^{j\omega t} \quad (\text{Equation 25})$$

Dividing Equation 25 by Equation 24 yields:

$$\frac{\tilde{p}_2}{\tilde{p}_1} = \frac{e^{j\tilde{k}x_2} + \tilde{R}e^{-j\tilde{k}x_2}}{e^{j\tilde{k}x_1} + \tilde{R}e^{-j\tilde{k}x_1}} = e^{j\tilde{k}(x_2-x_1)} \frac{[1 + \tilde{R}e^{-2j\tilde{k}x_2}]}{[1 + \tilde{R}e^{-2j\tilde{k}x_1}]} \quad (\text{Equation 26})$$

Using algebra, Equation 26 can be rewritten in terms of the complex reflection coefficient as follows:

$$\tilde{R} = \frac{[e^{j\tilde{k}x_2} - \left(\frac{\tilde{\delta p}_2}{\tilde{\delta p}_1}\right)e^{j\tilde{k}x_1}]}{-[e^{j\tilde{k}x_2} - \left(\frac{\tilde{\delta p}_2}{\tilde{\delta p}_1}\right)e^{j\tilde{k}x_1}]} \quad (\text{Equation 27})$$

From Equation 21, we can write:

$$\frac{\tilde{z}_{rel} - 1}{\tilde{z}_{rel} + 1} = \frac{[e^{j\tilde{k}x_2} - \left(\frac{\tilde{\delta p}_2}{\tilde{\delta p}_1}\right)e^{j\tilde{k}x_1}]}{-[e^{j\tilde{k}x_2} - \left(\frac{\tilde{\delta p}_2}{\tilde{\delta p}_1}\right)e^{j\tilde{k}x_1}]} \quad (\text{Equation 28})$$

Solving for the complex relative acoustic impedance yields:

$$\tilde{z}_{rel} = \frac{[e^{j\tilde{k}x_2} - \left(\frac{\tilde{\delta p}_2}{\tilde{\delta p}_1}\right)e^{-j\tilde{k}x_1}] - [e^{j\tilde{k}x_2} - \left(\frac{\tilde{\delta p}_2}{\tilde{\delta p}_1}\right)e^{j\tilde{k}x_1}]}{[e^{-j\tilde{k}x_2} - \left(\frac{\tilde{\delta p}_2}{\tilde{\delta p}_1}\right)] + [e^{j\tilde{k}x_2} - \left(\frac{\tilde{\delta p}_2}{\tilde{\delta p}_1}\right)e^{j\tilde{k}x_1}]} \quad (\text{Equation 29})$$

This simplifies to:

$$\tilde{z}_{rel} = \frac{-j[\sin \tilde{k}x_2 - \left(\frac{\tilde{\delta p}_2}{\tilde{\delta p}_1}\right)\sin \tilde{k}x_1]}{[\cos \tilde{k}x_2 - \left(\frac{\tilde{\delta p}_2}{\tilde{\delta p}_1}\right)\cos \tilde{k}x_1]} \quad (\text{Equation 30 - the Exact Equation})$$

This equation is exact.

a. Using the Exact Approach in a Computer Program

Using the microphone positions, x_2 and x_1 , and obtaining the pressure ratio as previously described (Equation 15 and following), this equation gives the most accurate estimation of boundary acoustic impedance. As before, the required frequency response measurements were made using a dynamic signal analyzer and stored to a disk

for later analysis using MATLAB, which employs Equation 30 to calculate and plot acoustic impedance. Further details appear in the next chapter and in the appendices.

3. The Low Frequency Approximation

If the complex value of “ kx ” is assumed to be small, Equation 30 simplifies to:

$$\tilde{z}_{rel} = \frac{-j[\tilde{k}x_2 - \left(\frac{\tilde{\delta p}_2}{\tilde{\delta p}_1}\right)\tilde{k}x_1]}{[1 - \left(\frac{\tilde{\delta p}_2}{\tilde{\delta p}_1}\right)]} \quad (\text{Equation 31 – Low Freq. Equation})$$

It can be shown that this approximation is equivalent to estimating the pressure at the boundary by linear extrapolation of the pressures at the microphones, while still estimating the velocity at the boundary as that estimated between the microphones using linear interpolation of the pressure field the same as the most simple approximation presented previously.

The derivation is as follows. We estimate the boundary acoustic pressure and velocity in the following equations:

$$\tilde{\delta p}|_{bdy} = \tilde{\delta p}_1 + x_1 \frac{\tilde{\delta p}_1 - \tilde{\delta p}_2}{(x_2 - x_1)} = \frac{\tilde{\delta p}_1}{(x_2 - x_1)} [x_2 - \left(\frac{\tilde{\delta p}_2}{\tilde{\delta p}_1}\right)x_1] \quad (\text{Equation 32})$$

$$\tilde{\delta u}|_{bdy} = \frac{-1}{j\omega\rho} \frac{(\tilde{\delta p}_2 - \tilde{\delta p}_1)}{(-x_2 - x_1)} = \frac{-j}{\omega\rho} \frac{\tilde{\delta p}_1 \left[\left(\frac{\tilde{\delta p}_2}{\tilde{\delta p}_1}\right) - 1\right]}{(x_2 - x_1)} \quad (\text{Equation 33})$$

Using Equations 32 and 33, the acoustic impedance of the boundary can be determined:

$$\tilde{z}_{bdy} \approx \frac{\tilde{\delta p}_1}{(x_2 - x_1)} \frac{[x_2 - \left(\frac{\tilde{\delta p}_2}{\tilde{\delta p}_1}\right)x_1]}{\frac{j}{\omega \rho_0} \frac{\tilde{\delta p}_1}{(x_2 - x_1)} \left(1 - \frac{\tilde{\delta p}_2}{\tilde{\delta p}_1}\right)} \quad (\text{Equation 34})$$

This leads to a final result for relative acoustic impedance that matches Equation

31:

$$\tilde{z}_{rel} = \frac{\tilde{z}_{bdy}}{\rho_0 c} = \frac{-j[\tilde{k}x_2 - \left(\frac{\tilde{\delta p}_2}{\tilde{\delta p}_1}\right)\tilde{k}x_1]}{[1 - \left(\frac{\tilde{\delta p}_2}{\tilde{\delta p}_1}\right)]} \quad (\text{Equation 35 - Low Freq. Equation})$$

a. Using the Low Frequency Approximation in a Computer Program

As mentioned previously, a procedure was developed to obtain the pressure ratio using a dynamic signal analyzer. This data are stored to a floppy disk and transferred to a MATLAB program that employs Equation 31 (or Equation 35) to calculate and plot an approximation of acoustic impedance. Low frequencies are inherently assumed. Further details appear in the next chapter and in the appendices.

D. IMPEDANCE MEASUREMENT THEORY USING ONE MICROPHONE

1. Measurement of Reflectivity

The acoustic impedance measurement tube can be used to measure both the pressure reflection coefficient as well as the surface acoustic impedance by measuring the complex incident and reflected pressure at a single point near the middle of the tube. In this case the driver is used to produce a short duration pulse instead of the continuous white noise used earlier in this chapter in C.1.

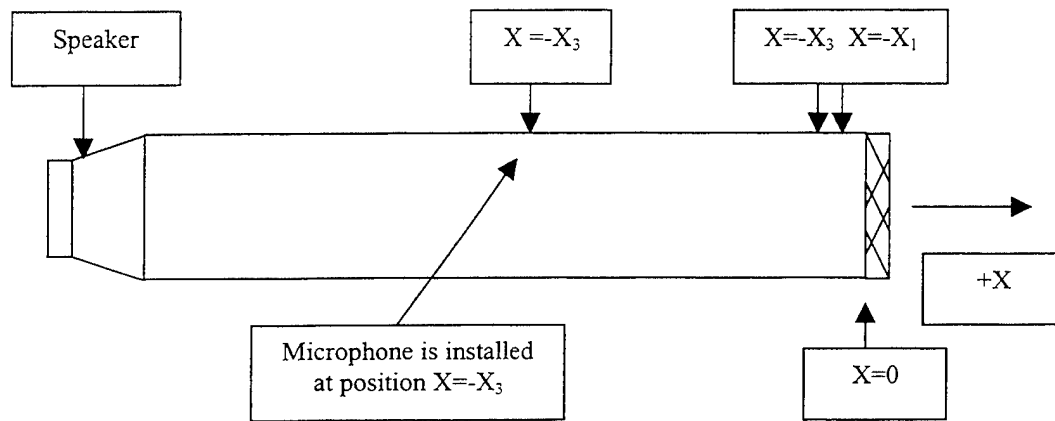


Figure 5. Acoustic impedance tube alignment for reflectivity measurement.

As schematized in Figure 5 above, one of the two microphones installed in the middle of the tube is designated to be in the x_3 position. If desired, for this experiment, a blank cover may be installed over the x_1 and x_2 microphone positions.

The following describes the measurement of the pressure reflection coefficient of a given material. Starting with the following equations expressing the superposition of the incident and reflected wave at a given point in the tube:

$$\tilde{\delta p}(x, t) = \tilde{\delta p}^+ e^{j(\omega t - kx)} e^{-\alpha x} + \tilde{\delta p}^- e^{j(\omega t + kx)} e^{\alpha x} \quad (\text{Equation 36})$$

$$\text{so} \quad \tilde{\delta p}(x, t) = \tilde{\delta p}^+ e^{j\omega t} [e^{-j\tilde{k}x} + \tilde{R}e^{j\tilde{k}x}] \quad (\text{Equation 37})$$

where $\tilde{k} \equiv k + j\alpha$ (Equation 38)

and $\tilde{R} = \frac{\tilde{\delta p}^-}{\tilde{\delta p}^+}$ (Equation 39)

where $\delta\tilde{p}^+$ and $\delta\tilde{p}^-$ are the complex pressure amplitudes of the incident and reflected waves, respectively.

We define the complex wave number in Equation 38 (as we did in Equation 20) and the complex reflection coefficient in Equation 39. Alpha is defined as the attenuation coefficient. It can be shown that:

$$\tilde{R} = \frac{\tilde{z}_{bdy} - \rho_0 c}{\tilde{z}_{bdy} + \rho_0 c} \quad \text{(Equation 40)}$$

where $\rho_0 c$ is the characteristic impedance of air based on conditions in the acoustic impedance measurement tube. If the complex wave number is known, then from measurements of the complex pressure at point x_3 alone, assuming incident and reflected waves are separated in time, the following results:

$$\tilde{\delta p}_3^{inc} = \tilde{\delta p}_i^+ e^{j\omega t} e^{j\tilde{k}x_3} \quad \text{(Equation 41)}$$

$$\tilde{\delta p}_3^{refl} = \tilde{\delta p}^- e^{j\omega t} e^{-j\tilde{k}x_3} = \tilde{R} \tilde{\delta p}_i^+ e^{j\omega t} e^{-j\tilde{k}x_3} \quad \text{(Equation 42)}$$

where $\tilde{\delta p}_3^{inc}$ and $\tilde{\delta p}_3^{refl}$ are the incident and reflected pressures at x_3 , respectively.

From above, it follows:

$$\frac{\tilde{\delta p}_3^{refl}}{\tilde{\delta p}_3^{inc}} = \tilde{R} e^{-2j\tilde{k}x_3} \quad \text{(Equation 43)}$$

$$\text{and: } \tilde{R} = \frac{\tilde{\delta p}_3^{refl}}{\tilde{\delta p}_3^{inc}} \times e^{2jkx_3} = \frac{\tilde{\delta v}_3^{refl}}{\tilde{\delta v}_3^{inc}} \times e^{2jkx_3} \quad (\text{Equation 44})$$

where $\frac{\tilde{\delta v}_3^{refl}}{\tilde{\delta v}_3^{inc}}$ is the measured microphone voltage ratio.

The exponential factor in Equation 44 may be obtained by measuring the complex voltage ratio of the reflected pulse to the incident pulse for the case where the complex reflection boundary has a reflection coefficient equal to one. This would be in the case of a perfectly rigid surface at the end of the acoustic impedance measurement tube. Using this technique, the complex reflectivity is determined by:

$$\tilde{R}_{sample} = \frac{(\tilde{\delta v}^{refl} / \tilde{\delta v}^{inc})_{sample}}{(\tilde{\delta v}^{refl} / \tilde{\delta v}^{inc})_{rigidwall}} \quad (\text{Equation 45 – Reflectivity Equation})$$

where the subscripts “sample” and “rigid wall” indicate the reflection boundary condition. Note it is important that the incident and reflected signals be referenced to the same zero of time.

A procedure was developed, using a dynamic signal analyzer, to apply a brief pulse excitation to the loud speaker, and to isolate a single occurrence of incident and its associated reflection. This procedure is covered in detail in Chapter III and Appendix J.

2. Measurement of Acoustic Impedance

Having calculated the reflectivity using Equation 45, it is a rather simple matter to calculate the acoustic impedance of the sample from this using Equations 21a and 22:

$$\tilde{z}_{rel} \equiv \frac{\tilde{z}_{bdy}}{\rho_0 c} = \frac{1 + \tilde{R}_{sample}}{1 - \tilde{R}_{sample}} \quad (\text{Equations 21a \& 22})$$

3. Using One Microphone Impedance Measurement Theory in a Computer Program

Using the theory described above, the procedure described above obtains the real and imaginary parts of the numerator and denominator ratios depicted in Equation 45 to a floppy disk. These files can be subsequently downloaded into a MATLAB program that calculates and plots the real and imaginary parts of a material's reflectivity as a function of frequency. This program also computes the acoustic impedance from the reflectivity using Equation 22 and plots it as well.

THIS PAGE INTENTIONALLY LEFT BLANK

III. DEVELOPMENT OF THE APPARATUS

A. ACOUSTIC IMPEDANCE MEASUREMENT TUBE DESCRIPTION

The new acoustic impedance measurement tube is approximately one meter long, with a two-inch (5 cm) diameter. It is mounted on two wooden brackets for support. On one end of the tube a compression horn driver is screwed firmly into place. The acoustic impedance tube is shown in Figure 6.

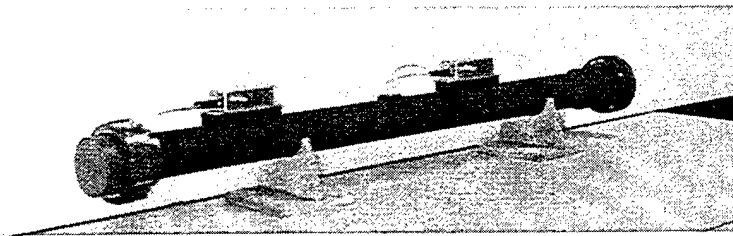


Figure 6. Shown above is the new acoustic impedance measurement tube.

On the opposite end of the tube the end cap sample holder (a calibration cup or a blank may be installed as well) is fastened into place by the retention ring. These are shown below in Figure 7.



Figure 7. End cap blank is featured along with the retention ring.

The acoustic impedance tube contains two pairs of microphones. One pair is mounted on the top middle of the tube while the other pair is installed very close to the sample end of the tube. A junction box is fastened into place near each microphone pair on the top of the tube. The junction box contains 1/8" phone jacks, into which the microphone plugs are inserted. It also contains a nine-volt battery that supplies power to the microphones. They are energized and de-energized by means of a micro-miniature toggle switch on the front of the junction box. On each side of the junction box are BNC connectors that provide the output signal from each microphone. The full acoustic impedance tube assembly is shown below in Figure 8.

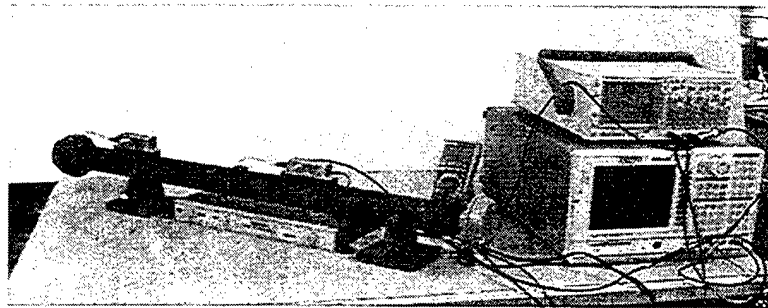


Figure 8. The acoustic impedance tube assembly is shown along with the dynamic signal analyzer in the foreground under the oscilloscope. The speaker/driver is installed on the tube on the right hand side. The sample cup is installed on the left hand side. Amplifier is shown under the impedance tube. The two junction boxes are on top of the tube.

Schematic drawings for the acoustic impedance measurement tube and its parts are contained in Appendix F.

B. SELECTED COMPONENTS OF THE ACOUSTIC IMPEDANCE MEASUREMENT TUBE

1. Microphone

The microphone selected for the measurements is the Mouser Electronics 25LM045, a small, rugged, electret microphone with a 0.39-inch diameter (1 cm). The

microphone is pictured below in Figures 9 and 10. The manufacturer specifications for this microphone are included in Appendix A. From Appendix A, the nominal sensitivity level of the microphones is -63 decibels referenced to one volt per microbar of pressure.

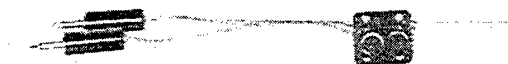


Figure 9. Front-end view of Mouser Electronics microphone pair.

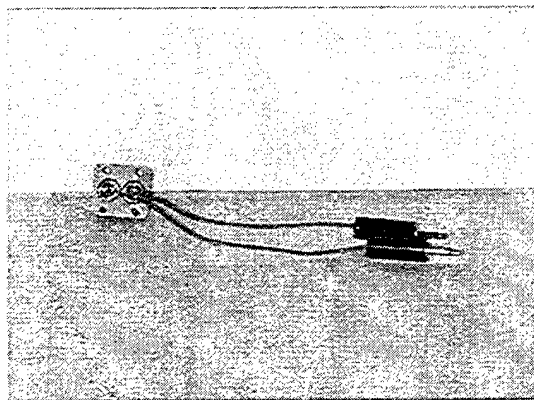


Figure 10. Reverse view of Mouser Electronics microphone pair.

The basic microphone circuit is also exhibited in Appendix A. These microphones are very sensitive, and are easily overdriven. Safe operating limits were established such that the microphone second harmonic distortion did not exceed one percent. These measures are described in detail below.

a. Second Harmonic Distortion

During the experimentation, described later in Chapter IV, it was noted that, with only several tenths of a volt rms drive to the speaker, there was significant distortion of the measured signals (and therefore errors in the acoustic impedances calculated from these signals). This distortion occurred for both drivers tested. Reducing the voltage applied to the drivers to a value of 50 mV rms improved the results dramatically. The source of the distortion was traced to the microphones overloading.

To investigate this phenomenon more thoroughly, an experiment was arranged where the Mouser microphones were placed in their calibration position (flush against the end of the tube as described later in this chapter) along with a laboratory precision microphone. One of the Mouser microphones was monitored on one channel of a dynamic signal analyzer, while the precision microphone (Larson-Davis 1/4-inch) was monitored on the other channel. A narrow band, power spectrum, single frequency sine wave was sent to the driver (Selenium DH200E). The magnitude of each microphone output voltage was monitored. The magnitude of the second harmonic component was compared to that of the fundamental.

The voltage of the driving sine wave was increased until the magnitude of the second harmonic component from the Mouser microphone reached a level of 40 decibels down (one percent) from the fundamental. Table 1 displays the results of these measurements, where six frequencies were tested. The (broadband) rms voltage of the driving signal was recorded using a voltmeter. The Mouser microphone output signal (broad band rms) was also recorded using an oscilloscope. Figure 11 displays this information graphically.

FREQUENCY	APPLIED VOLTAGE TO SELENIUM DH200E DRIVER (RMS)	MOUSER MICROPHONE BROAD BAND RMS OUTPUT VOLTAGE
256 Hz	38.5 mV	20 mV
496 Hz	116.7 mV	30 mV
922 Hz	214.5 mV	59 mV
1008 Hz	73.4 mV	43 mV
2016 Hz	72.0 mV	35 mV
3008 Hz	295.7 mV	35 mV

Table 1. Measured driving voltages required to produce second harmonic distortion to a level of one percent.

The above distortion measured in this experiment arises due to both loudspeaker and microphone non-linearity. This was, in fact, verified, by noting a non-negligible second harmonic component in the reference microphone signal. Loudspeaker non-linearity has no impact on the measurement of acoustic impedance with the apparatus. Hence, these distortion levels represent worst cases.

For further experiments, broadband speaker drive levels were maintained at a value of 35 mV rms, and so to ensure the resulting acoustic pressure measurements contained less than one percent second harmonic distortion.

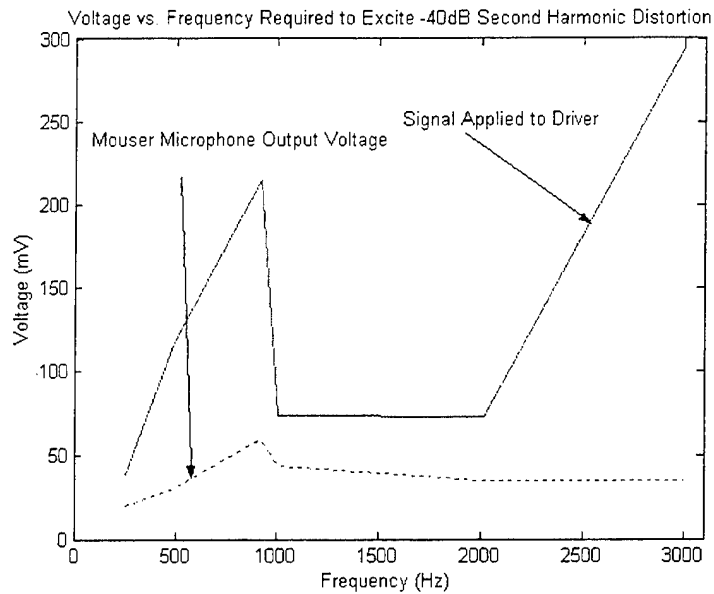


Figure 11. Voltage required to excite one percent or -40dB second harmonic distortion plotted as function of frequency.

What is important to note is that, regardless of the quality of the driver or speaker, if the microphones are high quality linear devices, they are able to accurately measure the sound field of the impedance tube. The acoustic impedance is determined by successfully measuring the pressure in the tube. If the microphones, however, distort the signal, the measurements don't represent reality. The conclusions, therefore, become erroneous. The one percent distortion described earlier represents both the speaker and the microphone distortion. The pressure measurements, therefore, should have less than a one percent error. The errors in the specific acoustic impedance extracted from measured pressure differences, of course, will be greater. They are also frequency dependent.

2. Microphone Power Supply Assembly

Each junction box in the acoustic impedance measurement tube apparatus is designed to supply power to two microphones, receive each microphone's signal, and output these signals via their respective BNC connectors. The signals are fed from the junction box BNC connectors into channels one and two of the Stanford Research Systems 785 dynamic signal analyzer for analysis.

Power is supplied to the microphones from a nine-volt dc battery (each via a 1000 ohm resistor). The Thevenin equivalent circuit source impedance of the microphones is approximated to be 1000 ohms. The selection of the capacitor is based on ensuring the impedance of the capacitor is well below the 1000 ohm impedance associated with the

microphone: $\frac{1}{2\pi fC} \ll 1k\Omega$. As a result: $C \gg \frac{1}{2\pi f1000} = \frac{1}{2\pi f}$ (capacitance, C ,

is expressed in microfarads and frequency, f , is expressed in kilohertz). For a 3dB drop in frequency to occur at 10 Hz, capacitance must be approximately sixteen microfarads. A twenty-two microfarad capacitor is used in the circuit.

Since the 3dB down frequency is $\frac{1}{2\pi RC}$, using a one kilo-ohm resistor and a twenty-two microfarad capacitor results in a -3dB frequency of about eight hertz. This is acceptable because the operating frequencies in the spectrum will be above eight hertz. A table is included in Appendix B documenting the parts used in assembling these junction boxes. The junction box used is exhibited in Figures 12 and 13 below.

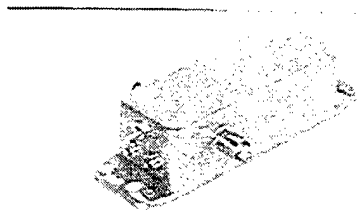


Figure 12. External close up view of microphone power supply junction box.

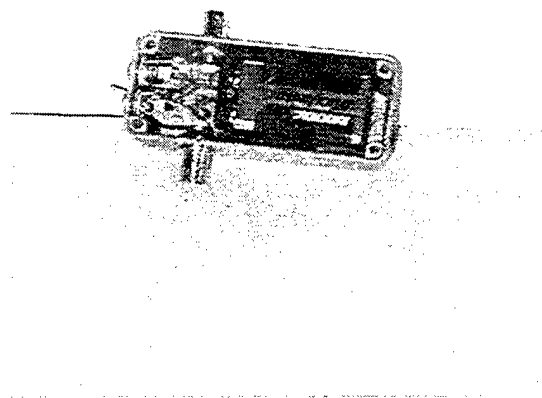


Figure 13. Internal view of junction box assembly including 9-volt battery.

3. Driver (Speaker)

The purpose of the driver is to provide a source of acoustic planar waves over a range of frequencies inside the acoustic impedance measurement tube. These waves will propagate inside the impedance tube and be measured by the microphones described earlier. The signal provided to the driver may originate from the SR-785 dynamic signal analyzer or the HP-3314A function generator (usually both signals are sent to the driver via an amplifier) depending on which measurement is being performed. Normally, for

the two-microphone measurement, a continuous, band limited white noise signal is provided from the SR-785. The HP-3314A normally provides a pulsed signal for the transient one microphone measurement. These techniques will be discussed further later in this chapter in part C. Having a driver that provides good, clean signals from 0 to 4 kHz (the lowest cut-off frequency for non-planar modes) is very important for the measurement. As a result, several drivers were tested to determine which one is best suited for the application described above.

a. *Drivers That Were Tested*

The following commercial drivers were tested in the manner that will be described subsequently: the Dayton Loudspeaker Company 260-098 horn driver; the Reflex Driver Unit; the Motorola KSN1142A horn driver; the Motorola DSN 1197A compact horn driver; the Selenium DH200E titanium compression driver; the Selenium tweeter compression driver; the University Sound 1828R reentrant driver; and the Selenium D-250 driver. Each of these drivers was very carefully evaluated. The best of these drivers were subsequently installed on the acoustic impedance measurement tube for impedance measurements.

b. *How the Drivers Were Tested*

Several compression horn drivers were evaluated for their suitability, using a test microphone (a high accuracy one-half inch microphone manufactured by Bruel and Kjaer) and a HP-35665 dynamic signal analyzer. The evaluation was performed in an anechoic chamber. Each driver was placed in a holder to radiate approximately 3 meters from the test microphone. The driver was fixed and facing the microphone. The Hewlett-Packard HP-3314A function generator or HP-35665 dynamic signal analyzer provided the test signal to the driver via a Techron 5507 power supply

amplifier. The signal received by the microphone was input to the HP-35665 dynamic signal analyzer. The test was set up as shown below in Figure 14.

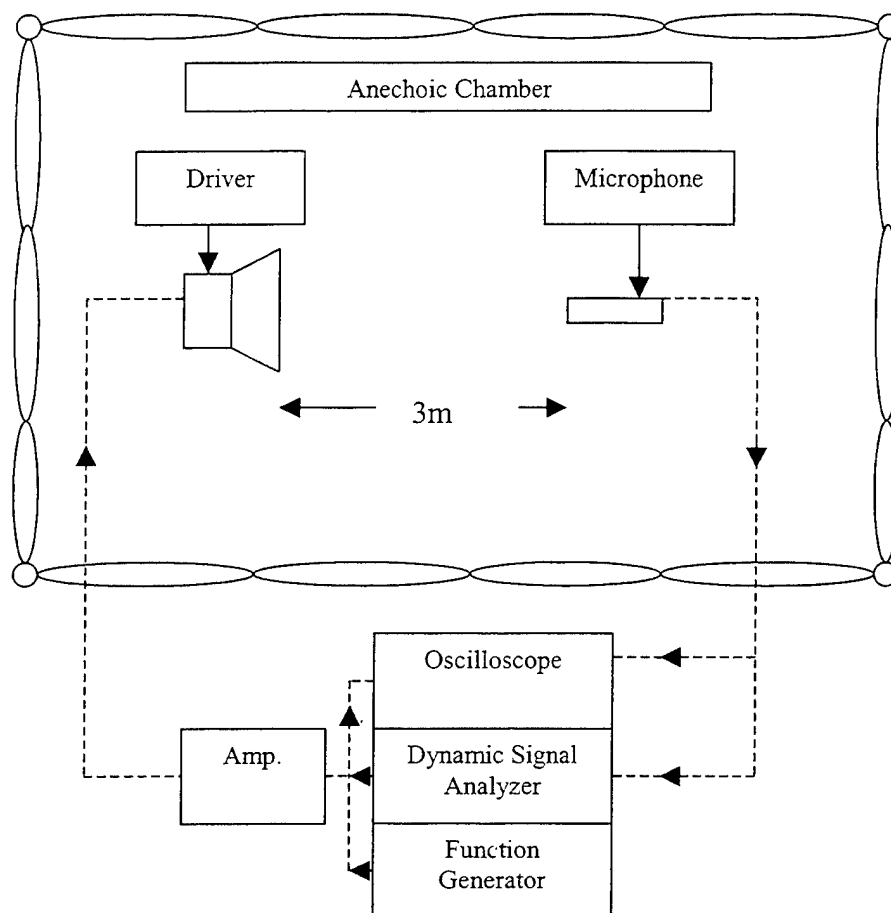


Figure 14. This is the set up for driver testing in the anechoic chamber.

First each driver was tested with a transient one-volt signal (a $\frac{1}{2}$ cycle of a 4 kHz cosine waveform) originating from the HP-3314A function generator and amplified via the Techron amplifier. The pulse was observed in the time domain on the HP-35665 dynamic signal analyzer. The display was immediately printed out and saved to a floppy disk by the HP-35665. Using the same signal, the time transient response and the narrow band frequency response magnitude spectrum were observed on the HP-

35665 (in the Fast Fourier Transform, FFT, mode) over a spectrum of 0 to 25.6 kHz. This display too, was immediately printed out and also saved electronically to a floppy disk.

Next each driver was tested with a swept sine signal provided by the HP-35665 dynamic signal analyzer via the Techron amplifier. The frequency response was monitored using the same analyzer over a spectrum from 50 Hz to 6 kHz. The display was plotted out on both a linear and logarithmic scale. Both displays were saved electronically to a floppy disk. During both procedures, the oscilloscope monitored both the input signal applied to the driver as well as the output signal measured by the microphone. This provided a very important back up indication to ensure the testing was conducted properly.

In summary, the following data were recorded for each driver: applied signal from the function generator to the driver, time-transient response received by the microphone (with dynamic signal analyzer in Fast Fourier Transform (FFT) mode), the time transient frequency response received by the microphone (over a range of 64 Hz to 25.6 kHz with dynamic signal analyzer in FFT mode), and the frequency response magnitude on both a linear and logarithmic scale (over a range of 50 Hz to 6.0 kHz with the dynamic signal analyzer in Swept Sine mode). These results were very closely compared to determine which driver had the most desirable properties. These results are presented next.

c. Driver Test Results

First, the response to the applied transient signal was compared for each driver. Each exhibited varying amounts of "ringing", which is an undesirable

characteristic of the output. Ideally the driver should generate a single pulse, with no ringing. Testing revealed that the Selenium DH200E titanium compression driver, shown below in Figure 15, exhibited the least amount of ringing of all units tested. Additionally the Selenium DH200E displayed acceptable frequency response characteristics over a band of frequencies that would be employed in the acoustic impedance measurement tube. The performance of the Selenium DH200E was weaker at the lower frequencies (below 500 Hz). Since frequencies greater than 4 kHz were not to be used during impedance measurements (due to the non-planar wave propagation discussed in II.B), results above this frequency were disregarded. The results of the Selenium DH200E testing are shown in Appendix C. The manufacturer specifications for the Selenium DH200E are included in Appendix D.

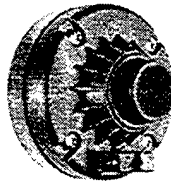


Figure 15. This is the Selenium DH200E driver.

It is important to note that although the Selenium driver exhibited the least amount of “ringing”. The University Sound 1828R reentrant driver exhibited slightly better output at the lower frequencies. As a result, the University Sound driver was also used in the later experiments. The measurement results using it will be compared to those of the Selenium driver in Chapter IV. The trade off here is better low frequency output for increased “ringing” by the driver. The results of the University Sound 1828R

testing are shown in Appendix E. The manufacturer specifications for the University Sound 1828R are included in Appendix F.

C. PROCEDURES

1. Computing Speed of Sound and "Absorption of the Day"

Essential to accurately measuring the acoustic impedance is a proper measurement of both the speed of sound and the absorption coefficient. The importance of the accurately knowing the speed of sound is evident in Equations 21a and 35 when relating the relative acoustic impedance to the boundary acoustic impedance. We measure the former, but are able to compute the latter with a good speed of sound measurement. The absorption is important in accurately determining the complex wave number as can be seen in Equations 20 and 42 shown earlier. Both of these parameters can vary depending on a number of factors.

Using the same settings described in below in C.3 for the HP-3314A function generator in the microphone calibration procedure, the speed of sound may be obtained as well as the absorption coefficient of the day. In this case the microphone calibration cup is replaced on the end of the acoustic impedance measurement tube with the blank rigid boundary assembly. Both microphones are installed in their normal position in the near center of the acoustic impedance measurement tube.

Data are collected using the SR-785, triggered externally from the HP-3314A function generator such that the direct and first reflected pulse are measured. The speed of sound, c , may be very easily measured using the relationship:

$$c = \frac{2 \times d}{\Delta t} \quad \text{(Equation 46)}$$

where " d " is the distance from the microphone to the reflection boundary, " t " is the time measured between the arrival of the direct and reflected pulses. The absorption coefficient may be obtained from measurement of the pressure amplitudes of the direct (P_{dir}) and reflected (P_{ref}) pulses using the following relationship:

$$e^{-2\alpha d} = \frac{P_{dir}}{P_{ref}} \quad \text{(Equation 47)}$$

By solving for " α ", the absorption coefficient may be readily obtained.

2. How the Samples Are Mounted

Prior to beginning the acoustic impedance measurement procedure, it is necessary to briefly introduce how the samples are mounted in the impedance tube. A 2- inch (5 cm) diameter sample of the material is cut from a bulk quantity. The sample is approximately 1.3 cm deep. This sample is inserted into a sample holder so its reflecting surface is flush with the flange of the holder. This holder is essentially an end piece with a void machined into it for insertion of the sample.

The sample holder is screwed into the end of the acoustic impedance measurement tube, opposite the driver assembly, using the retention ring. Figure 16 illustrates the microphones on the acoustic impedance measurement tube, aligned for sample measurement, just prior to the installation of the sample holder. The sample holder containing a ceiling tile sample is shown in the foreground, along with the retention ring.

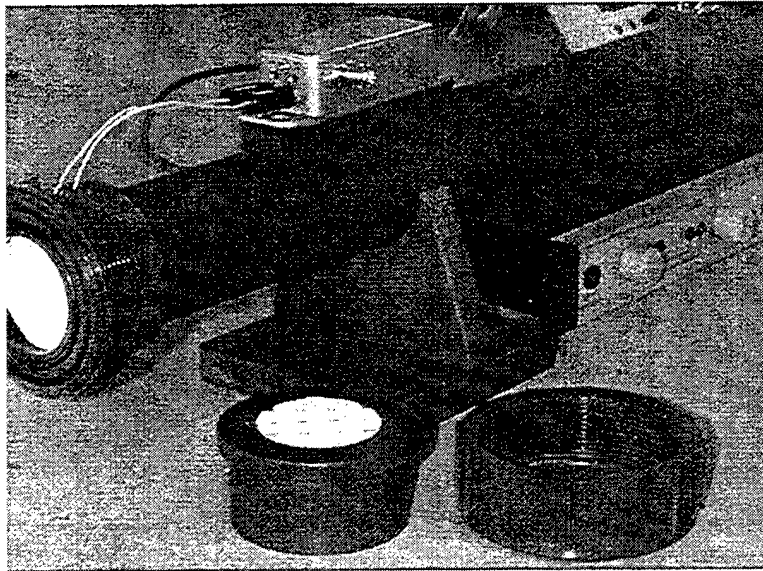


Figure 16. Microphones are installed in their sample measurement position. The end cup sample holder and the retention ring are featured in the foreground prior to installation.

3. Two-Microphone Continuous Excitation Acoustic Impedance Measurement

Having selected the essential components for the acoustic impedance tube, it is now time to present the procedures used in impedance measurement, starting with the two-microphone method. As mentioned earlier, the following components were used throughout the procedure: the acoustic impedance tube assembly (and its related components), an HP-467A amplifier (or a Techron 5507 amplifier), a voltmeter, a Stanford Research Systems Model SR-785 two-channel dynamic signal analyzer, and a Phillips PM-3384 oscilloscope. These components are assembled as shown below in Figure 17.

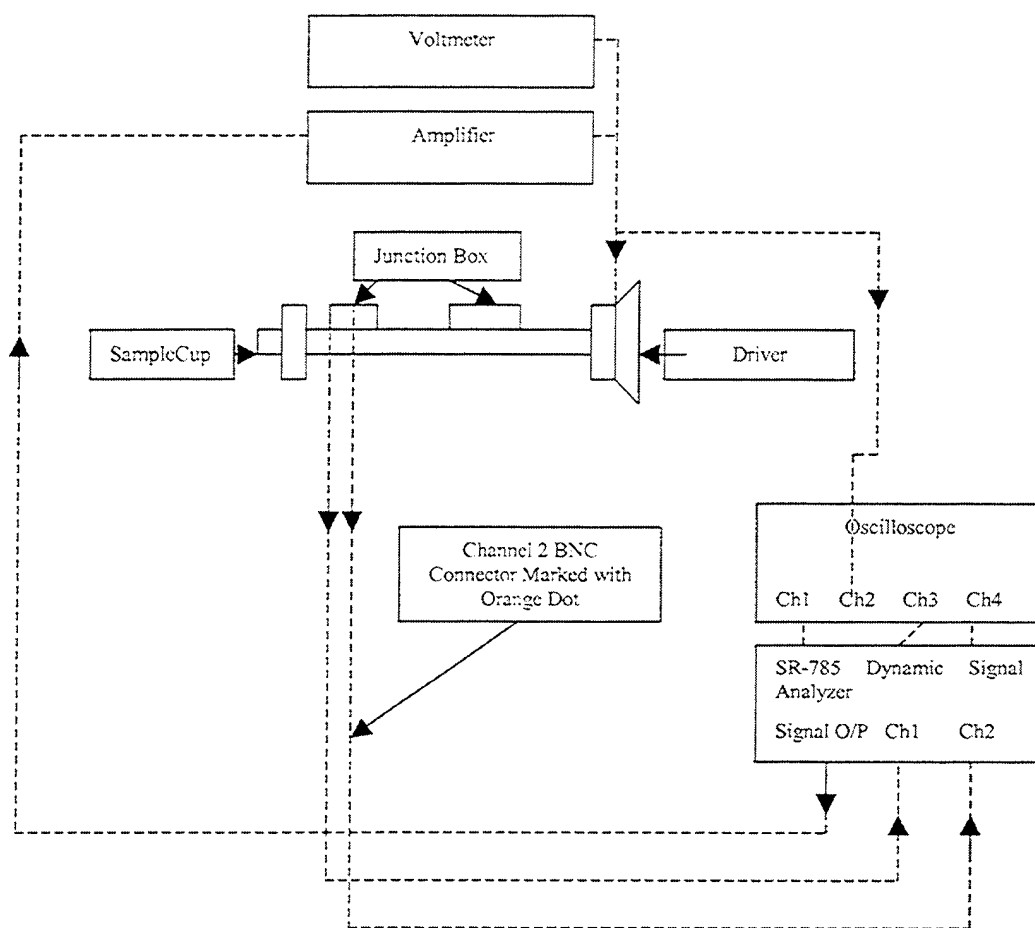


Figure 17. Acoustic impedance tube and associated equipment are set up in this configuration for an impedance measurement using the two-microphone continuous excitation method.

a. Microphone Calibration Procedure

In order to obtain an accurate acoustic impedance measurement, it is necessary to calibrate the microphones. (Actually only a relative calibration is required as explained further below.) There are several methods for doing this.

One method is to compare the Mouser Electronics 25LM045 to a calibrated reference microphone by using a transient signal. It could also be done using a

continuous signal. The first step of this procedure is to ensure that both microphones are installed in the specially designed microphone calibration cup. This cup is illustrated below in Figure 18. The normal microphone access used for impedance measurement (at the top end of the tube) will be covered with a blank cover. This enables both microphones to be nearly flush with the reflection boundary of the acoustic impedance tube so their responses may readily be compared.

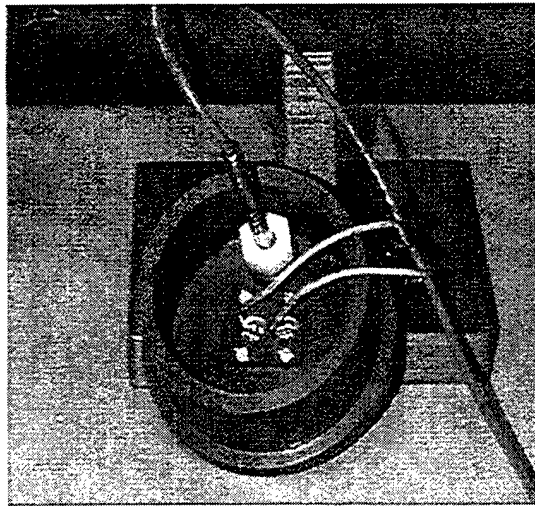


Figure 18. Microphone cup holder with test microphone inserted.

A Hewlett-Packard HP-3314A function generator and a power amplifier are used to provide the signal to the driver. The function generator is set to a one-half cycle "N" cycle burst mode, with the phase set to plus or minus 90 degrees, so the extrema of each half cycle are at the beginning and end of the burst. The HP-3314A frequency is nominally set to just below the first non-plane wave tube cutoff frequency (previously calculated to be approximately 4 kHz). The repetition rate is set at about 10 Hz to ensure incident and reflected pulses have adequately decayed prior to transmission of the next function generator pulse.

Data acquisition is achieved using the Stanford Research Systems SR-785 dynamic signal analyzer, which shall be referred to as the "SR-785". Data acquisition is triggered by the synchronous output of the HP-3314A. Triggering is set to coincide with the rising edge of the signal transmitted by the driver. (This is falling edge of the TTL trigger signal). Data acquisition is set to capture only the first arrival. It is important to note that, although this method can be used to calibrate each microphone prior to making a measurement, it is not actually needed nor used for the experimentation that followed. A simpler method is used that is discussed below. The technique mentioned above, however, may be used as an alternative.

The second method for calibrating the microphones is a much simpler approach that does not require a calibrated reference microphone. Essentially, an absolute calibration of each microphone is not needed. Only a reference calibration between the two microphones is needed. Recall, from Equations 15, 16, and 17, that ratios of microphone voltages are measured which are directly proportional to the acoustic pressures. These ratios are used in the acoustic impedance calculation as shown in Equations 18, 30, and 31. This technique is provided in the laboratory procedure illustrated in Appendix J. Instead of using a transient signal, a steady state, continuous, band-limited white noise signal is used. In this case the two microphones are placed at the end of the impedance tube in the specially designed microphone calibration cup previously described with the test microphone fitting blanked off. Figure 19 illustrates the microphones on the acoustic impedance measurement tube aligned in the calibration position. Instead of using the Hewlett-Packard HP-3314A function generator, a band-limited, white noise signal is generated by the SR-785 analyzer using the settings

downloaded electronically from the file "REIM.78S". As mentioned earlier, these settings are extensively provided for reference in Appendix G. It is very important to ensure drive signal is below 50 mV rms to avoid second harmonic distortion.

The response of each microphone should ideally be the same, but, due to manufacturing differences, there will be slightly varying phases and amplitudes over a broad frequency range. Using the averaging and automatic scaling features of the SR-785, the real and imaginary parts of the quotient of the microphone voltages are saved and downloaded as two separate ASCII files to a floppy disk. This quotient or ratio was discussed earlier in Chapter II as the frequency response ratios FR1 and FR2, (complex constants).

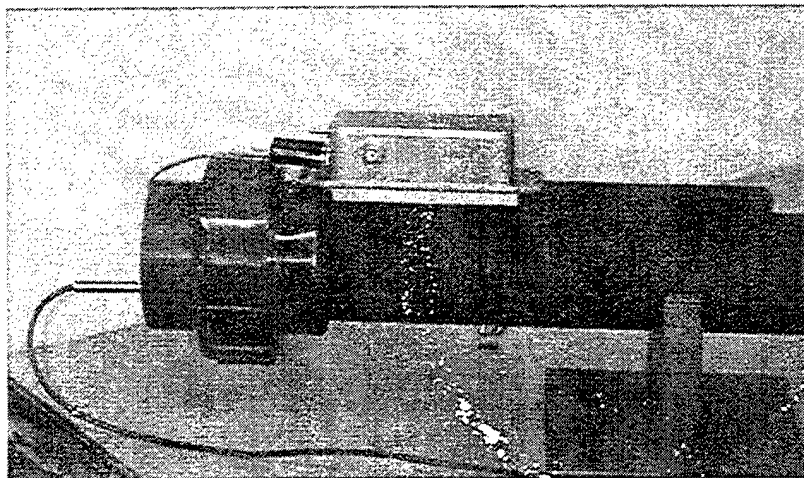


Figure 19. Microphones are aligned for calibration. Notice junction box has been advanced to support this alignment.

b. Sample Data Taking Procedure

Having saved the calibration data as describe in part a, the calibration cup is removed from the end of the tube. One can now measure as many samples as desired

without having to repeat the calibration between samples. (It is recommended that a calibration be performed at the beginning of each lab session.)

The two-microphone holder is unscrewed from the calibration cup. The microphones and junction box are repositioned to their normal measurement position. The microphone plate is bolted into the opening where the blank had previously been installed during the calibration procedure. The end of the acoustic impedance tube assembly should now look like Figure 20 shown below.

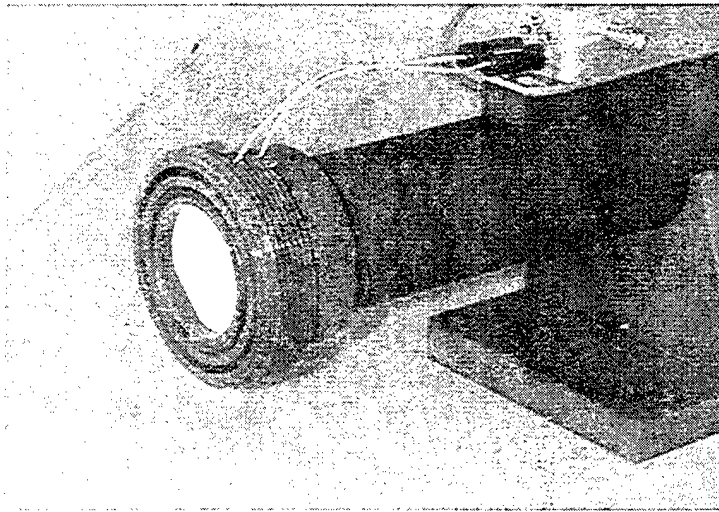


Figure 20. Microphones and junction box are returned to their normal sample measurement position. The sample cup and retention ring are removed.

Now the sample cup (containing a sample) is fastened to the end of the impedance tube. Again, the same band-limited, white noise signal is generated by the SR-785 analyzer (via the amplifier and driver) using the settings downloaded electronically from the file "REIM.78S". Using the averaging and automatic scaling features of the SR-785, the real and imaginary parts of the quotient of the microphone voltages are saved and downloaded as two separate ASCII files to a floppy disk just as in

the calibration procedure. This quotient or ratio was discussed earlier in Chapter II as the frequency response ratios FR1 and FR2, (complex constants).

The simple steps described above may be repeated for as many samples as desired and even an "open tube" measurement (where the sample cup is removed and the tube is left open to the atmosphere). The final step is to take the series of ratios saved to the disk under several files and use the previously mentioned MATLAB programs to compute and graphically plot the real and imaginary parts of the acoustic impedances. This is discussed next.

c. Processing the Sample Data Using MATLAB

As mentioned earlier, three MATLAB programs were developed to compute the acoustic impedance using the two-microphone continuous excitation technique. The programs function identically except that each uses a different equation for determining the acoustic impedance. The "Impedance.4" program computes the acoustic impedance using the Basic Equation (Equation 18). The "Impedance.5" and "Impedance.6" programs use the Low Frequency Equation (shown as both Equations 31 and 35) and the Exact Equation (Equation 30), respectively. A brief illustration of how these programs work is now provided, using the "Impedance.6" program as an example, where the Selenium DH200E driver is used with a speckled ceiling tile sample.

The program initially requests the user to input the file containing the real part of the microphone "calibration" data, that is the data from the real part of the microphone (that will be at position x_2 during the sample measurement) voltage divided by microphone (that will be at position x_1 during the sample measurement) voltage, when microphones are aligned in the calibration position. It reproduces the SR-785 trace as the

MATLAB plot shown in Figure 21. The program next requests the user input the file containing the imaginary part of the same ratio of the microphone voltages described above, when aligned in the calibration position. It reproduces the SR-785 trace as the MATLAB plot shown in Figure 22. After each plot, the user is asked to confirm that the plot matches what was viewed on the SR-785 during data gathering.

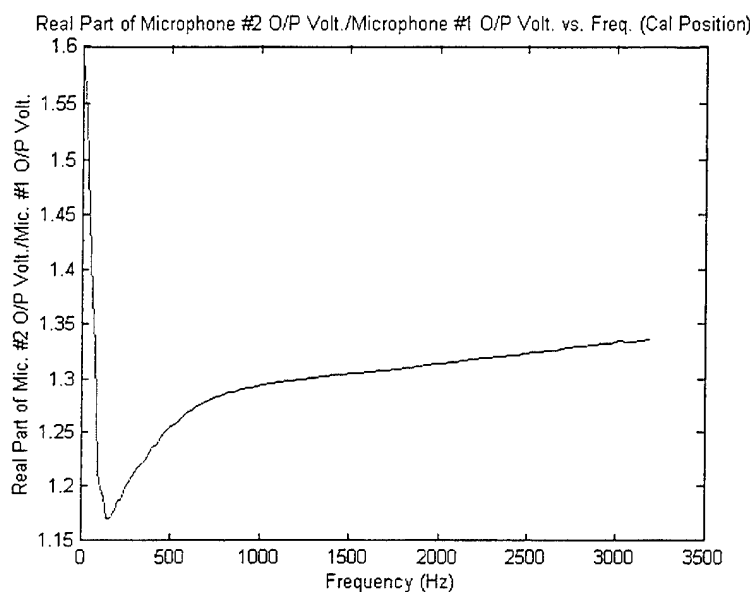


Figure 21. Real part of ratio of the microphone's output voltages is shown where microphones are in the calibration position.

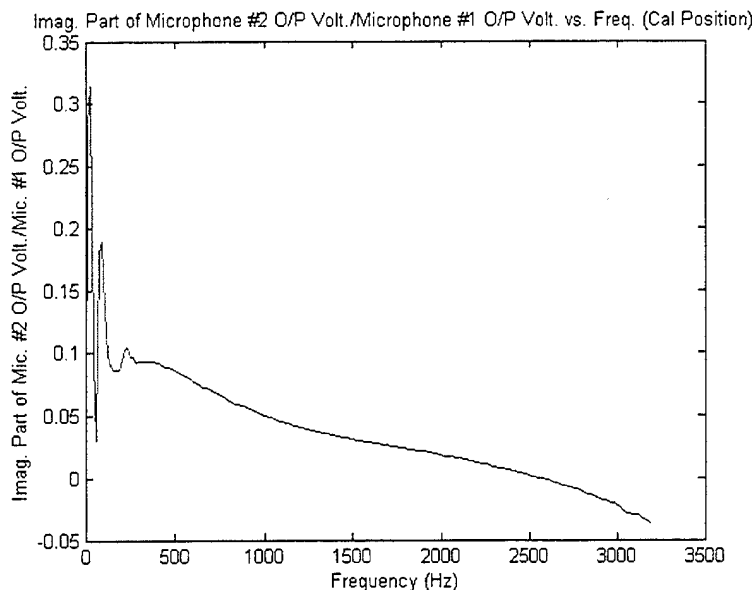


Figure 22. Imaginary part of ratio of the microphone's output voltages is shown where microphones are in the calibration position.

At this point the program requests the user to input the file containing the data from the real part of the microphone at position x_2 voltage divided by microphone at position x_1 when microphones are aligned in their normal position at the end of the tube with a sample installed. It reproduces the SR-785 trace as a MATLAB plot shown in Figure 23. The program next requests the user input the file containing the data from the imaginary part of the microphone at position x_2 voltage divided by microphone at position x_1 when microphones are aligned in their normal position. It reproduces the SR-785 trace as the MATLAB plot shown in Figure 24. After each plot the user is again asked to confirm the plot matches what was viewed on the SR-785 during testing.

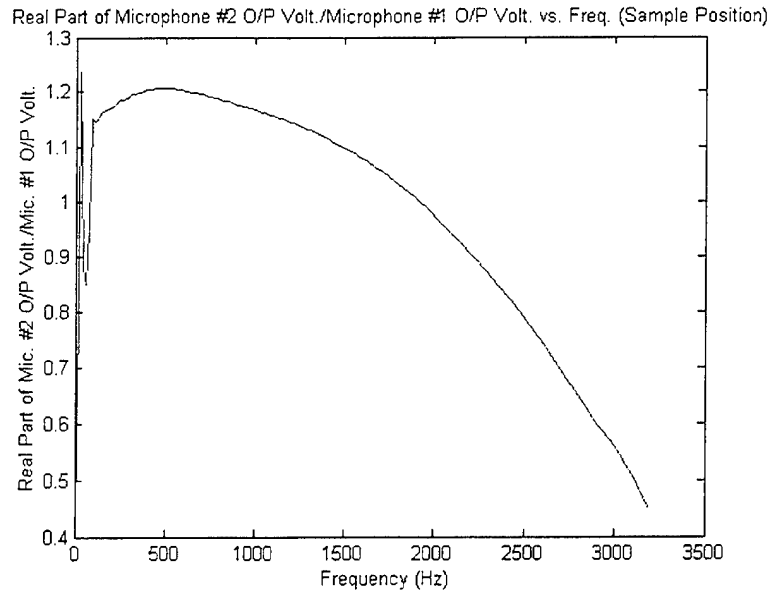


Figure 23. Real part of ratio of the microphone's output voltages is shown where microphones are in their normal position at top end of tube with sample installed.

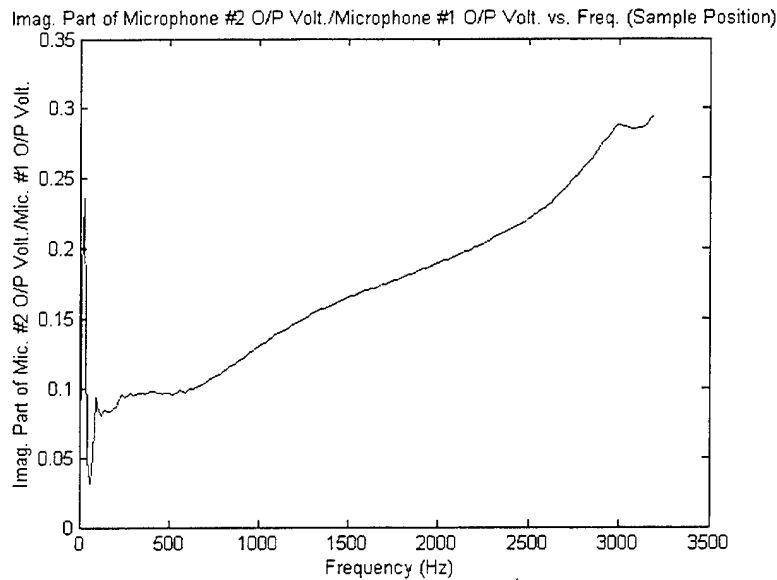


Figure 24. Imaginary part of ratio of the microphone's output voltages is shown where microphones are in their normal position at top end of tube with sample installed.

At this point all the required data has been entered, so the program requests the user input the name of the sample used. When this step is complete, it

rapidly calculates the normalized acoustic impedances using the Exact Equation, and provides four graphs. The first two graphs are of the real and imaginary parts of the acoustic impedance over a frequency range from 0 to 3.2 kHz, shown in Figures 25 and 26. The final two graphs are plots of the real and imaginary parts of the acoustic impedance, plotted on one graph and of the real versus imaginary parts of the acoustic impedance. These are shown in Figures 27 and 28, respectively.

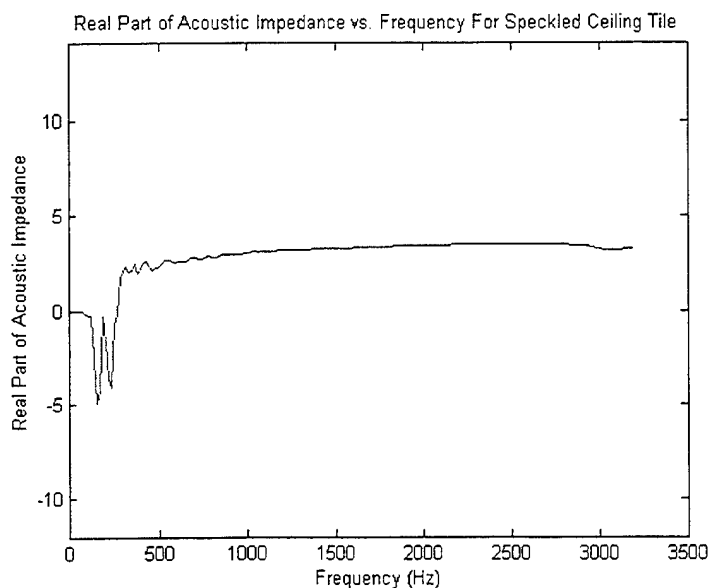


Figure 25. Real part of the acoustic impedance is plotted against the frequency for the speckled ceiling tile sample.

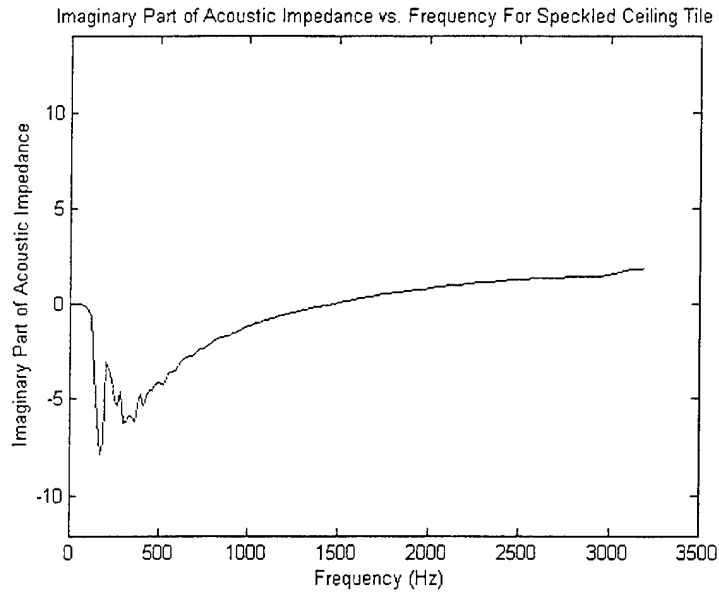


Figure 26. Imaginary part of the acoustic impedance is plotted against the frequency for the speckled ceiling tile sample.

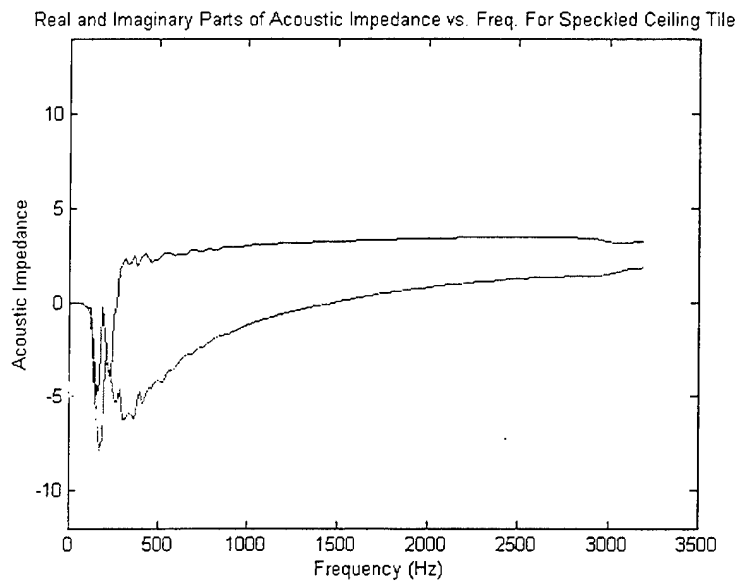


Figure 27. Real and imaginary parts of the acoustic impedance are plotted against the frequency for the speckled ceiling tile sample.

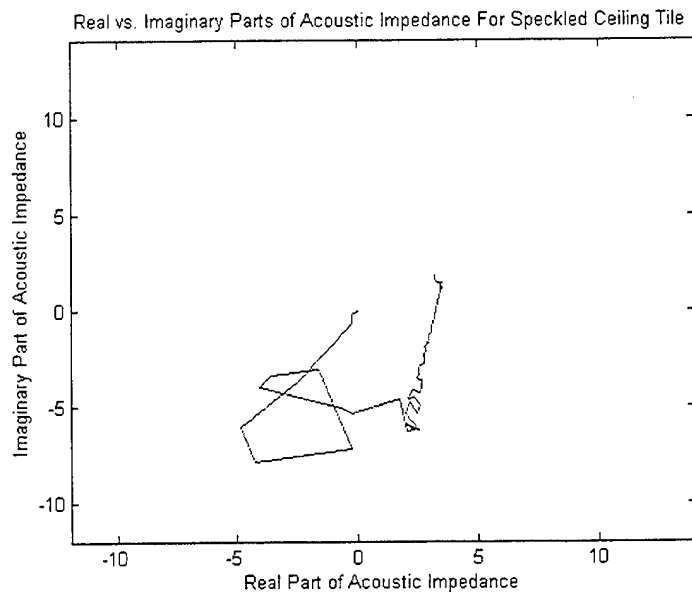


Figure 28. Real versus imaginary parts of the acoustic impedance is plotted for the speckled ceiling tile sample.

4. One-Microphone Transient Acoustic Impedance Measurement

Having selected the essential components for the acoustic impedance tube, it is now time to present the procedures used in impedance measurement with the one microphone transient method. This procedure is provided for reference in Appendix J. As mentioned earlier, the following components were used throughout the procedure: the acoustic impedance tube assembly (and its related components), the HP-3314A function generator, an HP-467A amplifier (or a Techron 5507 amplifier), a voltmeter, a Stanford Research Systems Model SR-785 two-channel dynamic signal analyzer, and a Phillips PM-3384 oscilloscope. These components are assembled as shown below in Figure 29.

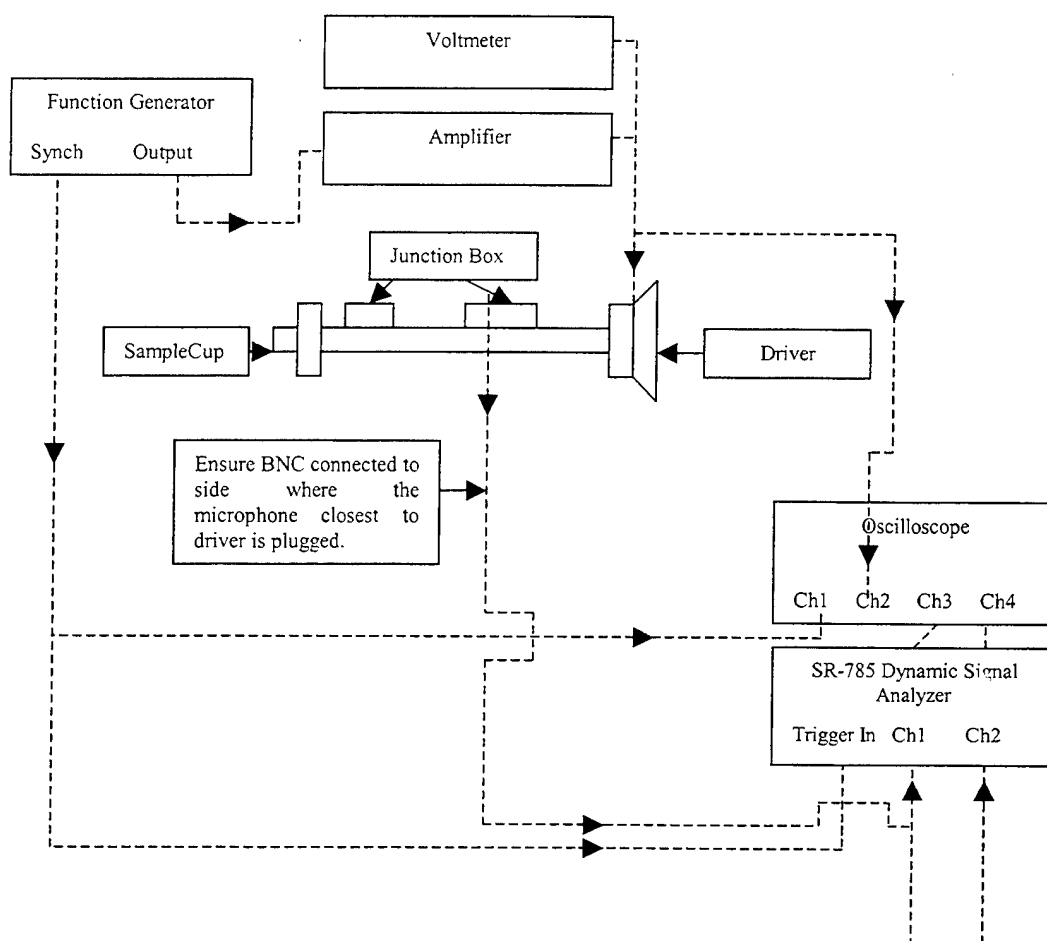


Figure 29. Acoustic impedance tube and associated equipment are set up in this configuration for an impedance measurement using the one microphone transient method.

a. Absorption Compensation Procedure

Only one microphone is used (one of the two microphones permanently installed in the middle of the tube is selected). This microphone is in the x_3 position illustrated in Figure 5 back in Chapter II. The same microphone measures both the incident and reflected pulse; therefore a calibration is not required. However, a correction, or compensation, must be made for the absorption that will reduce the amplitude of the reflected pulse. Recall from Chapter II.D.1, that the reflection coefficient is determined by Equation 45. By comparing the ratio of incident and

reflected pulse signals for a rigid wall boundary against that for any other sample material boundary, the effect of absorption is cancelled.

First a rigid boundary is installed at the end of the impedance tube as shown in Figure 30.

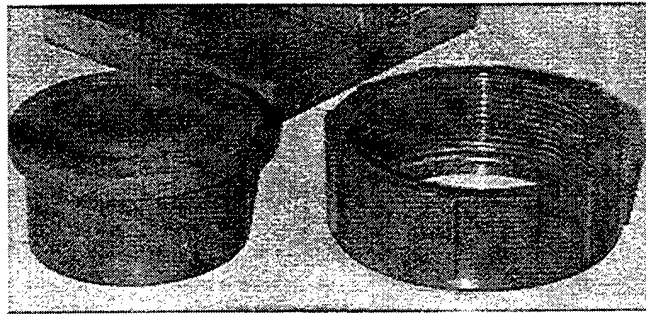


Figure 30. Rigid impedance tube boundary is shown with its retention ring.

The following parameters are set in the function generator to produce a half cycle burst pulse with $N=1$ cycle: 1 volt amplitude; 4000 Hz carrier frequency; 0 volts offset; 50% symmetry; negative 90 degrees phase; and $N=1$ cycle. The function generator provides a pulsed signal, shown in Figure 31, in the impedance tube.

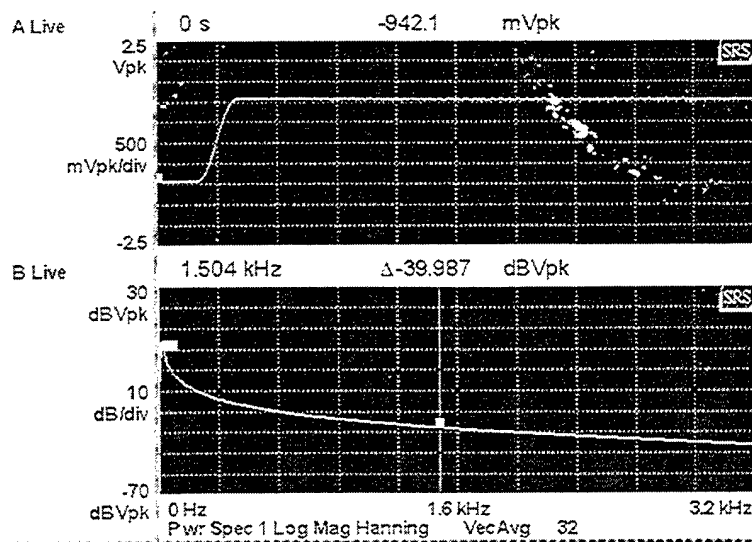


Figure 31. Above is pulsed transient signal and below is its frequency spectrum.

The measured signal from the microphone is monitored on the SR-785 dynamic signal analyzer and the oscilloscope as a back up indication. To set up the SR-785 for proper operation, settings are downloaded from a floppy disk file named "REFLWTIM.78S". These settings are included for reference in Appendix G. This provides the ability to apply a rectangular window of adjustable width over any portion of a force window time record. This is displayed in Figure 32. With this capability, we are able to shift and isolate an incident pulse and its associated reflected pulse on channels one and two, respectively, and make Fast Fourier Transform (FFT) frequency response measurements.

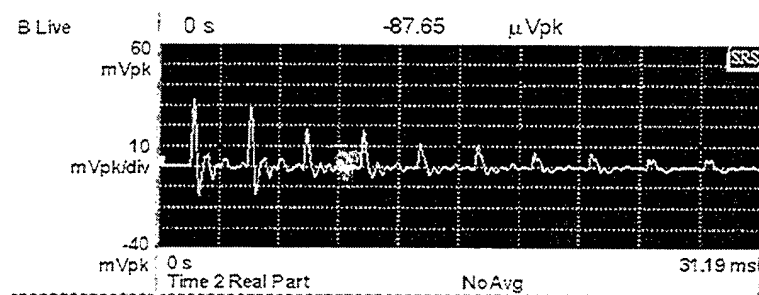


Figure 32. This is the window display on the SR-785 showing incident and reflected pulses over time.

When this is completed, the SR-785 "measurement option" parameter is changed from time transient to frequency response. The "REFLWTIM.78S" settings enable the ratio of the voltage of the reflected pulse to that of the incident pulse to be measured by the dynamic signal analyzer. In fact this is the very ratio that appears on the denominator of Equation 45, the Reflectivity Equation. The real and imaginary parts of this ratio are saved over the frequency spectrum from 0 to 3.2 kHz on a floppy disk in separate ASCII files. The absorption compensation measurements for the one-microphone transient excitation method are now complete.

b. Sample Data Taking Procedure

With the compensation complete, the user is free to measure as many samples as desired in rapid succession. This is accomplished by removing the rigid boundary from the end of the tube and installing a cup containing a sample. When the sample is installed, the user does not have to change any settings. In fact, it is important that the time delays employed during the compensation measurements remain unchanged for the sample measurements. Otherwise, a phase error will be introduced, and possibly a magnitude error, as well. The ratio that is now being measured by the SR-785 is again the ratio of the voltage of the reflected pulse to that of the incident pulse, but the sample is installed. This is the ratio that appears as the numerator in the Reflectivity Equation. The real and imaginary parts of this ratio are saved over the frequency spectrum from 0 to 3.2 kHz on a floppy disk in separate ASCII files.

The simple steps described above may be repeated for as many samples as desired and even an "open tube" measurement (where the sample cup is removed and the tube is left open to the atmosphere). The final step is to take the series of ratios saved to the disk under several files and use the previously mentioned MATLAB program to compute and graphically plot the real and imaginary parts of the acoustic reflectivity. This program also computes the acoustic impedance from the reflectivity value. This is discussed next.

c. Processing the Sample Data Using MATLAB

As mentioned earlier, a MATLAB program was developed to compute the reflectivity and acoustic impedance using the one-microphone transient excitation technique. The program functions similarly to the three previously discussed except that

it uses a different equation for determining the acoustic impedance. As mentioned earlier, it uses Equation 45, the Reflectivity Equation, to calculate the reflectivity of the sample over a frequency spectrum of 0 to 3.2 kHz. Additionally the program uses this value in Equation 22 to calculate the normalized acoustic impedance. A brief illustration of how the Reflectivity program works is now provided using the Selenium DH200E driver with a speckled ceiling tile sample.

The program initially requests the user to input the file containing the data from the real part of the microphone measurement of the ratio of the reflected pulse voltage over the incident pulse voltage when the rigid boundary is installed. It reproduces the SR-785 trace as a MATLAB plot shown in Figure 33. The program next requests the user input the file containing the data from the imaginary part of the same ratio of the microphone voltages described above when rigid boundary is installed. It reproduces the SR-785 trace as the MATLAB plot shown in Figure 34. After each plot the user is asked to confirm the plot matches what was viewed on the SR-785 during testing.

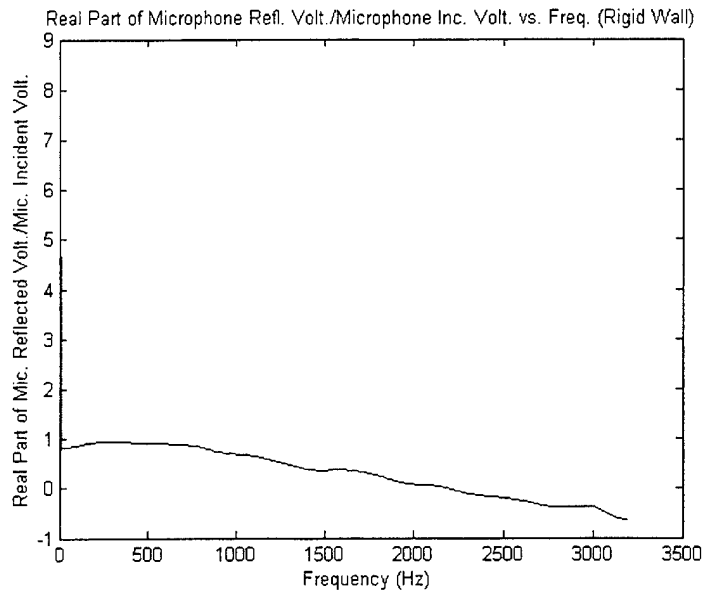


Figure 33. Real part of microphone reflected voltage over incident voltage with rigid boundary installed.

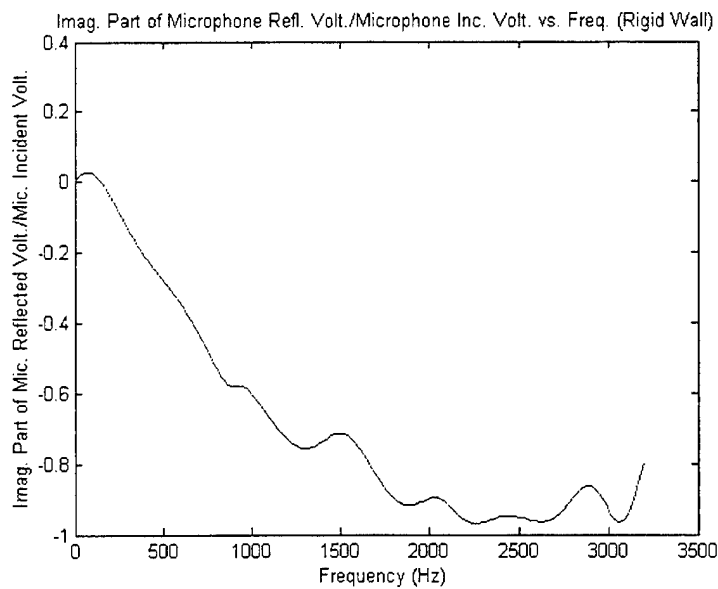


Figure 34. Imaginary part of microphone reflected voltage over incident voltage with rigid boundary installed.

The program next requests the user to input the file containing the data from the real part of the microphone measurement of the ratio of reflected pulse voltage over the incident pulse voltage when a sample is installed at the end of the tube. It reproduces the SR-785 trace as the MATLAB plot shown in Figure 35. Following this the user must input the file containing the imaginary part of the microphone measurement of the ratio of reflected pulse voltage over the incident pulse voltage when a sample is installed at the end of the tube. It reproduces the SR-785 trace as the MATLAB plot shown in Figure 36. After each plot the user is again asked to confirm the plot matches what was viewed on the SR-785 during testing.

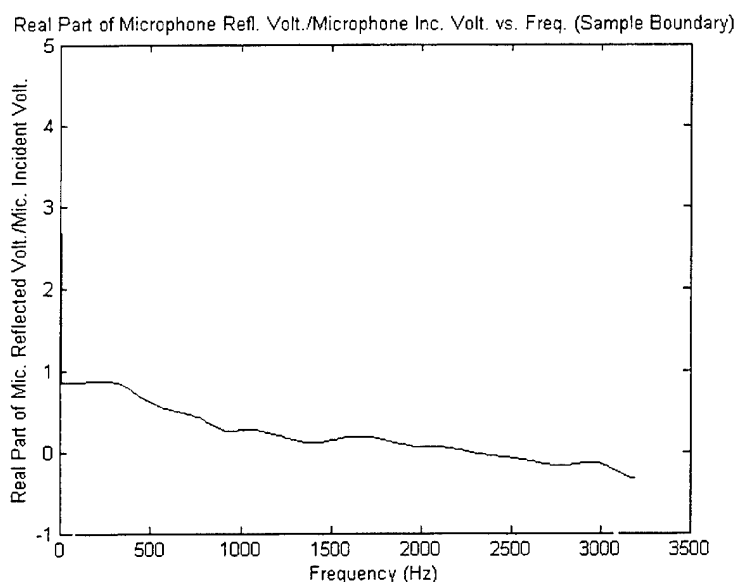


Figure 35. Real part of microphone reflected voltage over incident voltage with sample boundary installed.

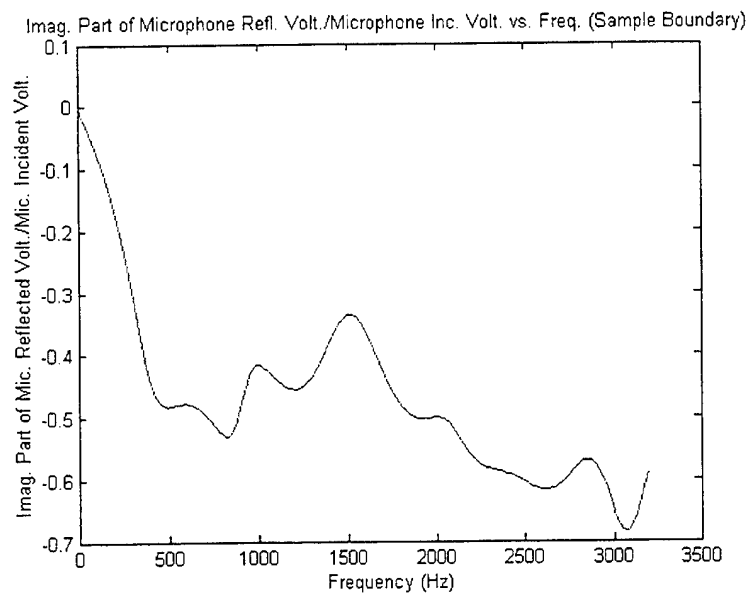


Figure 36. Imaginary part of microphone reflected voltage over incident voltage with sample boundary installed.

At this point all the required data has been entered so the program requests the user input the name of the sample used. When this step is complete, it rapidly calculates the reflectivity using the Reflectivity Equation and from this the acoustic impedance using Equation 22. It provides a total of eight graphs. The first two graphs are of the real and imaginary parts of the reflectivity over a frequency spectrum from 0 to 3.2 kHz shown in Figures 37 and 38. The next two graphs are plots of the real and imaginary parts of the reflectivity together and of the real versus imaginary parts of the reflectivity (not shown). The program then plots the real and imaginary parts of the acoustic impedance over a frequency spectrum from 0 to 3.2 kHz shown in Figures 39 and 40. The last two graphs are plots of the real and imaginary parts of the acoustic impedance together and of the real versus imaginary parts of the acoustic impedance. These are not shown.

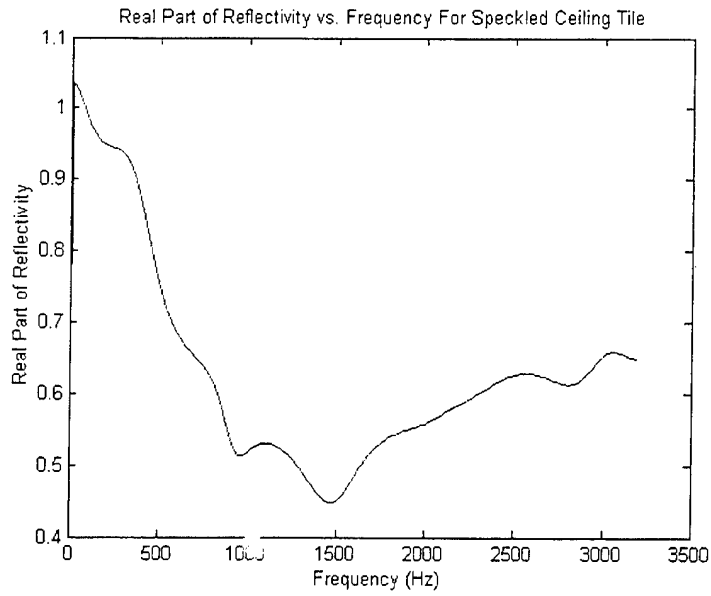


Figure 37. Real part of the reflectivity versus the frequency is shown for a speckled ceiling tile.

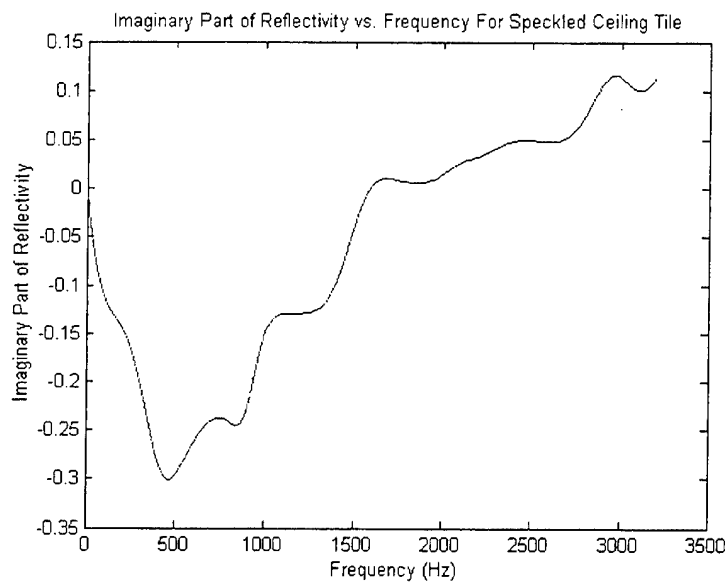


Figure 38. Imaginary part of the reflectivity versus the frequency is shown for a speckled ceiling tile.

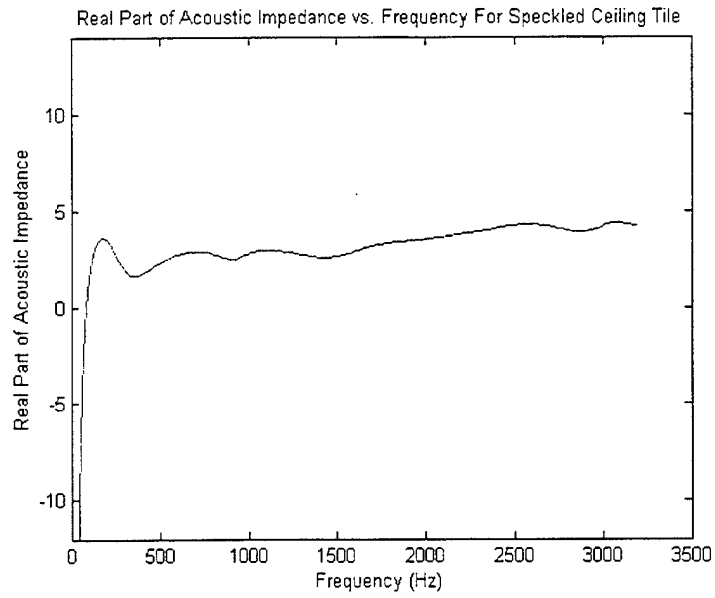


Figure 39. Real part of the acoustic impedance versus the frequency is shown for a speckled ceiling tile.

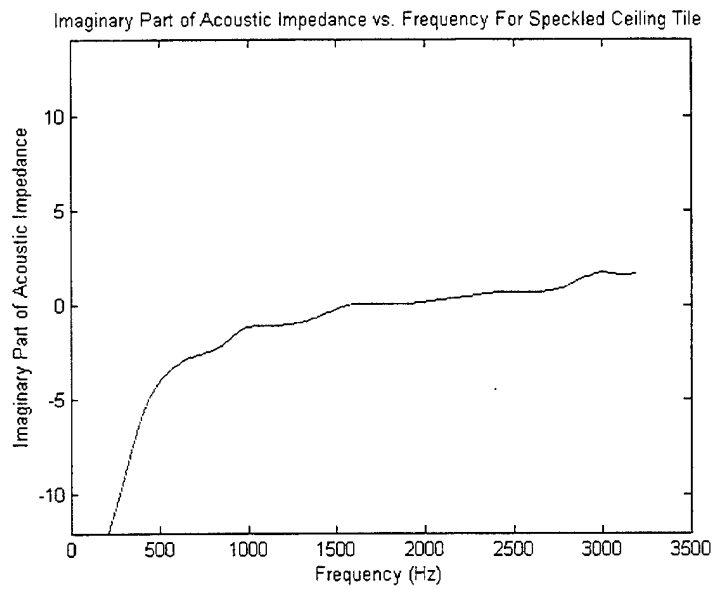


Figure 40. Imaginary part of the acoustic impedance versus the frequency is shown for a speckled ceiling tile.

THIS PAGE INTENTIONALLY LEFT BLANK

IV. EXPERIMENTAL RESULTS

A. TEST CASE: THE OPEN TUBE

1. Expected Open Tube Results Based On Theory

Before presenting the experimental results, it is necessary to briefly touch on open tube theory. This is very important because it provides a theoretical value for acoustic impedance with which the measurement techniques previously described may be compared. No such theory exists for the sample materials that will be subsequently measured.

The impedance of an open pipe is approximated by an equivalent impedance circuit. This circuit consists of a real impedance $\rho_0 c$ (the density of air times the speed of sound in air) in parallel with an imaginary impedance $j\omega\rho_0 l_{eff}$ (the density of air times an effective length). (Reference 1) The circuit is shown in Figure 41.

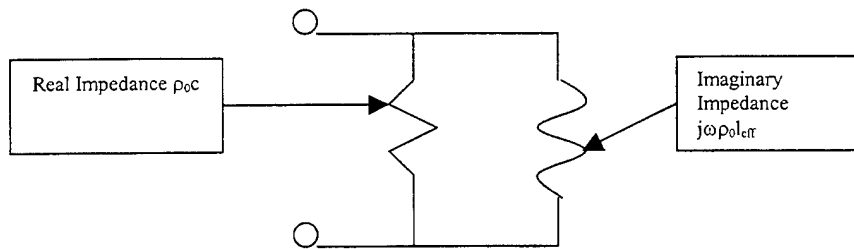


Figure 41. Open pipe impedance circuit is presented above.

The effective length is a property of the pipe diameter and flange end condition. From Reference 1, chapter 10, the value for an un-flanged open pipe is 0.6 times the radius of the pipe, while the value for a flanged open pipe is 0.85 times the radius of the pipe. The acoustic impedance measurement tube's effective radius lies somewhere

between these two values, but it is possibly closer to the flanged open pipe. By referring to Figure 20, one can clearly see a substantial difference between the inner and outer radius at the end of the impedance tube when it is open. The inner radius measures 5 cm while the outer radius measures 9 cm, making it very nearly a flanged open pipe.

The normalized specific acoustic impedance for an open pipe is shown in Equation 48:

$$\frac{\tilde{z}}{\rho_0 c} = \frac{j\omega l_{eff}}{c + j\omega l_{eff}} = \frac{j\omega l_{eff}/c}{1 + j\omega l_{eff}/c} = \frac{jkl_{eff}}{1 + jkl_{eff}} \quad (\text{Equation 48})$$

This theoretical value for the acoustic impedance of an open tube will now be compared with the measured results.

2. Open Tube Experimental Results

Having conducted the acoustic impedance measurement experiment in accordance with the documented procedure set forth in Appendix J (using a 50 mV rms signal as prescribed), the first results presented are those obtained using the Selenium DH200E driver with the impedance tube open at the end. This is one of the most important measurements made, since it is the only one where the actual acoustic impedance measurements may be compared with a theoretical value. Figures 42 and 43 illustrate the real and imaginary parts of the acoustic impedance measured for an open tube. Plotted are curves computed using: the approximation delineated by Equations 31 and 35 (Low Frequency Approximation Equation), the exact formula from Equation 30 (Exact Equation), and, lastly, the method using the measured reflectivity from Equations 45 (Reflectivity Equation) and 22.

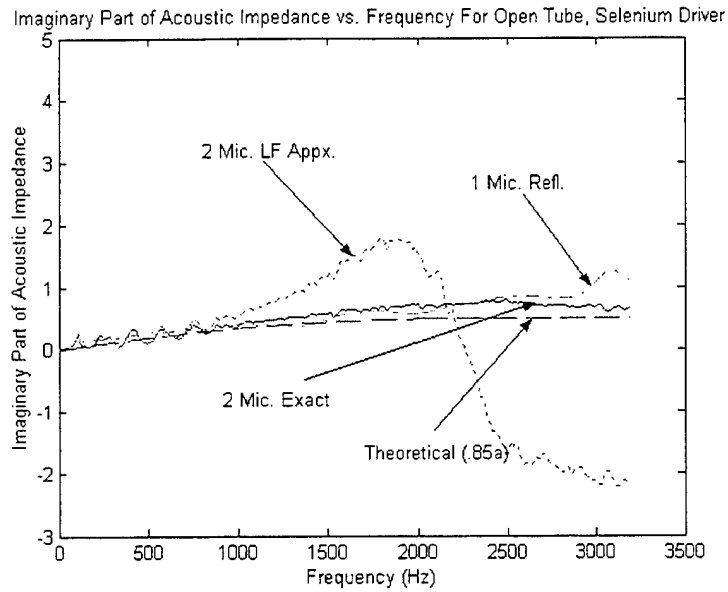


Figure 42. Real part of acoustic impedance versus frequency for an open tube using a Selenium driver.

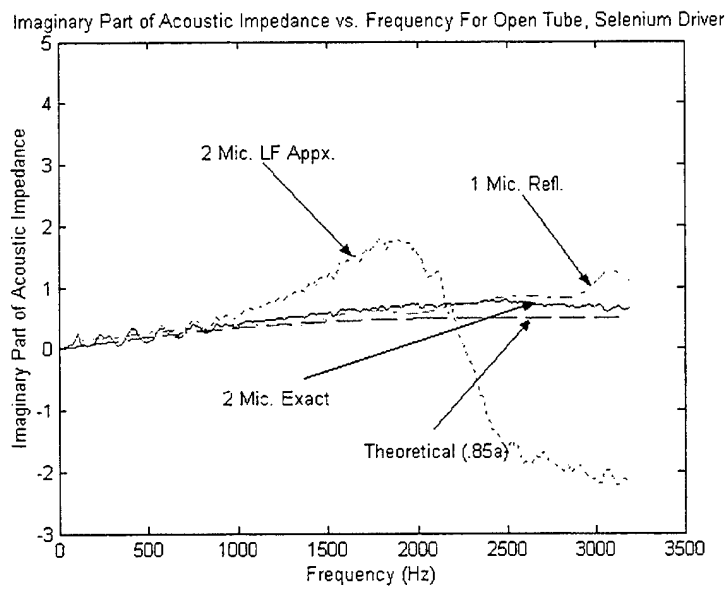


Figure 43. Imaginary part of acoustic impedance versus frequency for an open tube using a Selenium driver.

As one can note from the above two figures, the comparisons are highly favorable between measured impedance and theoretical values for all but the two-microphone, low frequency approximation results. This is consistent with our expectations, as the low frequency approximation is valid only for small values of kx , and the value of kx_2 equals one for a frequency of 2.1 kHz. Another important thing to note is the close agreement between the one microphone transient excitation method (using the measured reflectivity) with the two-microphone "exact" technique. A trend that will be increasingly apparent throughout the analysis (and those subsequent) is that the performance of the one microphone technique degrades at very high and very low frequencies. Typically, at the higher frequencies (usually above 2.5 kHz), the real and imaginary parts of the acoustic impedance start to oscillate about the "exact" value.

Presented for comparison are open tube acoustic impedance measurements made exactly as described above except that a University Sound driver is used in lieu of the Selenium driver. The results are shown in Figures 44 and 45.

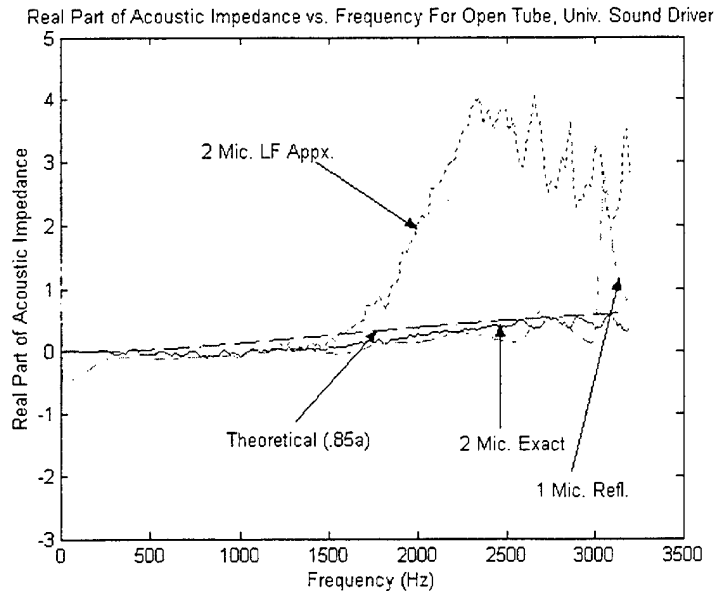


Figure 44. Real part of acoustic impedance versus frequency for an open tube using a University Sound driver.

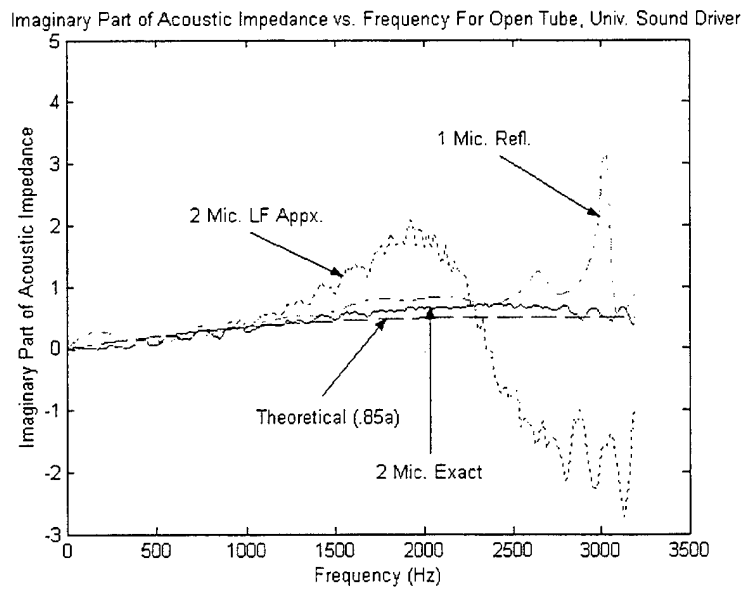


Figure 45. Imaginary part of acoustic impedance versus frequency for open tube using a University Sound driver.

Notice, again, that the two-microphone, exact results compare very favorably with the theoretical open tube results. As noted before, the two-microphone low frequency approximation is very crude and virtually not usable at frequencies above 1000 Hz. The one microphone method degrades considerably above 2.5 kHz.

Overall, in comparing the Selenium driver with the University Sound driver, it is clear from the above figures, that the Selenium driver yields significantly better results at the higher frequencies (for example those above 2.0 kHz). The University Sound driver yields very slightly better results at the lower frequencies (in this case those below 600 Hz). In summary, the trend to note is that the Selenium driver yields better overall results than the University Sound driver. This is a trend that will continue throughout the analyses when material samples are inserted at the end of the tube.

B. RESULTS USING SAMPLE MATERIALS

After noting highly encouraging results from the open tube impedance measurements, three sample materials were installed at the end of the tube: a speckled ceiling tile sample, an insulation material sample, and a ceiling tile sample with perforated holes. These sample materials are pictured below in Figure 46. The following results are presented.

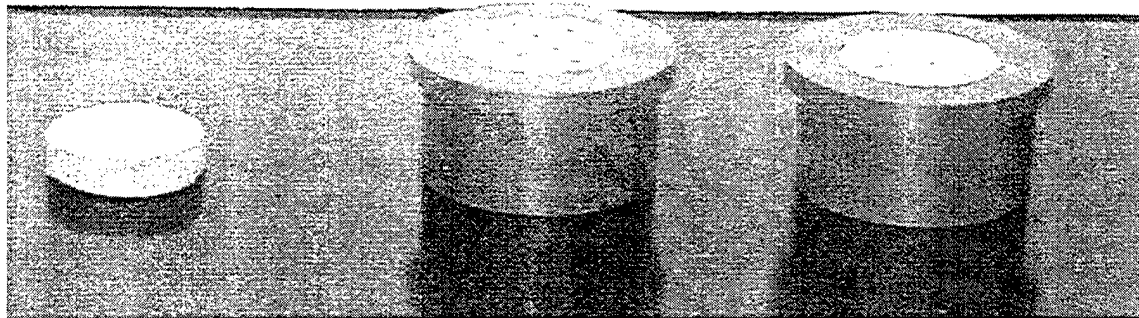


Figure 46. Shown from left to right are the three samples measured: an insulation sample, a ceiling tile sample with perforated holes (in sample cup), and a speckled ceiling tile sample (in sample cup).

1. Speckled Ceiling Tile Sample

After noting highly encouraging results from the open tube impedance measurements, a speckled ceiling tile sample was placed in the cup holder at the end of the tube. Once again, the procedures documented in Appendix J were followed to obtain the acoustic impedance measurements with a 50 mV drive signal used. These results are presented using the two-microphone exact and approximation methods and the one-microphone measurement derived from the reflectivity described earlier. The results are plotted together in Figures 47 and 48 for comparison.

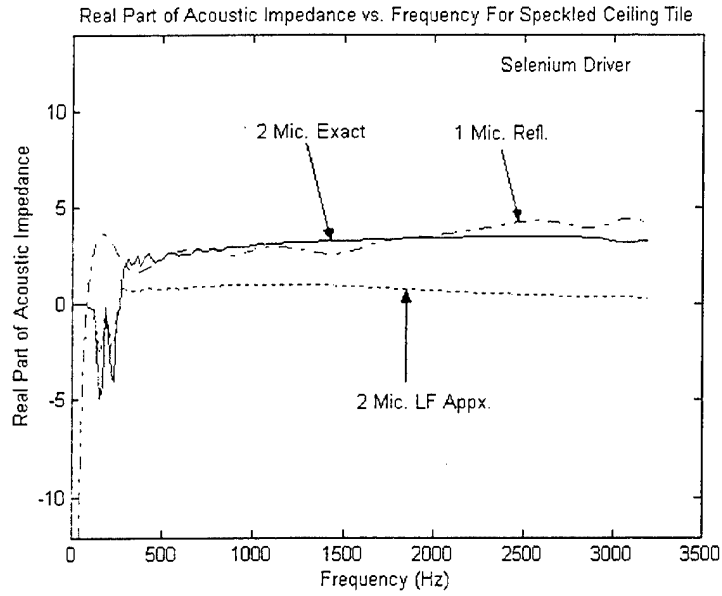


Figure 47. Real part of acoustic impedance versus frequency for a speckled ceiling tile sample using the Selenium driver.

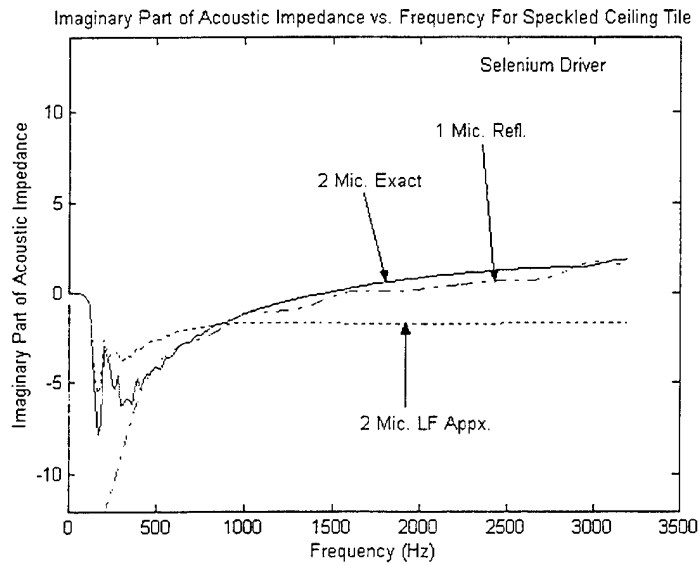


Figure 48. Imaginary part of acoustic impedance versus frequency for a speckled ceiling tile sample using the Selenium driver.

Interestingly, the normalized results shown above are significantly different from those obtained for the open tube. The approximate formulas from Equations 31 or 35 are consistent with the exact measurement up to about 300 Hz before there is significant digression. This is to be expected, and occurs consistently throughout the analyses. The one-microphone measurement tracks very well with the two-microphone exact measurement at frequencies above 1000 Hz for the imaginary part of the acoustic impedance (and above 500 Hz for the real part). Lastly the one-microphone measurement results are poor below 500 Hz, and can't be used for a valid comparison. In fact, significant problems are evident in the one and two-microphone measurements below 300 Hz, in that negative values for the real part of the impedance are shown. Negative real impedance values are physically impossible for a passive material. The one-microphone technique also exhibits slight oscillation at the very highest frequencies used (over 2.8 kHz for example).

2. Insulation Sample

The next results provided for analysis are those obtained using an insulation type of material that is very similar to the speckled ceiling tile discussed in part B. Not surprisingly, the results and trends are very similar as well. Again, a 50 mV drive signal is applied to avoid second harmonic distortion of the microphone. The results presented are those using the Selenium driver. Again the two-microphone, continuous exact (Equation 30) and low frequency approximation (Equations 31 or 35) methods, as well as the one-microphone, transient measurement (Equations 45 and 22), are plotted together to enable comparison.

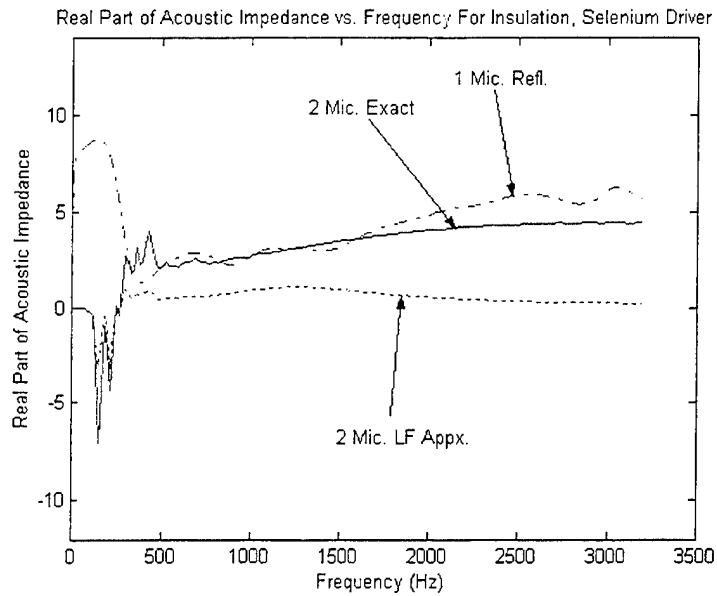


Figure 49. Real part of acoustic impedance versus frequency for an insulation sample using the Selenium driver.

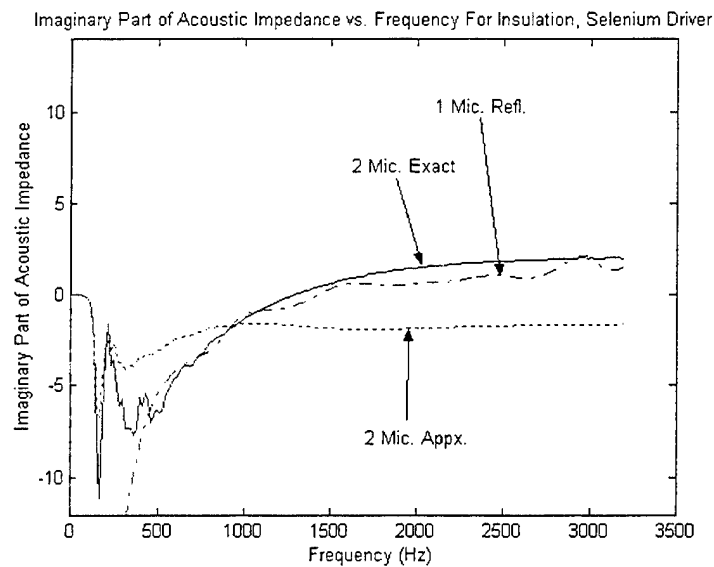


Figure 50. Imaginary part of acoustic impedance versus frequency for an insulation sample using the Selenium driver.

Since the insulation material is similar to that of the speckled ceiling tile analyzed in part B, the trends exhibited during the impedance measurements are similar as well. The agreement between the one-microphone method and two-microphone methods is almost as good as it was in the case of the speckled ceiling tile sample. The one-microphone method exhibits slightly more oscillation at frequencies greater than 2.8 kHz than it did for the speckled ceiling tile.

Again, the results for frequencies below 500 Hz were poor for both techniques. In addition to this, the values for the real part of the acoustic impedance reached physically impossible negative values for the two-microphone technique at frequencies below 300 Hz. Furthermore, the one-microphone method exhibits enormous divergence at frequencies below 300 Hz before reaching very negative values (these are very hard to see on Figure 49).

3. Ceiling Tile Sample (With Hole Perforations)

The third sample to be tested with the acoustic impedance measurement tube was a ceiling tile sample that had hole perforations about 4mm in diameter spaced about 1 cm apart in a repeating square pattern. The measurements were made in accordance with the procedure documented in Appendix J using the Selenium driver to which a 50 mV signal was applied. As mentioned earlier in Chapter I, the measurements were also made using the original impedance tube that utilizes the standing wave ratio method pictured in Figure 1. Shown below are the acoustic impedance measurement results using both techniques. They are plotted together for comparison in Figures 51 and 52.

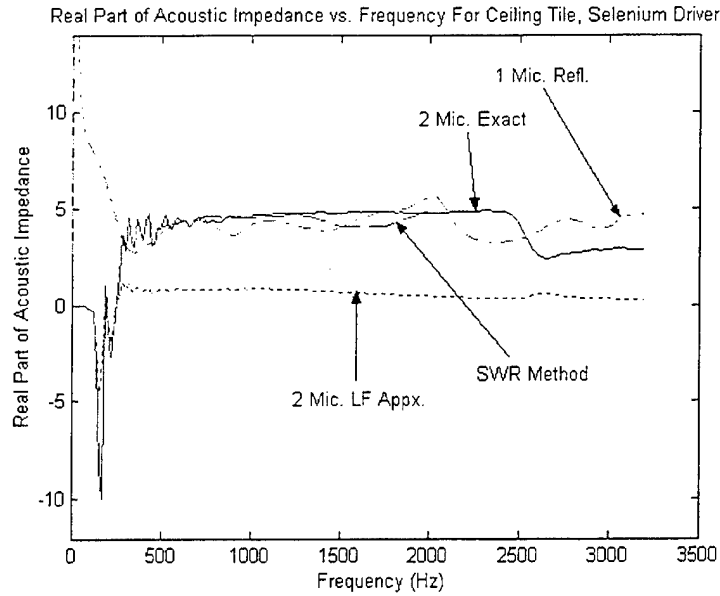


Figure 51. Real part of acoustic impedance versus frequency for a ceiling tile sample using the Selenium driver and a 50 mV signal.

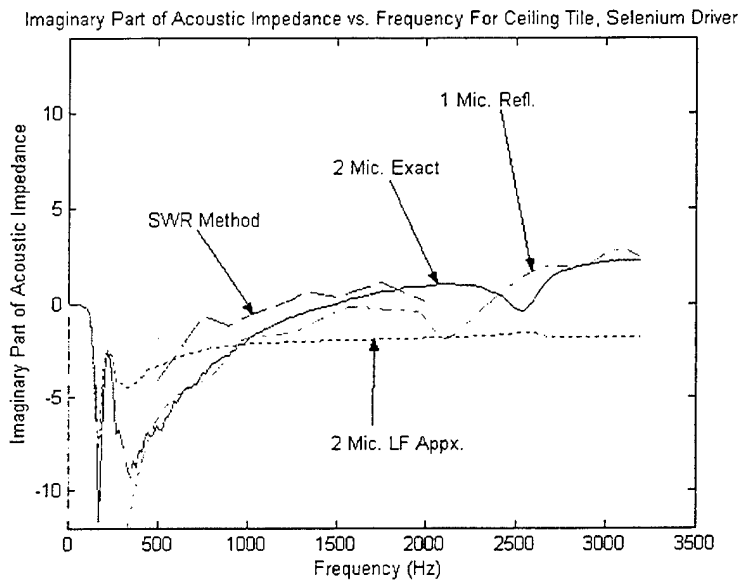


Figure 52. Imaginary part of acoustic impedance versus frequency for ceiling tile sample using the Selenium driver with a 50 mV signal applied.

There is excellent overall agreement between the two-microphone exact and one-microphone impedance measurement at frequencies over 500 Hz. The only exceptions

occur on the imaginary acoustic impedance measurement graph at frequencies near 2.0 kHz and 2.5 kHz where the value briefly "dips" on the one microphone and two-microphone methods respectively. Again, the two-microphone approximation method deviates significantly at frequencies over 300 Hz.

Both techniques used on the new acoustic impedance measurement tube compare favorably with the measurements using the older acoustic impedance measurement tube that utilizes the standing wave ratio method described earlier in Chapter II (although the imaginary impedance values deviate somewhat). This is very encouraging because the two-microphone method can be performed much more rapidly over a wider range of frequencies than the standing wave ratio technique on the other tube.

THIS PAGE INTENTIONALLY LEFT BLANK

V. SUMMARY

A. CONCLUSIONS

The purpose of this the investigation described in this thesis was the development of an acoustic impedance measurement tube employing fixed microphones that can be used quickly to measure the acoustic impedance of any material placed in the cup holder at the end of the tube, over a frequency band of 0 to 3.2 kHz. A new laboratory experiment was developed using this impedance tube. This experiment used two methods for impedance measurement. One method was the two-microphone continuous excitation method, and the other was the one-microphone transient excitation method. This was accomplished in several steps.

First a brief review was made of some of the different methods used in acoustic impedance measurement. Using basic definitions and theory, three principal equations were developed for analysis using two microphones: the Basic Equation, the Exact Equation, and the Low Frequency Approximation Equation. Additionally, an equation was developed for analysis using one microphone: the Reflectivity Equation. Four MATLAB programs were developed that use these equations to compute the acoustic impedances from the raw laboratory data.

Next several components were investigated for the acoustic impedance tube: the microphone, the junction box/power supply assembly, and the driver. A careful study was made of second harmonic distortion in the signal from the Mouser microphone. The junction boxes were carefully designed and constructed for optimal conveyance of the microphone signal to the dynamic signal analyzer. Lastly, eight drivers were tested to

determine which best suited the needs of the experiment. Two drivers, the Selenium DH200E and the University Sound 1828R, were selected for use.

Having developed the apparatus and theory, it was necessary to establish a test procedure that would integrate these and provide a means for measuring the acoustic impedance of a sample material. This was accomplished for the two-microphone continuous excitation method and the one-microphone transient excitation method. A laboratory handout was produced, to enable students to conduct acoustic impedance measurements using this apparatus.

The final step was to validate the effectiveness of this acoustic impedance measurement tube and its developed techniques. This was successfully accomplished by making "open tube" measurements and comparing the results to established theory over the frequency range of 0 to 3.2 kHz. The measurements made using the two-microphone technique and the one microphone technique both compared favorably with the theory. Additionally, measurements were made using: an insulation sample, a speckled ceiling tile sample, and a ceiling tile sample with perforated holes. Again, the results using the two-microphone method and one microphone methods compared favorably with each other, and, where available, with the results using the old impedance tube apparatus. The Selenium and University Sound drivers were also compared and it was determined that the Selenium driver yielded better results overall for this application.

B. RECOMMENDATIONS

Although the acoustic impedance measurement tube was successfully developed, along with a useful procedure and software, there are still some modifications that can further improve the performance of this apparatus. One is the development of a filter that

would improve the acoustic impedance measurement results at the low end of the frequency band (below 1000 Hz, for example) by boosting the drive signal at these frequencies. Two additional developments that would improve the educational value of this apparatus are: cutting of more samples from bulk material and production of a Helmholtz resonator for a reflector. Additional samples of a wider variety of materials can validate the performance of the apparatus over a wider range of acoustic impedance. It is important to note that a Helmholtz resonator can be developed and used with this apparatus to demonstrate important acoustic theory. One last area worth exploring is the use of a higher quality microphone. Linearity is the most important quality of a microphone used in this apparatus; sensitivity is not a problem. Use of a higher quality microphone would, no doubt, yield better results.

THIS PAGE INTENTIONALLY LEFT BLANK

APPENDIX A: MOUSER ELECTRONICS 25LM045 SPECIFICATIONS

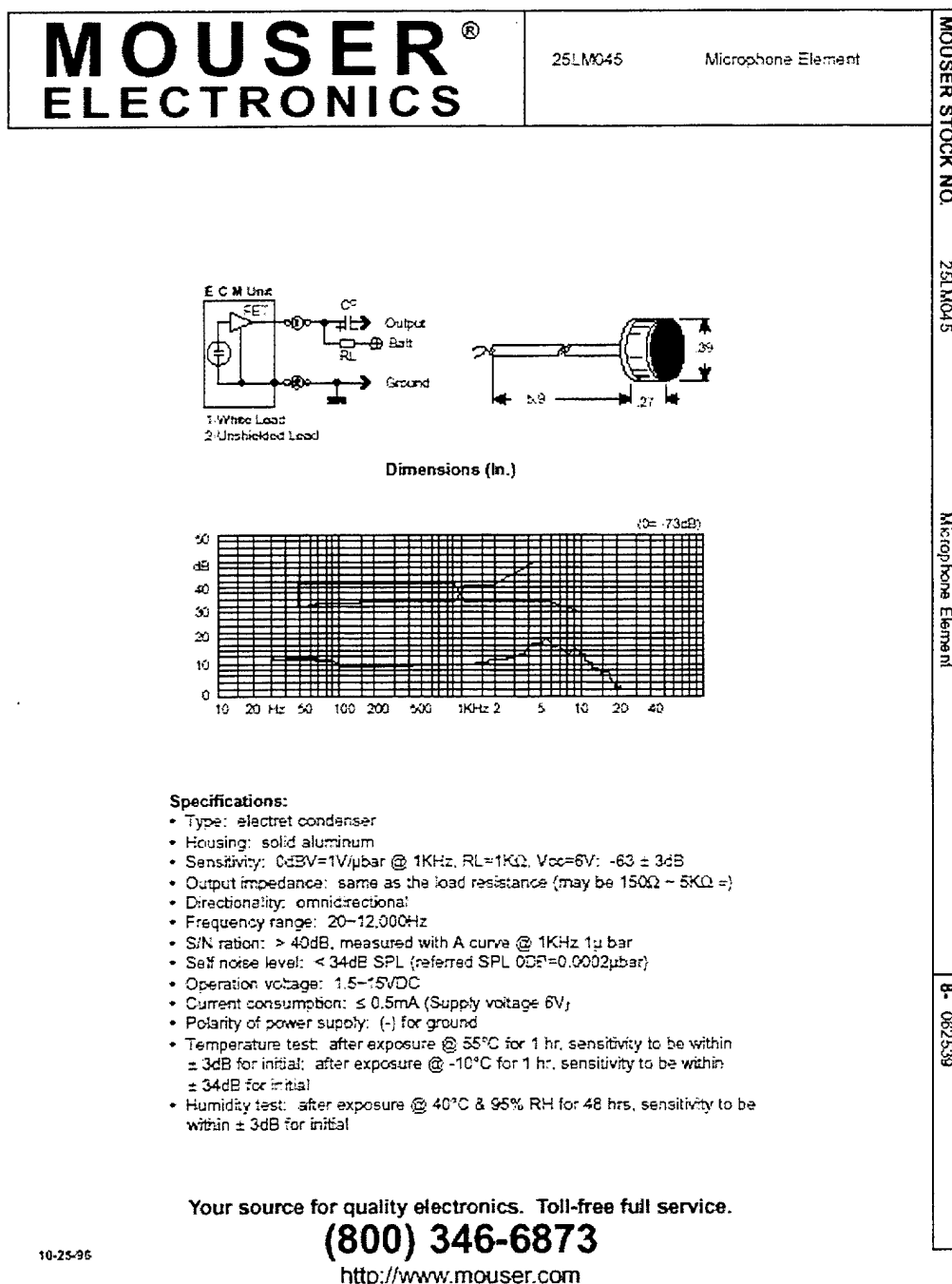


Figure 53. Mouser microphone data specifications.

THIS PAGE INTENTIONALLY LEFT BLANK

APPENDIX B: LIST OF PARTS FOR ACOUSTIC IMPEDANCE TUBE

Item Description	Manufacturer/Supplier Phone Number	Part Number
1/8" Panel mount phone jacks	Radio Shack 899-2100	274-251
Microminiature toggle switch, 3A/125VAC, 1/4" hole	Radio Shack 899-2100	275-624
Heavy duty 9V battery snap connectors (5 pkg.)	Radio Shack 899-2100	270-324
Battery Holder	Allied Electronics (800)-433-5700	839-1295
1/8" Phone plugs (2 pkg.)	Radio Shack 899-2100	274-286
Metal connector box	Allied Electronics (800)-433-5700	806-1870
Omni directional electret condenser microphone	Mouser Electronics (800)-346-6873	25LM045

Selenium DH200E Titanium Compression Driver	Parts Express (800)-338-0531	264-225
BNC bulkhead receptacle (jack)	Amphenol RFX (800)-627-7100 or Amphenol Comm. Network and Products Div. (203)-743-9272	31-221-RFX (for Amphenol RFX) or 999-226B (for Amphenol Comm.)
1000 ohm precision resistor	Digi-Key Corporation (800)-344-4539	1.00KXBK-ND
22 microfarad capacitor	Digi-Key Corporation (800)-344-4539	ECS-F1CE226K

Table 2. List of Parts For Microphone Junction Box Assembly

APPENDIX C: ANALYSIS OF SELENIUM DH200E DRIVER

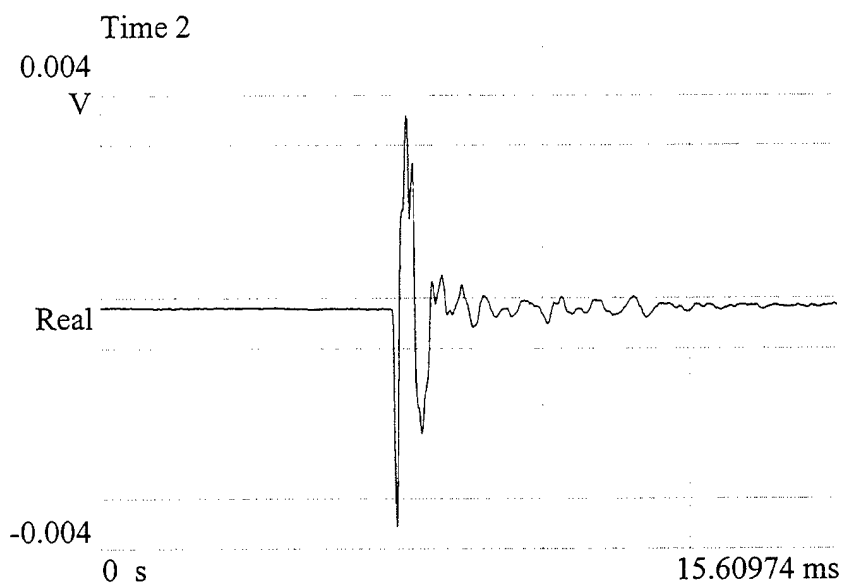


Figure 54. Selenium driver pulse-excitation time response on the HP-35665.

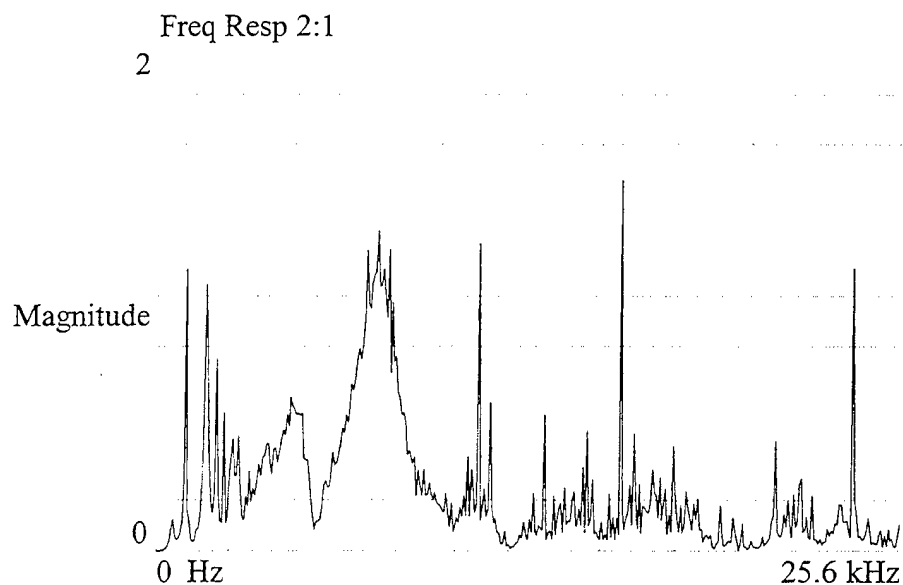


Figure 55. Selenium driver pulse-excitation narrow band frequency response on the HP-35665 (FFT mode).

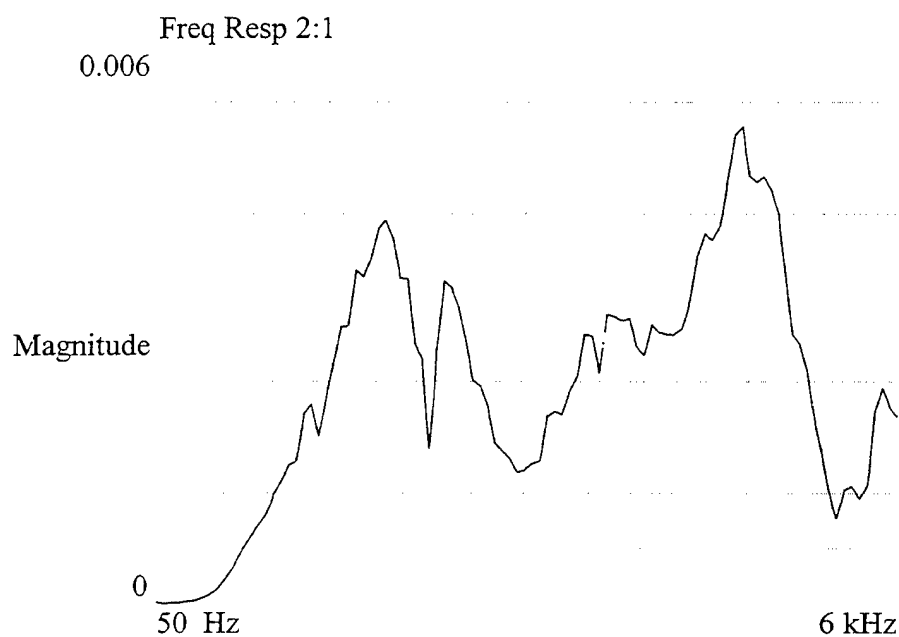


Figure 56. Selenium driver pulse-excitation narrow band frequency response on the HP-35665 (Swept Sine mode).

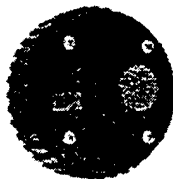
APPENDIX D: SELENIUM DH200E DRIVER SPECIFICATIONS

SELENIUM LOUDSPEAKERS

11 East Rochester Ave. P.O. Box 104, PA 16041-0104
Tel: 810-285-2045 • 800-962-0473 • Fax: 810-285-2044
E-Mail: Sales@selecusa.com • www.Selenium-USA.com

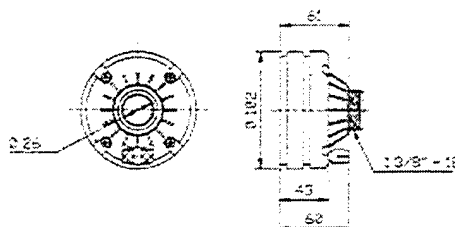
DH200E

Professional Series



This 1" compressive driver delivers exceptional smoothness, clarity and detail as a full range driver in compact 2-way systems and as a VHF device in 3-way mid/high enclosures. Utilizing a titanium diaphragm on a 48 mm kapton former, the DH200E is the result of extensive research and development and the use of the latest materials to provide sonic

excellence and a high level of reliability. With a usable frequency range from 2000Hz to 20,000Hz and power handling at 200 Watts (program 62KHz), the DH200E provides wide band response, high power handling and high SPL for professional use. The matching horn exhibits a nominal dispersion of 60 x 40 degrees with outstanding off-axis uniformity and extremely low throat distortion.



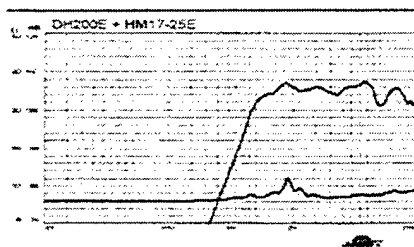
Dimensions: mm.

SPECIFICATIONS: DH200E

Nominal Impedance	8	Ohms
Power Handling (Cont. Program)*		
W/Crossover 2000 Hz 12dB/Octave	200	Watts
Sensitivity (1W/1m)	125	dB SPL
Frequency Response	1500 - 20000	Hz
Flux Density	15,500 (1.55)	Gauss (Ts)
Recommended Crossover	2000	Hz
Voice Coil Diameter	48 (1.81)	mm (in)
Former Material	Kapton	
Diaphragm Material	Titanium	
Baffle Cutout	115 x 115 (4.5 X 4.5)	mm (in)
Sound Dispersion (HzV)	60X40	Degrees
Magnet Weight	429 (15)	g (oz)
Net Weight	1570 (3.4)	g (lb)

WARNING: Must be connected with an appropriate crossover.

* Specifications to handle normal speech and music program material with 5% permissible maximum distortion on amplifier. Products are actually tested using RMS measurement standards: Continuous, *Program = 2 x WRMS.



Frequency Response and Impedance curve measured in anechoic chamber.

Ring Radiator Titanium Diaphragm
RPH0720

HM17-25E - 60 x 40 Matching Horn



Specifications subject to change without notice.

Updated 01-Jan-1998

Figure 57. Specifications for Selenium DH-200E driver.

THIS PAGE INTENTIONALLY LEFT BLANK

APPENDIX E: ANALYSIS OF UNIVERSITY SOUND 1828R DRIVER

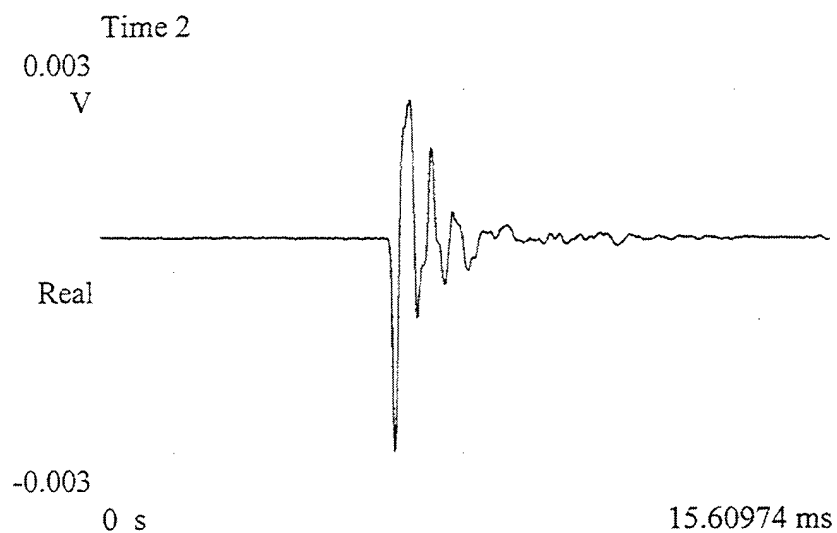


Figure 58. University Sound driver pulse-excitation time response on HP-35665.

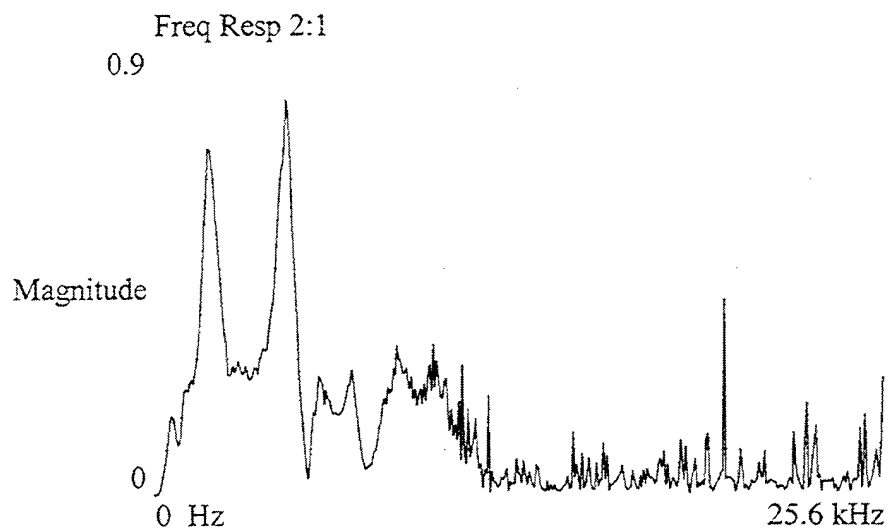


Figure 59. University Sound driver pulse-excitation narrow band frequency response on the HP-35665 (FFT mode).

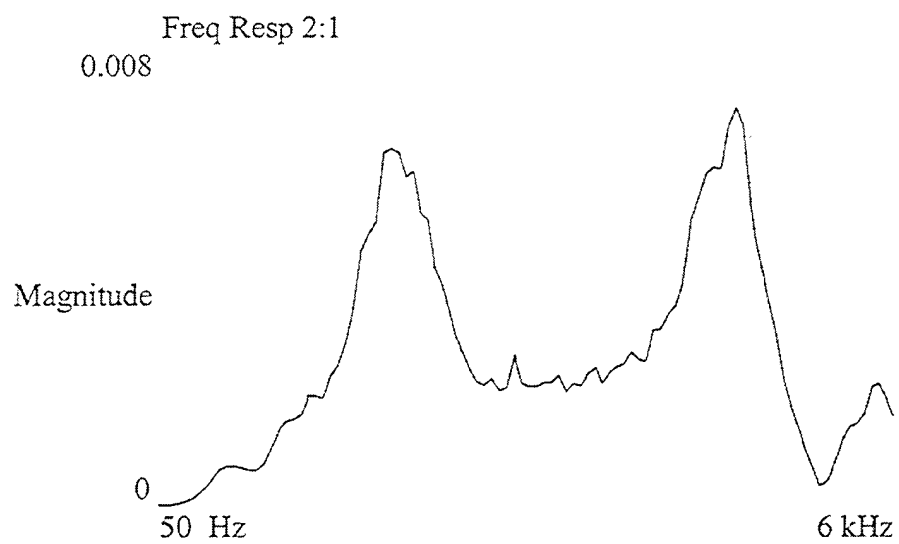


Figure 60. University Sound driver pulse-excitation narrow band frequency response on the HP-35665 (Swept Sine mode).

APPENDIX F: UNIVERSITY SOUND 1828R DRIVER SPECIFICATIONS

1828T 1828C Convertible Drivers



General Product Description

The 1828T and 1828C are heavy-duty convertible drivers for use in medium power public address installations.

The drivers have rugged phenolic diaphragms, 1.5 inch diameter voice coils, and "rim centered" ferrite magnet structures for long life and reliability under extreme operating conditions.

The transformer model (1828T) includes connections for 70V/25V distributed systems and a power tap selector panel. The exterior is finished in durable waterproof paint, and all metal parts have been treated for resistance to high humidity and fungus.

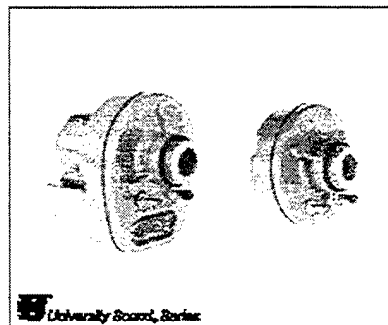
Ideal for both indoor and outdoor applications, these drivers are well suited for any installation requiring rugged and reliable performance.

Architects' and Engineers' Specifications

The loudspeaker(s) shall be of the compression-driver type having a rugged phenolic diaphragm and a high-temperature rated one and one-half inch voice coil.

The loudspeaker(s) shall exhibit essentially flat power response from 400 to 3,000 Hz with a smoothly rolled-off response beyond. Their sensitivity, when mounted on a FC100 horn, will be 105 dB (1 W/1 M) with a 500 to 5,000 Hz pink noise signal applied.

The loudspeaker(s) will be capable of handling a 50 watt, 500 to 5,000 Hz pink noise signal with a 6 dB crest factor for a period of eight hours.



The 1828T shall have a height of 12.7 cm (5.0 in.), a width of 10.2 cm (4.0 in.), and a depth of 13.3 cm (5.2 in.).

The 1828C shall have a diameter of 8.31 cm (3.3 in.), and a height of 10.2 cm (4.0 in.). Both shall have a throat opening of 2.54 cm (1.0 in.) with a 1-3/8"-18 thread for mounting.

The loudspeakers are the 1828T which includes a 70V/25V line matching transformer (see Table 1) and weighs no more than 2.3 kg (5 lb), and the University Sound 1828C, which has a nominal impedance of 8 ohms and weighs no more than 2.2 kg (4.7 lb).

Specifications:

Frequency Response:

200-10,000 Hz ± 5 dB (see Figure 2)

Power Handling, 8 Hours, 6 dB Crest Factor:

30 watts (500-5,000 Hz pink noise)

Impedance, Nominal:

8 ohms

Minimum:

5.5 ohms (FC100 horn)

Sound Pressure Level at 1 Meter, 1 Watt Input Averaged, Pink Noise Band-Limited from 300-5,000 Hz:

105 dB (FC100 horn)

Voice Coil Diameter:

3.31 cm (1.30 in.)

Magnet Weight:

0.23 kg (0.52 lb)

Magnet Material:

Stentum Iron

Flux Density:

1.25 Tesla

Construction:

Rugged weatherproof finish for outdoor use

Mechanical Construction of Driver:

1-3/8"-18 x 7.62" long thread allows the 1828 to be mounted on any horn

Dimensions, 1828T:

Height 12.7 cm (5.0 in.)

Width 10.2 cm (4.0 in.)

Depth 13.3 cm (5.2 in.)

Dimensions 1828C:

Diameter 8.31 cm (3.3 in.)

Height 10.2 cm (4.0 in.)

Net Weight:

1828T 2.3 kg (5.0 lb)

1828C 2.2 kg (4.7 lb)

Shipping Weight:

1828T 2.5 kg (5.5 lb)

1828C 2.4 kg (5.2 lb)

Recommended Horns:

FC100 Cobrelex HS Cobrelex TL

Electro-Voice

Figure 61. University Sound Driver product specifications.

Installation

For use with compound horns, remove both protective plastic caps and the plastic foam loading plug from the rear. Note: front end is the one with wiring terminals.

Next, screw the large horn section onto the rear of the driver and the small section onto the front. Hand tighten to slightly compress rubber gaskets.

For use with all other horn types, rear cap and foam plug are left in place and firmly hand tightened with horn attached to the front directly to the driver terminals.

Transformer Model (1826T)

A transformer and power selection panel is installed in the back of the housing. Power taps for the transformer are listed in Table 1.

Low-Frequency Driver Protector

When frequencies below the low-frequency cutoff for the horn assembly are fed to the driver, excessive current may be drawn by the driver. For protection of driver, amplifier, and transformer (if driver with built-in transformer is used), capacitor(s), in series with driver, or transformer primary are recommended. Table 1 indicates

recommended values. The values shown are for 200 Hz. Values for other frequencies can be determined by using the formula:

$$C = \left[C_{200} \times \frac{200}{f} \right] \quad C_{200} = \text{Values shown in the following table}$$

$f = \text{New Frequency}$

For drivers without transformers: 8-ohm driver, 25 V - 100 mF 150 Vdc or 150 V non-polarized electrolytic, or two 150 Vdc electrolytics of two times required value in series, back to back, for 70 volt lines.

Table 1. Series Protection Capacitors for 200 Hz and Below

Power	70-Volt Lines		25-Volt Lines	
	Impedance	Capacitance	Impedance	Capacitance
30 W	165	5 mF	-	-
15 W	200	2 mF	-	-
8 W	625	1 mF	-	-
5 W	1250	0.5 mF	150	5 mF
2 W	-	-	312	2 mF
1 W	-	-	625	1 mF
1/2 W	-	-	1250	0.5 mF

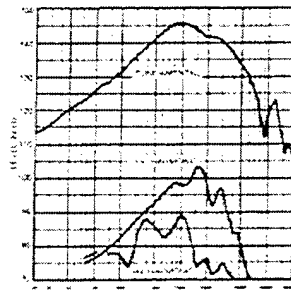


Figure 1.
Distortion Response - Plane Wave Tube (1 inch)
(3 watt input)

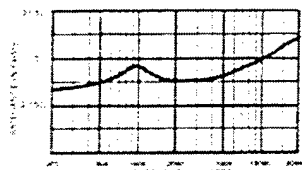


Figure 3.
Impedance Response - Plane Wave Tube (1 inch)

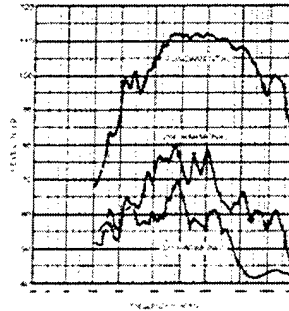


Figure 2.
Distortion Response - FC100 Horn
(1 watt / 1 meter)

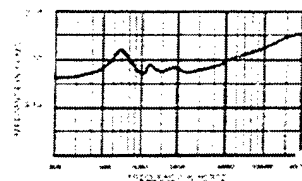


Figure 4.
Impedance Response - FC100 Horn

www.electrovoice.com - Telcel Communications, Inc. - www.telcel.com
© Telcel Communications, Inc. 10/01/01
Part Number 1826T-01 Rev A



U.S.A. and Canada only
For customer orders, contact the Customer Service department at
800/252-2417 Fax: 949/252-0417
For warranty repair or service information, contact the Service
Repair Department at 949/252-2417
For technical assistance, contact Technical Support at 949/252-2417
Please refer to the Engineering Data Sheet for complete information.
(Some of the subject is changed with the new)

Figure 62. University Sound performance specifications.

APPENDIX G: "REIM.78S" AND "REFLWTIM.78S" SETTINGS

The "REIM.78S" settings are:

Input	Ch 1	Ch 2
Source	Analog	Analog
Config	Dual Chan.	Dual Chan.
Mode	A	A
Ground	Ground	Ground
Coupling	AC	AC
Range	-6 dBVpk	-4 dBVpk
AA Filter	On	On
A-Wt Filter	Off	Off
Auto Range	Up Only	Up Only
Auto Offset	On	On
EU	Off	Off
EULabel	m/s	m/s
EU/Volt	1 EU/V	1 EU/V
User Label	EU	EU
Ta1		1
Tach Level	0.00 V	0.00 V
Tach Trigger	TTL	TTL
Tach Slope	Rising	Rising
Tach Holdoff	Off	Off
ShowTach	Off	Off
Xdcr		
Measure	Display A	Display B
Measurement	Freq. Resp.	Freq. Resp.
View	Real Part	Imag. Part
Units		
dB Units	Off	Off

Peak Units	off	off
PSD Units	Off	Off
Phase Units	deg	deg
dBm Ref	50	50
Base Freq	102.4 kHz	102.4 kHz
Span	3.2 kHz	3.2 kHz
Start Freq	0 Hz	0 Hz
Lines	200	200
Window	Hanning	Hanning
Force	976.563 s	976.563 s
Expo	50.00%	50.00%

Average	Display A	Display B
Comp. Average	Yes	Yes
Type	Linear / Fix Len	Linear / Fix Len
Display	RMS	RMS
Number	256	256
Time Incr	100.00%	100.00%
Reject	On	On
Preview	Off	Off
Prv Time	2 s	2 s

Display	Display A	Display B
Ymax	1.9	400 m
Y/div	100 m	100 m
Xcenter	50	50
X/div polar	10	10
Ycenter	50	50
Y/div polar	10	10
Pan	0	0
Zoom	x1	x1
Format	Dual	Dual
X Axis	Linear	Linear

Grid	On	On
Grid Div	10	10
Grid Type	Rectangular	Rectangular
Phase Suppress	0.0000e+000	0.0000e+000
d/dx Window	0.5	0.5

Marker	Display A	Display B
MarkerOn	Link	
Mode	Normal	Normal
Seeks	Max	Max
Width	Spot	Spot
Relative	Off	Off
X Relative	Off	Off
X Rel	0	0
Y Rel	0	0
# Harmonics	1	1
Display	Fundamental	Fundamental
Readout	Absolute	Absolute
Sideband Sep	0	0
# Sidebands	10	10
Band Exclude	none	none

Band

Waterfall	Display A	Display B
Wfall Display	Normal	Normal
Wfall Storage	Off	Off
Storage Mode	All	All
Total Count	69	69
Skip	30	30
View Count	10	10
Trace Height	70%	70%
Angle	-30°	-30°
Fast Angles	Off	Off
Threshold	0%	0%

Hidden Lines	Invisible	Invisible
Paused Draw	Normal	Normal

Source

Source 0 [0=Off, 1=On]

Type 2 [0=Sine, 1=Chirp, 2=Noise, 3=Arb]

Sine Freq 1 10.24 kHz

Sine Amp 1 500.0 mVpk

Sine Freq 2 51.2 kHz

Sine Amp 2 0.0 mVpk

Sine Offset 0.0 mV

Chirp Amp 1000.0 mV

Chirp Burst 100.00 %

Source Display Display A

Noise Amp 1000.0 mV

Noise Type BL White

Noise Burst 100.000 %

Arb Amp 100.00 %

Arb Rate 262.1 kHz

Arb Source Arb. Buffer

Arb Start 0

Arb Length 4 kPts

Trigger

Arming Mode Auto Arm

Trigger Source Source

Trigger Level 0 %

Trigger Slope Falling

Delay1 0 s

Delay2 0 s

Source Mode Continuous

Start RPM Off

Start RPM 50

Delta RPM Abs. Change

Delta RPM 10
 Time Step 100 ms
 Capture
 Capt Channels Ch1+Ch2
 Capt Mode 1 Shot
 Capt Length 488 kPts/ch
 Capt Rate 262.1 kHz
 Auto Pan On
 Playback Start 0
 Playback Len 488 kPts/ch
 Playback Mode 1-Shot

The "REFLWTIM.78S" settings are:

Input	Ch 1	Ch 2
Source	Analog	Analog
Config	Dual Chan.	Dual Chan.
Mode	A	A
Ground	Ground	Ground
Coupling	AC	AC
Range	-12 dBVpk	-12 dBVpk
AA Filter	On	On
A-Wt Filter	Off	Off
Auto Range	Up Only	Up Only
Auto Offset	On	On
EU	Off	Off
EU		
EU/Volt	1 EU/V	1 EU/V
User Label	EU	EU
Tachs/Rev	1	1
Tach Level	0.00 V	0.00 V
Tach Trigger	TTL	TTL
Tach Slope	Rising	Rising
Tach Holdoff	Off	Off
ShowTach	Off	Off
Xdcr		
Measure	Display A	Display B
Measurement	WinTime 1	WinTime 2
View	Real Part	Real Part
Units	Vpk	Vpk

dB Units	Off	Off
Peak Units	pk	pk
PSD Units	Off	Off
Phase Units	deg	deg
dBm Ref	50	50
Base Freq	102.4 kHz	102.4 kHz
Span	3.2 kHz	3.2 kHz
Start Freq	0 Hz	0 Hz
Lines	200	200
Window	Force/Exp	Force/Exp
Force	2.92969 ms	2.92969 ms
Expo	50.00%	50.00%

Average	Display A	Display B
Comp. Average	Yes	Yes
Type	Exp. / Cont.	Exp. / Cont.
Display	Vector	Vector
Number	32	32
Time Incr	100.00%	100.00%
Reject	On	
Preview	Off	Off
Prv Time	2 s	2 s

Display	Display A	Display B
Ymax	350 m	350 m
Y/div	50 m	50 m
Xcenter	50	50
X/div polar	10	10
Ycenter	50	50
Y/div polar	10	10
Pan	0	0
Zoom	x1	x1
Format	Dual	Dual
X Axis	Linear	Linear
Grid	On	On
Grid Div	10	10
Grid Type	Rectangular	Rectangular
Phase Suppress	0.0000e+000	0.0000e+000
d/dx Window	0.5	0.5

Marker	Display A	Display B
MarkerLink	Link	
Mode	Normal	Normal
Seeks	Max	Max
Width	Spot	Spot
Relative	Off	Off

X Relative	Off	Off
X Rel	0	0
Y Rel	0	0
# Harmonics	1	1
Display	Fundamental	Fundamental
Readout	Absolute	Absolute
Sideband Sep	0	0
# Sidebands	10	10
Band Exclude	none	none
Band		
Waterfall	Display A	Display B
Wfall Display	Normal	Normal
Wfall Storage	Off	Off
Storage Mode	All	All
Total Count	69	69
Skip	30	30
View Count	10	10
Trace Height	70%	70%
Angle	-30°	-30°
Fast Angles	Off	Off
Threshold	0%	0%
Hidden Lines	Invisible	Invisible
Paused Draw	Normal	Normal

Source

Source 0	[0=Off, 1=On]
Type 2	[0=Sine, 1=Chirp, 2=Noise, 3=Arb]
Sine Freq 1	10.24 kHz
Sine Amp 1	500.0 mVpk
Sine Freq 2	51.2 kHz
Sine Amp 2	0.0 mVpk
Sine Offset	0.0 mV
Chirp Amp	1000.0 mV
Chirp Burst	100.00 %
Source Display	Display A
Noise Amp	500.0 mV
Noise Type	BL White
Noise Burst	100.000 %
Arb Amp	100.00 %
Arb Rate	262.1 kHz
Arb Source	Arb. Buffer
Arb Start	0
Arb Length	4 kPts

Trigger
Arming Mode Auto Arm

Trigger Source Ext TTL
Trigger Level 0 %
Trigger Slope Falling
Delay1 1.58691 ms
Delay2 4.5166 ms
Source Mode Continuous
Start RPM Off
Start RPM 50
Delta RPM Abs. Change
Delta RPM 10
Time Step 100 ms

Capture
Capt Channels Ch1+Ch2
Capt Mode 1 Shot
Capt Length 488 kPts/ch
Capt Rate 262.1 kHz
Auto Pan On
Playback Start 0
Playback Len 488 kPts/ch
Playback Mode 1-Shot
Playback Speed Normal

Memory
Capt Memory 489 Blks
Wfall Memory 488 Blks
Arb Memory 2 Blks

System
Output To RS232
GPIB Address 10
Override REM Yes
Band Rate 9600 bd
Word Length 8 bits
Parity None
Key Click Off
Alarms On
Alarm Vol Noisy
Done Vol Noisy
Audible Ovld On
Screen Saver On
Saver Delay 10 m
Freq Format Exact Bin
Node Info No

Output

Print Screen Key	ASCII Dump
Printer Type	PCX 8 bit
Bitmap Area	Graphs
Plotter Type	PostScript
Destination	Disk File
GPIB Control	SR785
Plotter Address	2
Print Bright	12%
Print Dim	White
Print Black	Black
Print Graph	Black on White
Text Pen	1
Grid Pen	1
Trace Pen	1
Marker Pen	1

THIS PAGE INTENTIONALLY LEFT BLANK

APPENDIX H: IMPEDANCE MEASUREMENT TUBE DRAWINGS

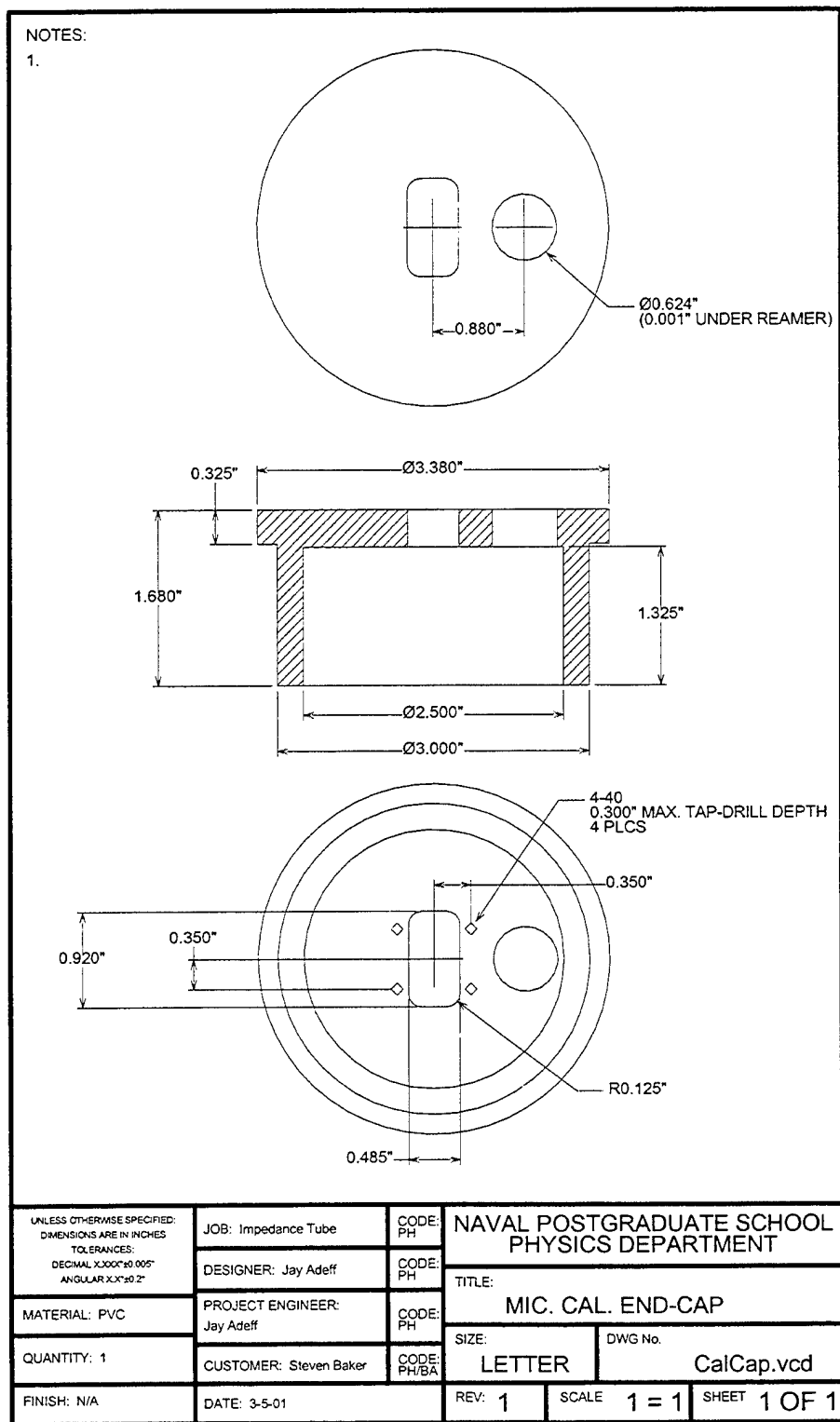
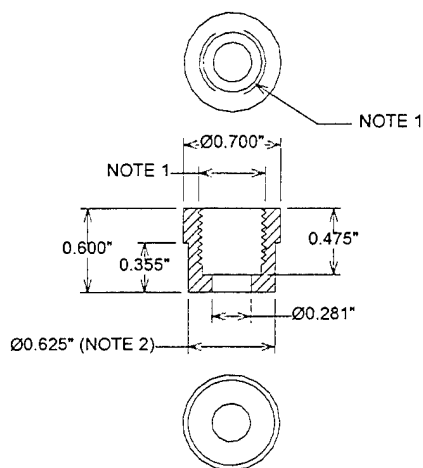


Figure 63. Microphone calibration cup drawing.

NOTES:

1. 1/2-13 thread. Use 7/16" flat bottom end-mill for tap drill to a depth of 0.475". Run bottoming tap to a depth of 0.400".

2. Press fit into Mic. Cal. End-Cap (DWG # CalCap.vcd).

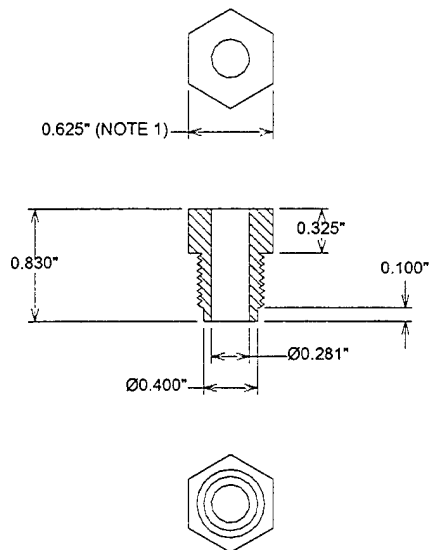


UNLESS OTHERWISE SPECIFIED: DIMENSIONS ARE IN INCHES TOLERANCES: DECIMAL X.XXX \pm 0.005" ANGULAR X.X \pm 0.2°	JOB: IMPEDANCE TUBE	CODE: PH	NAVAL POSTGRADUATE SCHOOL PHYSICS DEPARTMENT		
	DESIGNER: Jay Adeff	CODE: PH	TITLE: CAL. MIC. BOSS		
MATERIAL: PVC	PROJECT ENGINEER: Jay Adeff	CODE: PH	SIZE:	DWG No.	
QUANTITY: 1	CUSTOMER: S. Baker	CODE: PH/Ba	LETTER	CalMicBoss.vcd	
FINISH: N/A	DATE: 3-5-01	REV: 1	SCALE	1 = 1	SHEET 1 OF 1

Figure 64. Calibration microphone end fitting drawing.

NOTES:

1. Use standard 1/2-13 nylon cap-head bolt. Reduce head to dimensions shown.



UNLESS OTHERWISE SPECIFIED: DIMENSIONS ARE IN INCHES TOLERANCES: DECIMAL X.XXX" ± 0.005 " ANGULAR X.X" ± 0.2 "	JOB: IMPEDANCE TUBE	CODE: PH	NAVAL POSTGRADUATE SCHOOL PHYSICS DEPARTMENT		
	DESIGNER: Jay Adeff	CODE: PH	TITLE: Calibration Mic. Retainer		
MATERIAL: Nylon	PROJECT ENGINEER: Jay Adeff	CODE: PH	SIZE:	DWG No.	
QUANTITY: 1	CUSTOMER: S. Baker	CODE: PH/Ba	LETTER	CalMicRetainer.vcd	
FINISH: N/A	DATE: 3-5-01	REV: 1	SCALE	1 = 1	SHEET 1 OF 1

Figure 65. Calibration microphone retainer drawing.

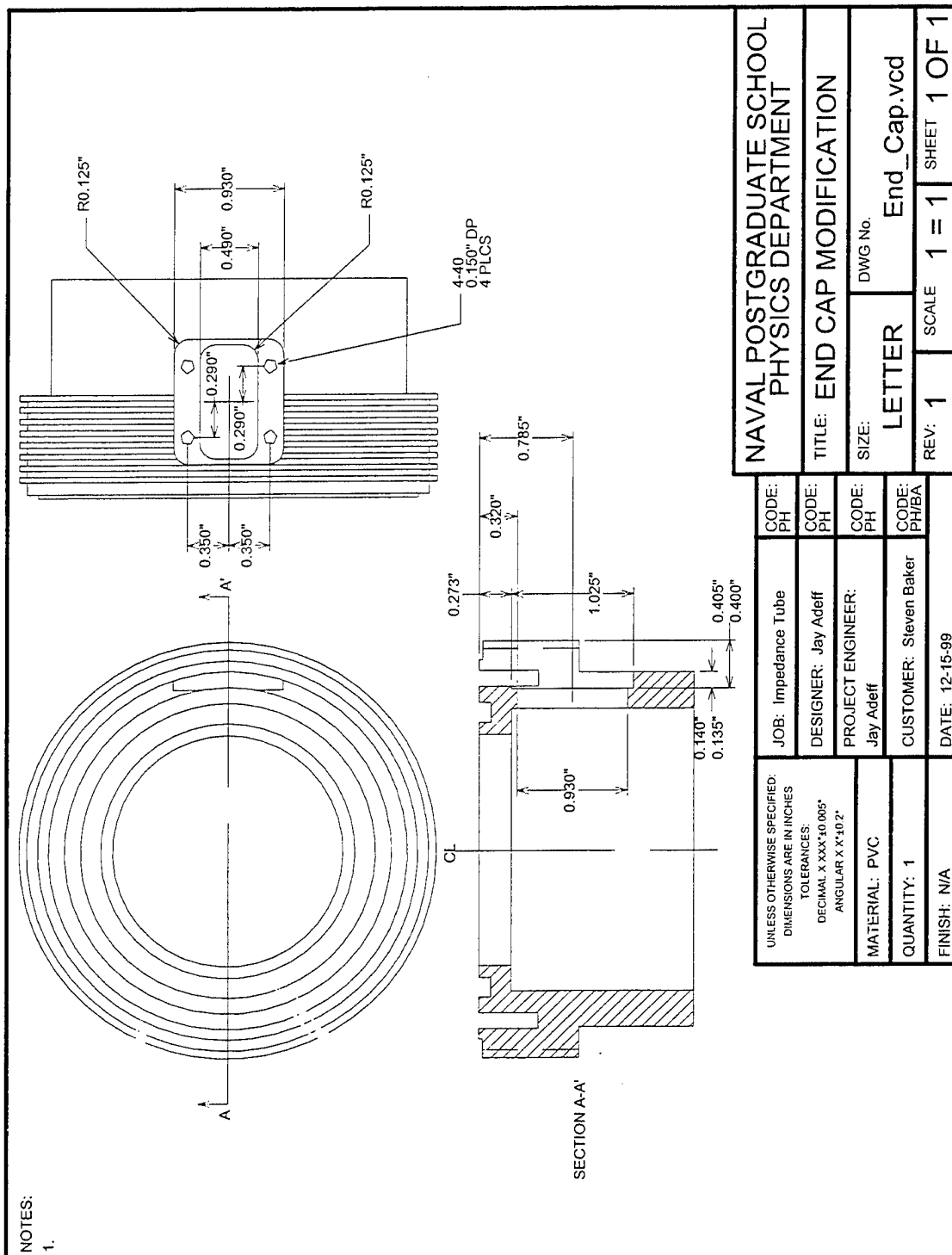
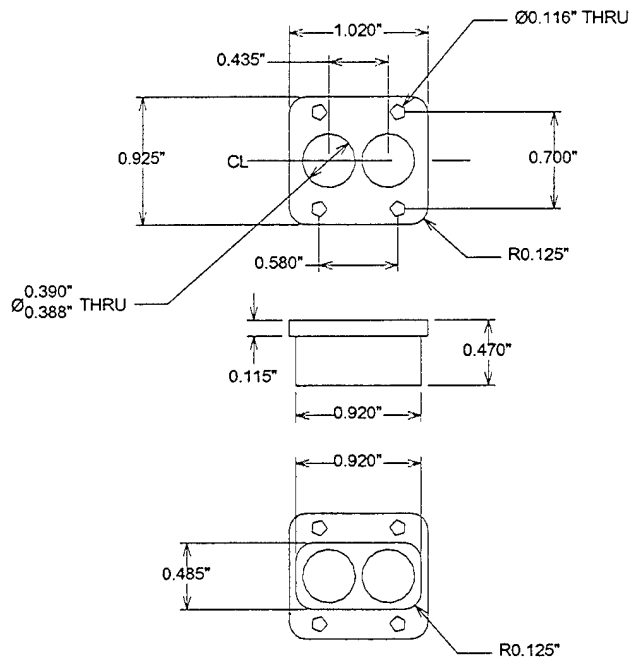


Figure 66. End cap modification drawing.

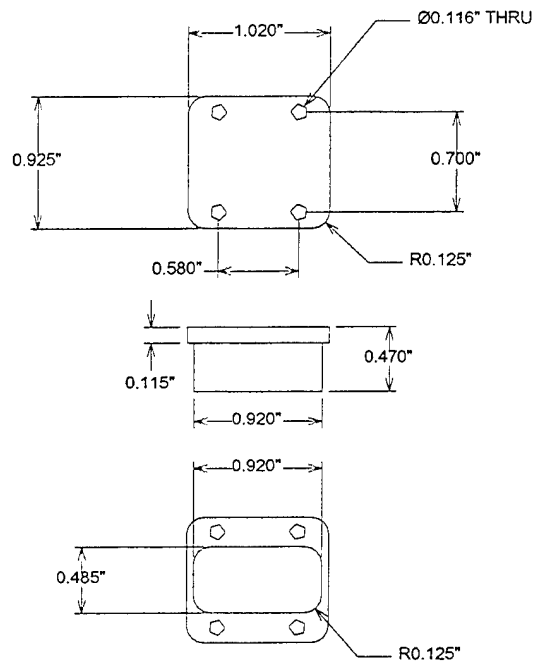
NOTES:
1.



UNLESS OTHERWISE SPECIFIED DIMENSIONS ARE IN INCHES TOLERANCES: DECIMAL X.XXX"±0.005" ANGULAR X.X°±0.2°	JOB: Impedance Tube	CODE: PH	NAVAL POSTGRADUATE SCHOOL PHYSICS DEPARTMENT		
	DESIGNER: Jay Adeff	CODE: PH			
MATERIAL: PVC	PROJECT ENGINEER: Jay Adeff	CODE: PH	TITLE: MICROPHONE PLATE 1		
QUANTITY: 2	CUSTOMER: Steve Baker	CODE: PH/BA	SIZE: LETTER	DWG No. Mic_Plate1.vcd	
FINISH: N/A	DATE: 12-15-99	REV: 1	SCALE 1 = 1	SHEET 1 OF 1	

Figure 67. Microphone holder plate drawing.

NOTES:
1.

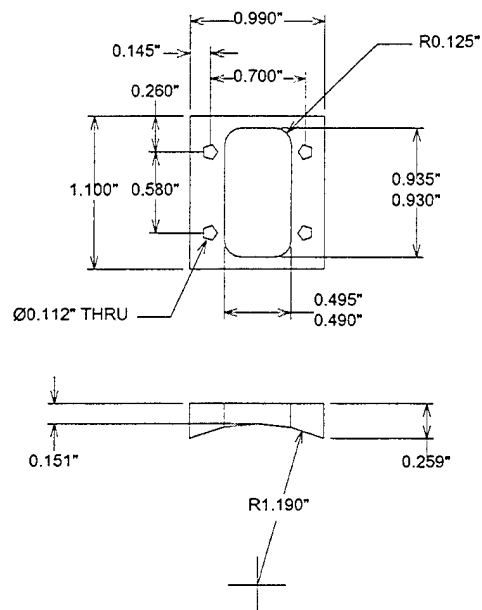


UNLESS OTHERWISE SPECIFIED: DIMENSIONS ARE IN INCHES TOLERANCES: DECIMAL X.XXX \pm 0.005" ANGULAR X.X \pm 0.2°	JOB: Impedance Tube	CODE: PH	NAVAL POSTGRADUATE SCHOOL PHYSICS DEPARTMENT	
	DESIGNER: Jay Adeff	CODE: PH		
MATERIAL: PVC	PROJECT ENGINEER: Jay Adeff	CODE: PH	TITLE: Microphone Plate Blank	
QUANTITY: 2	CUSTOMER: Steve Baker	CODE: PH/BA	SIZE: LETTER	DWG No. Mic_Plate2.vcd
FINISH: N/A	DATE: 2-9-01	REV: 1	SCALE 1 = 1	SHEET 1 OF 1

Figure 68. Microphone blank cover plate drawing.

NOTES:

1.



UNLESS OTHERWISE SPECIFIED: DIMENSIONS ARE IN INCHES TOLERANCES: DECIMAL X.XXX \pm 0.005" ANGULAR X.X \pm 0.2°	JOB: Impedance Tube	CODE: PH	NAVAL POSTGRADUATE SCHOOL PHYSICS DEPARTMENT		
	DESIGNER: Jay Adeff	CODE: PH	TITLE: MIC. PLATE BOSS		
	PROJECT ENGINEER: Jay Adeff	CODE: PH	SIZE:	DWG No.	
	CUSTOMER: Steve Baker	CODE: PH/BA	LETTER	MicPlateBoss.vcd	
MATERIAL: PVC	DATE: 1-7-00	REV: 1	SCALE	1 = 1	SHEET 1 OF 1
QUANTITY: 1					
FINISH: N/A					

Figure 69. Microphone holder plate drawing.

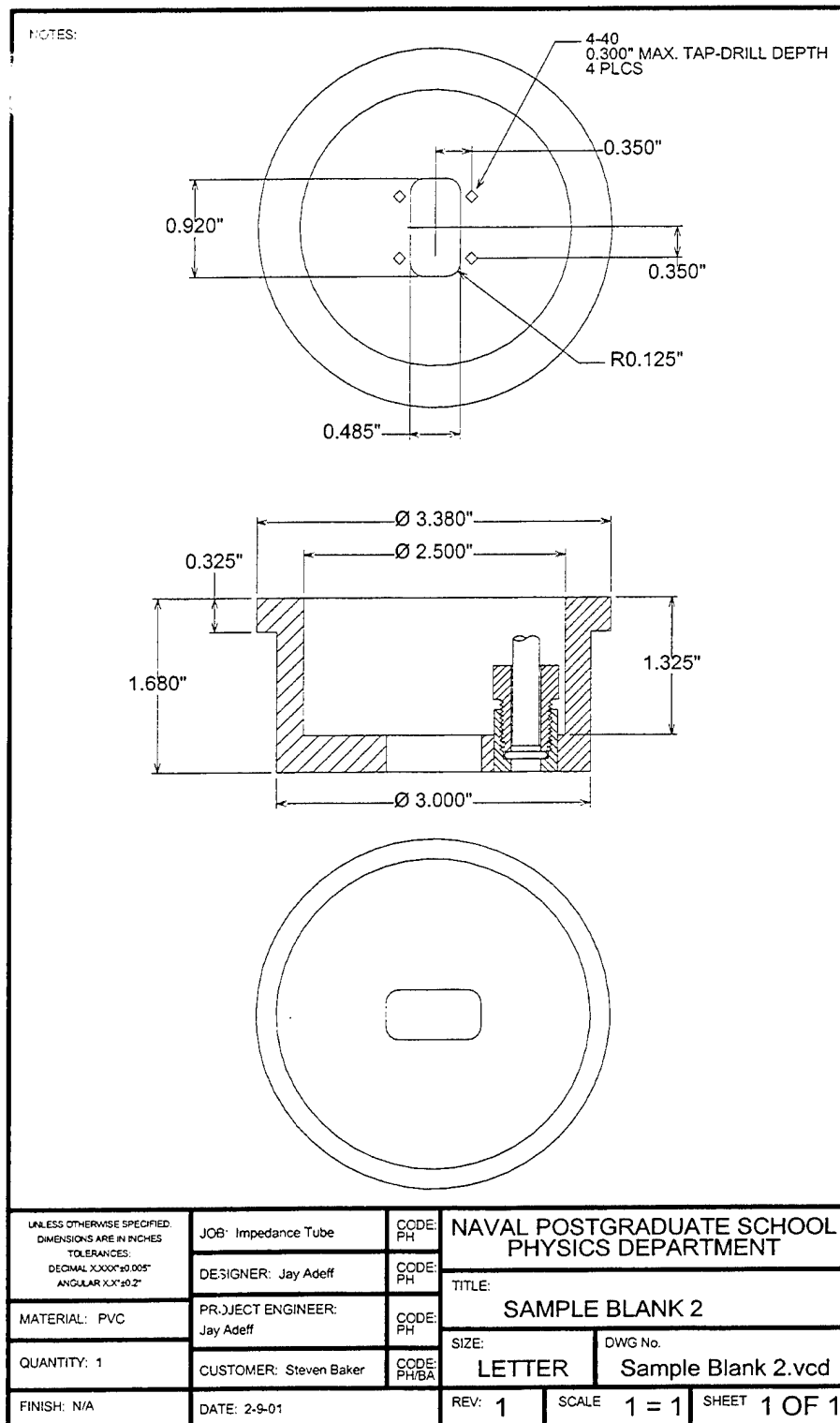
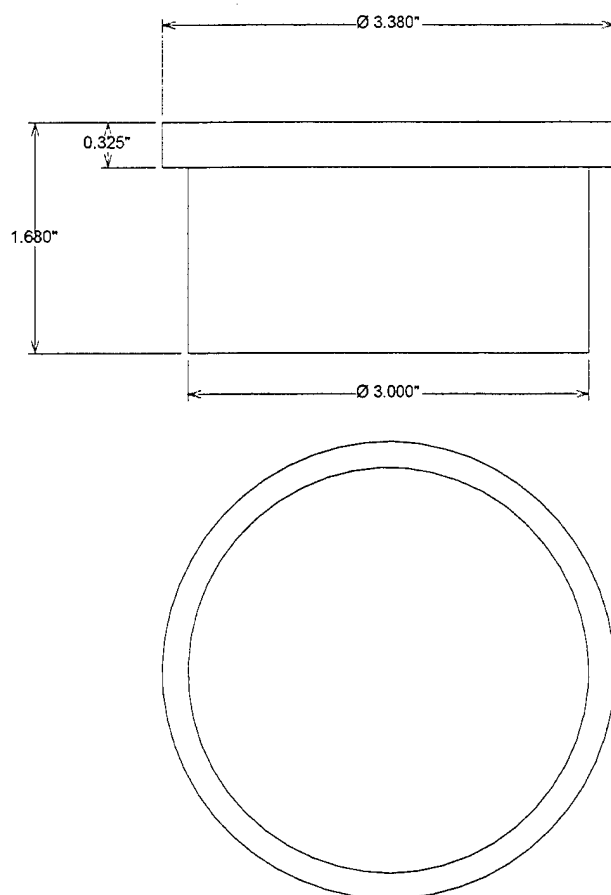


Figure 70. End tube sample holder with microphone access port drawing.

NOTES:

1.



UNLESS OTHERWISE SPECIFIED: DIMENSIONS ARE IN INCHES TOLERANCES DECIMAL X.XXX"±0.005" ANGULAR X.X°±0.2°	JOB: Impedance tube	CODE: PH	NAVAL POSTGRADUATE SCHOOL PHYSICS DEPARTMENT		
	DESIGNER: Jay Adeff	CODE: PH	TITLE: SAMPLE BLANK		
MATERIAL: PVC	PROJECT ENGINEER: Jay Adeff	CODE: PH	SIZE:	DWG No.	
QUANTITY: 1	CUSTOMER: Steven Baker	CODE: PH/BA	LETTER	Sample Blank.vcd	
FINISH: N/A	DATE: 1-4-00	REV: 1	SCALE	1 = 1	SHEET 1 OF 1

Figure 71. End tube blank plate drawing.

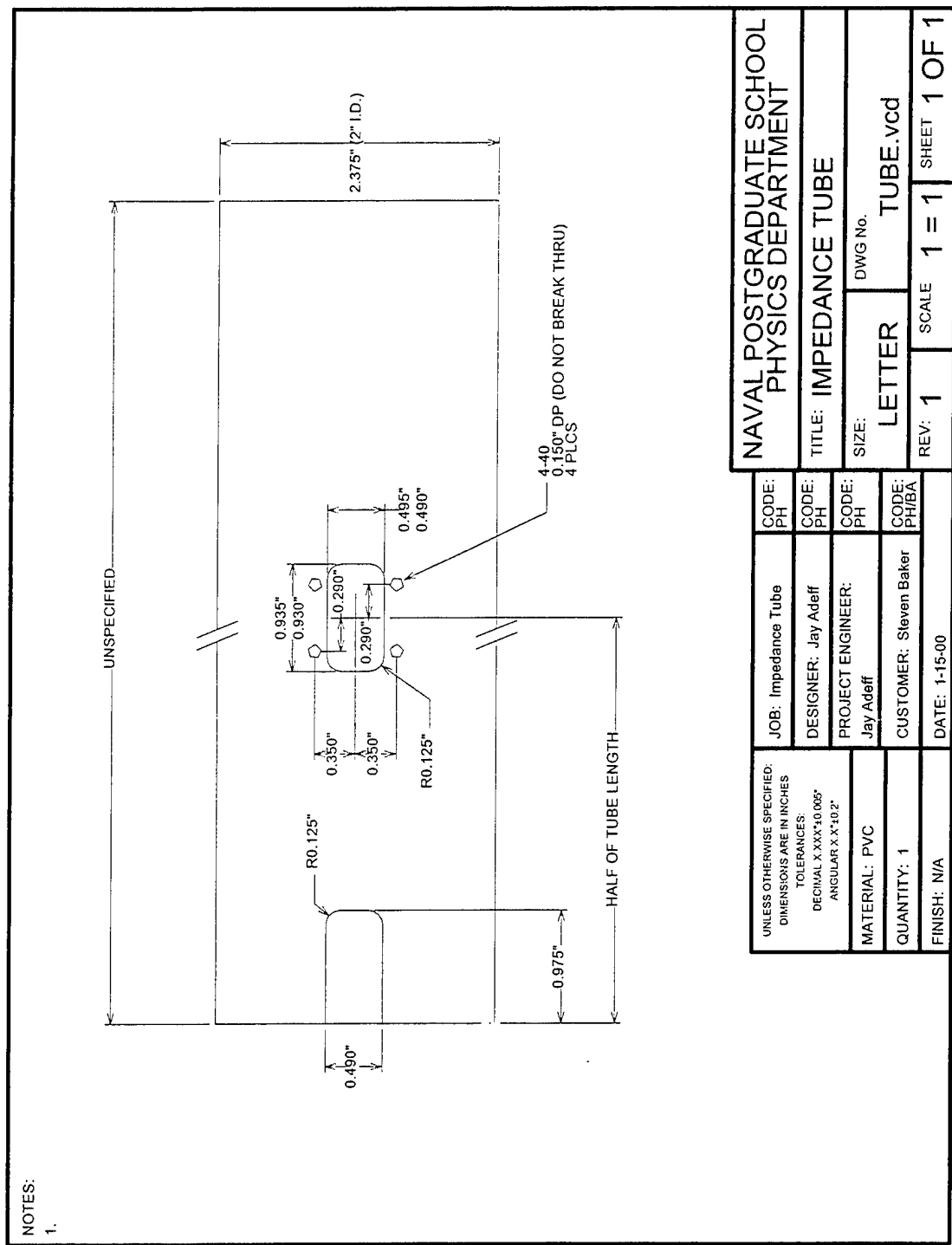


Figure 72. Acoustic impedance measurement tube drawing.

APPENDIX I: COMPUTER PROGRAMS USED FOR IMPEDANCE TUBE

1. The following program is called "Impedance.5", run on the MATLAB R12 version. It uses the approximation outlined from Equations 31 and 35:

```
%This program is designed to compute acoustic impedance given 4
data files obtained
%from the microphone calibration and a measurement using a sample
installed
%at the end of the tube. A second more detailed approximation is
used.

clear
n=1;
while n==1

    disp('')
    disp('The first graph will display the real part of the ratio
of')
    disp('Microphone #2 output voltage over Microphone #1 output
voltage')
    disp('with the Microphones in the calibration position.')
    disp('')
    disp('Please type in name of your file in which this data is
saved.')
    y = input('Ensure you type file exactly as it was saved. ','s');
    p=eval(['load('' y '')']);

    figure (1)
    plot(p(:,1),p(:,2))
    xlabel('Frequency (Hz)')
    ylabel('Real Part of Mic. #2 O/P Volt./Mic. #1 O/P Volt.')
    title('Real Part of Microphone #2 O/P Volt./Microphone #1 O/P
Volt. vs. Freq. (Cal Position)')

    disp('')
    disp('Does this graph accurately reflect your trace saved from
the SRS-785?')
    x=input('Enter 1 to mean YES, 0 to mean NO '); %User verifies
graph is correct
    if x == 0
        disp('') %Erroneous graph
        aborts program
        disp('There is an error.')
        disp('Please verify file name typed in correctly')
        disp('and that trace was saved properly on the SRS-785.')
        break
    end
end
```

```

disp('
')
disp('The second graph will display the imaginary part of the
ratio of')
disp('Microphone #2 output voltage over Microphone #1 output
voltage')
disp('with the Microphones in the calibration position.')
disp('
')
disp('Please type in name of your file name in which this data is
saved')
y1 = input('Again ensure file name is typed exactly. ','s');
p1=eval(['load('' y1 '')']);

figure (2)
plot(p1(:,1),p1(:,2))
xlabel('Frequency (Hz)')
ylabel('Imag. Part of Mic. #2 O/P Volt./Mic. #1 O/P Volt.')
title('Imag. Part of Microphone #2 O/P Volt./Microphone #1 O/P
Volt. vs. Freq. (Cal Position)')

disp('
')
disp('Does this graph accurately reflect your trace saved from
the SRS-785?')
x1=input('Enter 1 to mean YES, 0 to mean NO '); %User verifies
graph is correct
if x1 == 0
    disp('
') %Erroneous graph
aborts program
    disp('There is an error.')
    disp('Please verify file name was typed in correctly')
    disp('and that trace was saved properly on the SRS-785.')
    break
end

disp('
')
disp('The third graph will display the real part of the ratio
of')
disp('Microphone #2 output voltage over Microphone #1 output
voltage')
disp('with the Microphones in the sample measurement position.')
disp('
')
disp('Please type in next file name in which your data is saved')
y2 = input('Again ensure file name is typed exactly. ','s');
p2=eval(['load('' y2 '')']);

figure (3)
plot(p2(:,1),p2(:,2))
xlabel('Frequency (Hz)')
ylabel('Real Part of Mic. #2 O/P Volt./Mic. #1 O/P Volt.')
title('Real Part of Microphone #2 O/P Volt./Microphone #1 O/P
Volt. vs. Freq. (Sample Position)')

disp('
')
disp('Does this graph accurately reflect your trace saved from
the SRS-785?')

```

```

        x2=input('Enter 1 to mean YES, 0 to mean NO '); %User verifies
graph is correct
        if x2 == 0
            disp('') %Erroneous graph
        aborts program
            disp('There is an error.')
            disp('Please verify file name was typed in correctly')
            disp('and that trace was saved properly on the SRS-785.')
            break
        end

        disp('')
        disp('The fourth graph will display the imaginary part of the
ratio of')
        disp('Microphone #2 output voltage over Microphone #1 output
voltage')
        disp('with the Microphones in the sample measurement position.')
        disp('')
        disp('Please type in next file name in which your data is saved')
        y3 = input('Again ensure file name is typed exactly. ','s');
        p3=eval(['load('' y3 ''')']);

        figure (4)
        plot(p3(:,1),p3(:,2))
        xlabel('Frequency (Hz)')
        ylabel('Imag. Part of Mic. #2 O/P Volt./Mic. #1 O/P Volt.')
        title('Imag. Part of Microphone #2 O/P Volt./Microphone #1 O/P
Volt. vs. Freq. (Sample Position)')

        disp('')
        disp('Does this graph accurately reflect your trace saved from
the SRS-785?')
        x3=input('Enter 1 to mean YES, 0 to mean NO '); %User verifies
graph is correct
        if x3 == 0
            disp('') %Erroneous graph
        aborts program
            disp('There is an error.')
            disp('Please verify file name was typed in correctly')
            disp('and that trace was saved properly on the SRS-785.')
            break
        end

        n=0; % Change n value to exit the
while loop
        end

        if n == 1 % If above loop aborted n is
still 1
            disp('Program cannot be completed. Please try again.')
        else

            disp('')
            q = input('Please enter name of sample used: ','s');

```

```

        fr1 = p(:,2)+j*p1(:,2);           % Loads in complex ratio from
calibration
        fr2 = p2(:,2)+j*p3(:,2);           % Load in complex ratio from
measurement
        c = 343.0;                         % Speed of Sound in air (m/s)
        w = 2*pi*p(:,1);                   % Converts frequencies to
"omegas"
        b1 = 0.0144018;                     % Position of 1st microphone
from tube wall (m)
        b2 = 0.0254508;                     % Position of 2nd microphone
from tube wall (m)
        z1 = -j*(w/c).*(b2-((fr2./fr1)*b1))./(1-(fr2./fr1)); %
Complex acoustic impedance

        figure (5)
        plot(p(:,1),real(z1))
        axis([0,3500,-12,14])
        xlabel('Frequency (Hz)')
        ylabel('Real Part of Acoustic Impedance')
        title(['Real Part of Acoustic Impedance vs. Frequency For
',q])

        figure (6)
        plot(p(:,1),imag(z1))
        axis([0,3500,-12,14])
        xlabel('Frequency (Hz)')
        ylabel('Imaginary Part of Acoustic Impedance')
        title(['Imaginary Part of Acoustic Impedance vs. Frequency
For ',q])

        figure (7)
        plot(p(:,1),real(z1),p(:,1),imag(z1))
        axis([0,3500,-12,14])
        xlabel('Frequency (Hz)')
        ylabel('Acoustic Impedance')
        title(['Real and Imaginary Parts of Acoustic Impedance vs.
Freq. For ',q])

        figure (8)
        plot(real(z1),imag(z1))
        axis([-12,14,-12,14])
        xlabel('Real Part of Acoustic Impedance')
        ylabel('Imaginary Part of Acoustic Impedance')
        title(['Real vs. Imaginary Parts of Acoustic Impedance For
',q])

end

```

2. The next program is called "Impedance.6", run on the MATLAB R12 version.

It uses the exact impedance formula derived from Equation 30:

```

    %This program is designed to compute acoustic impedance given 4
data files obtained

```

```

    %from the microphone calibration and a measurement using a sample
installed

```

```

    %at the end of the tube. The exact formula is used.

```

```

clear
n=1;
while n==1

```

```

    disp(' ')
    disp('The first graph will display the real part of the ratio
of')

```

```

    disp('Microphone #2 output voltage over Microphone #1 output
voltage')

```

```

    disp('with the Microphones in the calibration position.')

```

```

    disp(' ')

```

```

    disp('Please type in name of your file in which this data is
saved.')

```

```

    y = input('Ensure you type file exactly as it was saved. ','s');

```

```

    p=eval(['load('' y '')']);

```

```

    figure (1)

```

```

    plot(p(:,1),p(:,2))

```

```

    xlabel('Frequency (Hz)')

```

```

    ylabel('Real Part of Mic. #2 O/P Volt./Mic. #1 O/P Volt.')

```

```

    title('Real Part of Microphone #2 O/P Volt./Microphone #1 O/P
Volt. vs. Freq. (Cal Position)')

```

```

    disp(' ')

```

```

    disp('Does this graph accurately reflect your trace saved from
the SRS-785?')

```

```

    x=input('Enter 1 to mean YES, 0 to mean NO '); %User verifies
graph is correct

```

```

    if x == 0

```

```

        disp(' ')

```

```

        %Erroneous graph

```

```

    aborts program

```

```

        disp('There is an error.')

```

```

        disp('Please verify file name typed in correctly')

```

```

        disp('and that trace was saved properly on the SRS-785.')

```

```

        break

```

```

    end

```

```

    disp(' ')

```

```

    disp('The second graph will display the imaginary part of the
ratio of')

```

```

    disp('Microphone #2 output voltage over Microphone #1 output
voltage')

```

```

    disp('with the Microphones in the calibration position.')

```

```

    disp(' ')

```

```

    disp('Please type in name of your file name in which this data is
saved')

```

```

    y1 = input('Again ensure file name is typed exactly. ','s');

```

```

    p1=eval(['load('' y1 '')']);

```

```

    figure (2)

```

```

        plot(p1(:,1),p1(:,2))
        xlabel('Frequency (Hz)')
        ylabel('Imag. Part of Mic. #2 O/P Volt./Mic. #1 O/P Volt.')
        title('Imag. Part of Microphone #2 O/P Volt./Microphone #1 O/P
Volt. vs. Freq. (Cal Position)')

        disp(' ')
        disp('Does this graph accurately reflect your trace saved from
the SRS-785?')
        x1=input('Enter 1 to mean YES, 0 to mean NO '); %User verifies
graph is correct
        if x1 == 0
            disp(' ') %Erroneous graph
            aborts program
            disp('There is an error.')
            disp('Please verify file name was typed in correctly')
            disp('and that trace was saved properly on the SRS-785.')
            break
        end

        disp(' ')
        disp('The third graph will display the real part of the ratio
of')
        disp('Microphone #2 output voltage over Microphone #1 output
voltage')
        disp('with the Microphones in the sample measurement position.')
        disp(' ')
        disp('Please type in next file name in which your data is saved')
        y2 = input('Again ensure file name is typed exactly. ','s');
        p2=eval(['load('' y2 ''')]);

        figure (3)
        plot(p2(:,1),p2(:,2))
        xlabel('Frequency (Hz)')
        ylabel('Real Part of Mic. #2 O/P Volt./Mic. #1 O/P Volt.')
        title('Real Part of Microphone #2 O/P Volt./Microphone #1 O/P
Volt. vs. Freq. (Sample Position)')

        disp(' ')
        disp('Does this graph accurately reflect your trace saved from
the SRS-785?')
        x2=input('Enter 1 to mean YES, 0 to mean NO '); %User verifies
graph is correct
        if x2 == 0
            disp(' ') %Erroneous graph
            aborts program
            disp('There is an error.')
            disp('Please verify file name was typed in correctly')
            disp('and that trace was saved properly on the SRS-785.')
            break
        end

        disp(' ')

```

```

disp('The fourth graph will display the imaginary part of the
ratio of')
disp('Microphone #2 output voltage over Microphone #1 output
voltage')
disp('with the Microphones in the sample measurement position.')
disp(' ')
disp('Please type in next file name in which your data is saved')
y3 = input('Again ensure file name is typed exactly. ','s');
p3=eval(['load('' y3 '')']);

figure (4)
plot(p3(:,1),p3(:,2))
xlabel('Frequency (Hz)')
ylabel('Imag. Part of Mic. #2 O/P Volt./Mic. #1 O/P Volt.')
title('Imag. Part of Microphone #2 O/P Volt./Microphone #1 O/P
Volt. vs. Freq. (Sample Position)')

disp(' ')
disp('Does this graph accurately reflect your trace saved from
the SRS-785?')
x3=input('Enter 1 to mean YES, 0 to mean NO '); %User verifies
graph is correct
if x3 == 0
    disp(' ') %Erroneous graph
    aborts program
    disp('There is an error.')
    disp('Please verify file name was typed in correctly')
    disp('and that trace was saved properly on the SRS-785.')
    break
end

n=0; % Change n value to exit the
while loop
end

if n == 1 % If above loop aborted n is
still 1
    disp('Program cannot be completed. Please try again.')
else

    disp(' ')
    q = input('Please enter name of sample used: ','s');

    fr1 = p(:,2)+j*p1(:,2); % Loads in complex ratio from
calibration
    fr2 = p2(:,2)+j*p3(:,2); % Load in complex ratio from
measurement
    c = 343.0; % Speed of Sound in air (m/s)
    w = 2*pi*p(:,1); % Converts frequencies to
"omegas"
    b1 = 0.0144018; % Position of 1st microphone
from tube wall (m)
    b2 = 0.0254508; % Position of 2nd microphone
from tube wall (m)

```



```

A = sin((w/c)*b2);
B = sin((w/c)*b1);
C = cos((w/c)*b2);
D = cos((w/c)*b1);

z1 = -j*(A - ((fr2./fr1).*B))./(C - ((fr2./fr1).*D)); %
Complex acoustic impedance

figure (5)
plot(p(:,1),real(z1))
axis([0,3500,-12,14])
xlabel('Frequency (Hz)')
ylabel('Real Part of Acoustic Impedance')
title(['Real Part of Acoustic Impedance vs. Frequency For
',q])

figure (6)
plot(p(:,1),imag(z1))
axis([0,3500,-12,14])
xlabel('Frequency (Hz)')
ylabel('Imaginary Part of Acoustic Impedance')
title(['Imaginary Part of Acoustic Impedance vs. Frequency
For ',q])

figure (7)
plot(p(:,1),real(z1),p(:,1),imag(z1))
axis([0,3500,-12,14])
xlabel('Frequency (Hz)')
ylabel('Acoustic Impedance')
title(['Real and Imaginary Parts of Acoustic Impedance vs.
Freq. For ',q])

figure (8)
plot(real(z1),imag(z1))
axis([-12,14,-12,14])
xlabel('Real Part of Acoustic Impedance')
ylabel('Imaginary Part of Acoustic Impedance')
title(['Real vs. Imaginary Parts of Acoustic Impedance For
',q])

end

```

3. The last program is called "Reflectivity", also run on the MATLAB R12 version. It uses the reflectivity formula derived from Equation 45 and the simple relationship between reflectivity and impedance defined in Equation 22:

```

%This program is designed to compute acoustic impedance given 4
data files obtained
%from the microphone calibration and a measurement using a sample
installed
%at the end of the tube.

```

```

clear
n=1;
while n==1

    disp('')
    disp('The first graph will display the real part of the ratio
of')
    disp('the microphone reflected pulse voltage over the microphone
incident')
    disp('pulse voltage for a rigid wall at the end of the tube.')
    disp('')
    disp('Please type in name of your file in which this data is
saved.')
    y = input('Ensure you type file exactly as it was saved. ','s');
    p=eval(['load('' y '')']);

    figure (1)
    plot(p(:,1),p(:,2))
    xlabel('Frequency (Hz)')
    ylabel('Real Part of Mic. Reflected Volt./Mic. Incident Volt.')
    title('Real Part of Microphone Refl. Volt./Microphone Inc. Volt.
vs. Freq. (Rigid Wall)')

    disp('')
    disp('Does this graph accurately reflect your trace saved from
the SRS-785?')
    x=input('Enter 1 to mean YES, 0 to mean NO '); %User verifies
graph is correct
    if x == 0
        disp('') %Erroneous graph
        aborts program
        disp('There is an error.')
        disp('Please verify file name typed in correctly')
        disp('and that trace was saved properly on the SRS-785.')
        break
    end

    disp('')
    disp('The second graph will display the imaginary part of the
ratio of')
    disp('the microphone reflected pulse voltage over the microphone
incident')
    disp('pulse voltage for a rigid wall at the end of the tube.')
    disp('')
    disp('Please type in name of your file name in which this data is
saved')
    y1 = input('Again ensure file name is typed exactly. ','s');
    p1=eval(['load('' y1 '')']);

    figure (2)
    plot(p1(:,1),p1(:,2))
    xlabel('Frequency (Hz)')
    ylabel('Imag. Part of Mic. Reflected Volt./Mic. Incident Volt.')
    title('Imag. Part of Microphone Refl. Volt./Microphone Inc. Volt.
vs. Freq. (Rigid Wall)')

```

```

disp(' ')
disp('Does this graph accurately reflect your trace saved from
the SRS-785?')
x1=input('Enter 1 to mean YES, 0 to mean NO '); %User verifies
graph is correct
if x1 == 0
    disp(' ') %Erroneous graph
aborts program
    disp('There is an error.')
    disp('Please verify file name was typed in correctly')
    disp('and that trace was saved properly on the SRS-785.')
    break
end

```

```

disp(' ')
disp('The third graph will display the real part of the ratio
of')
disp('the microphone reflected pulse voltage over the microphone
incident')
disp('pulse voltage for a sample at the end of the tube.')
disp(' ')
disp('Please type in next file name in which your data is saved')
y2 = input('Again ensure file name is typed exactly. ','s');
p2=eval(['load('' y2 ''')]);

```

```

figure (3)
plot(p2(:,1),p2(:,2))
xlabel('Frequency (Hz)')
ylabel('Real Part of Mic. Reflected Volt./Mic. Incident Volt.')
title('Real Part of Microphone Refl. Volt./Microphone Inc. Volt.
vs. Freq. (Sample Boundary)')

```

```

disp(' ')
disp('Does this graph accurately reflect your trace saved from
the SRS-785?')
x2=input('Enter 1 to mean YES, 0 to mean NO '); %User verifies
graph is correct
if x2 == 0
    disp(' ') %Erroneous graph
aborts program
    disp('There is an error.')
    disp('Please verify file name was typed in correctly')
    disp('and that trace was saved properly on the SRS-785.')
    break
end

```

```

disp(' ')
disp('The fourth graph will display the imaginary part of the
ratio of')
disp('the microphone reflected pulse voltage over the microphone
incident')
disp('pulse voltage for a sample at the end of the tube.')
disp(' ')

```

```

disp('Please type in next file name in which your data is saved')
y3 = input('Again ensure file name is typed exactly. ','s');
p3=eval(['load('' y3 '')']);

figure (4)
plot(p3(:,1),p3(:,2))
xlabel('Frequency (Hz)')
ylabel('Imag. Part of Mic. Reflected Volt./Mic. Incident Volt.')
title('Imag. Part of Microphone Refl. Volt./Microphone Inc. Volt.
vs. Freq. (Sample Boundary)')

disp(' ')
disp('Does this graph accurately reflect your trace saved from
the SRS-785?')
x3=input('Enter 1 to mean YES, 0 to mean NO '); %User verifies
graph is correct
if x3 == 0
    disp(' ') %Erroneous graph
    aborts program
    disp('There is an error.')
    disp('Please verify file name was typed in correctly')
    disp('and that trace was saved properly on the SRS-785.')
    break
end

n=0; % Change n value to exit the
while loop
end

if n == 1 % If above loop aborted n is
still 1
    disp('Program cannot be completed. Please try again.')
else
    disp(' ')
    q = input('Please enter name of sample used: ','s');

    fr1 = p(:,2)+j*p1(:,2); % Loads in complex ratio from
rigid bdy
    fr2 = p2(:,2)+j*p3(:,2); % Load in complex ratio from
sample bdy

    r = fr2./fr1; % Complex reflectivity

    z = (1+r)./(1-r); % Compute impedance from
reflectivity

    figure (5)
    plot(p(:,1),real(r))
    xlabel('Frequency (Hz)')
    ylabel('Real Part of Reflectivity')
    title(['Real Part of Reflectivity vs. Frequency For ',q])

    figure (6)

```

```

        plot(p(:,1),imag(r))
        xlabel('Frequency (Hz)')
        ylabel('Imaginary Part of Reflectivity')
        title(['Imaginary Part of Reflectivity vs. Frequency For
',q])

        figure (7)
        plot(p(:,1),real(r),p(:,1),imag(r))
        xlabel('Frequency (Hz)')
        ylabel('Reflectivity')
        title(['Real and Imaginary Parts of Reflectivity vs. Freq.
For ',q])

        figure (8)
        plot(real(r),imag(r))
        xlabel('Real Part of Reflectivity')
        ylabel('Imaginary Part of Reflectivity')
        title(['Real vs. Imaginary Parts of Reflectivity For ',q])

        figure (9)
        plot(p(:,1),real(z))
        axis([0,3500,-12,14])
        xlabel('Frequency (Hz)')
        ylabel('Real Part of Acoustic Impedance')
        title(['Real Part of Acoustic Impedance vs. Frequency For
',q])

        figure (10)
        plot(p(:,1),imag(z))
        axis([0,3500,-12,14])
        xlabel('Frequency (Hz)')
        ylabel('Imaginary Part of Acoustic Impedance')
        title(['Imaginary Part of Acoustic Impedance vs. Frequency
For ',q])

        figure (11)
        plot(p(:,1),real(z),p(:,1),imag(z))
        axis([0,3500,-12,14])
        xlabel('Frequency (Hz)')
        ylabel('Acoustic Impedance')
        title(['Real and Imaginary Parts of Acoustic Impedance vs.
Freq. For ',q])

        figure (12)
        plot(real(z),imag(z))
        axis([-12,14,-12,14])
        xlabel('Real Part of Acoustic Impedance')
        ylabel('Imaginary Part of Acoustic Impedance')
        title(['Real vs. Imaginary Parts of Acoustic Impedance For
',q])

    end

```

APPENDIX J: LABORATORY TEST PROCEDURE

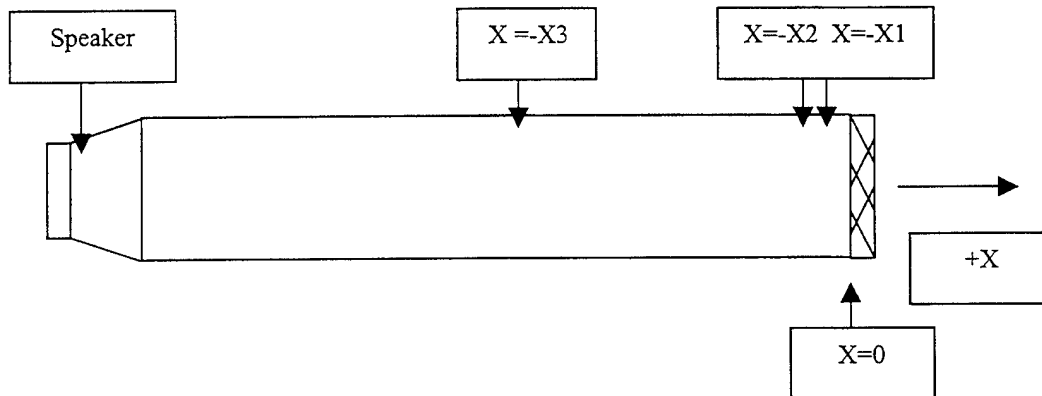
ACOUSTIC LABORATORY

IMPEDANCE TUBE

OBJECTIVE: To measure the complex specific acoustic impedance of different materials in an impedance tube using two different techniques.

EQUIPMENT: Impedance tube with sample holders, rigid termination, microphone calibration fixture, HP 3314A function generator, HP 467A amplifier, voltmeter, Stanford Research Systems Model SR785 2 channel dynamic signal analyzer, Phillips PM3384 Oscilloscope.

THEORY: Acoustic impedance may be calculated by two methods using this apparatus.



One method uses two microphones located at positions x_1 and x_2 in the figure above with a band-limited, continuous white noise signal. By measuring the pressure wave with two microphones at positions x_1 and x_2 , the following equation may be used to determine relative acoustic impedance:

$$\tilde{z}_{rel} = \frac{-j[\sin \tilde{k}x_2 - \left(\frac{\tilde{\partial p}_2}{\tilde{\partial p}_1}\right)\sin \tilde{k}x_1]}{[\cos \tilde{k}x_2 - \left(\frac{\tilde{\partial p}_2}{\tilde{\partial p}_1}\right)\cos \tilde{k}x_1]} \quad (\text{Exact Equation})$$

Another method uses one microphone, located at position x_3 in the figure above, with a transient, pulsed signal. By measuring the incident and reflected pulse

signals with a rigid reflection termination and then with a sample in place, reflectivity may be determined by the following equation:

$$\tilde{R}_{sample} = \frac{(\tilde{\delta v}^{refl} / \tilde{\delta v}^{inc})_{sample}}{(\tilde{\delta v}^{refl} / \tilde{\delta v}^{inc})_{rigidwall}} \quad \text{(Reflectivity Equation)}$$

From the computed value of reflectivity, one can determine the relative acoustic impedance from the following relationship:

$$\tilde{Z}_{rel} \equiv \frac{\tilde{Z}_{bdy}}{\rho_0 c} = \frac{1 + \tilde{R}_{sample}}{1 - \tilde{R}_{sample}}$$

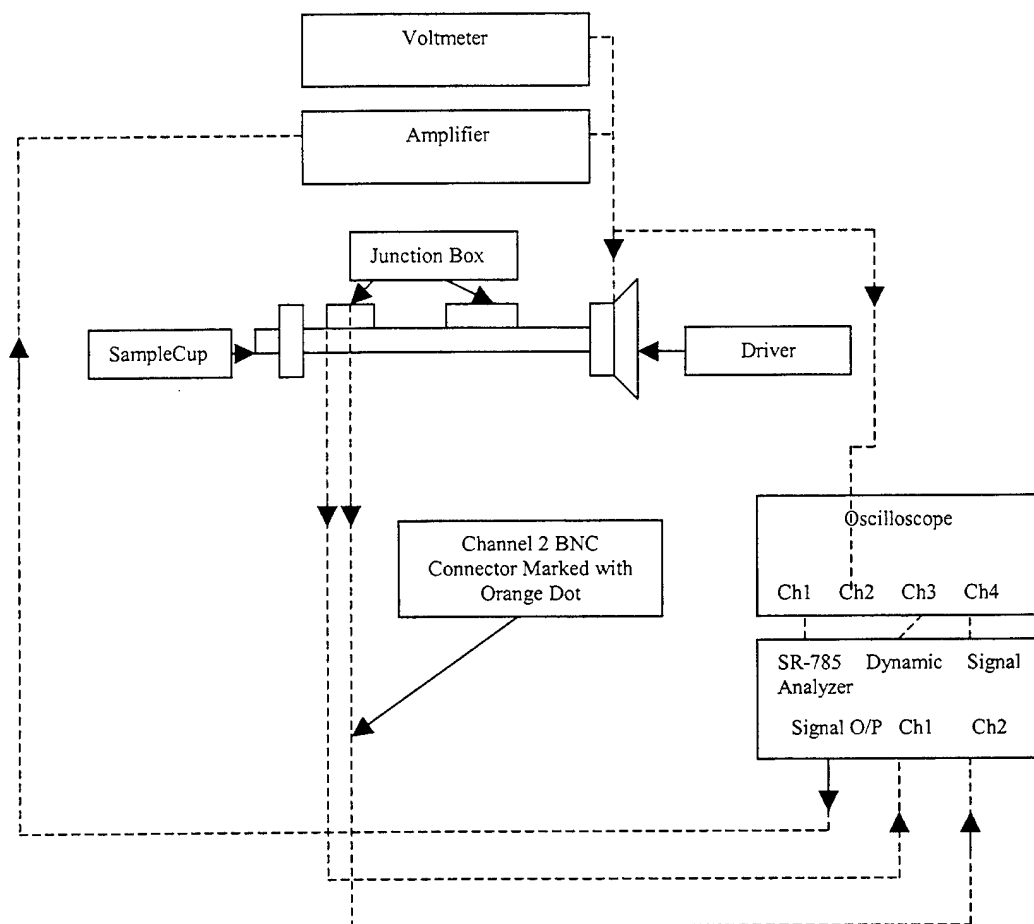
PROCEDURES:

1. a) The lower frequency limit of the impedance tube is determined by the output of the source which rolls off with decreasing frequency. The upper limit is set by the cut-off frequency of the first non-planar standing wave. Show that this is found from the formula: $ka = 1.84$ (where a is the tube radius).

TWO-MICROPHONE, CONTINUOUS EXCITATION METHOD

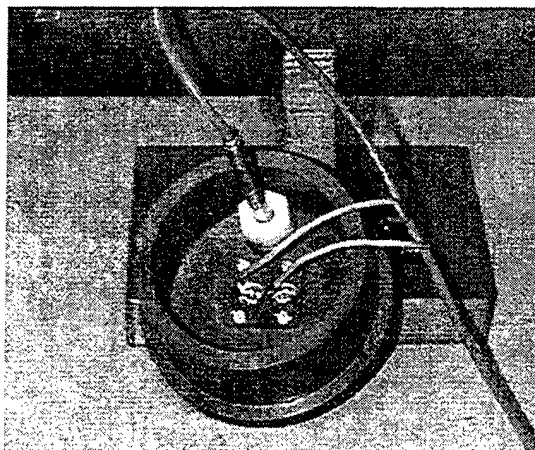
SET UP:

1. a) Set up the apparatus according to the block diagram:



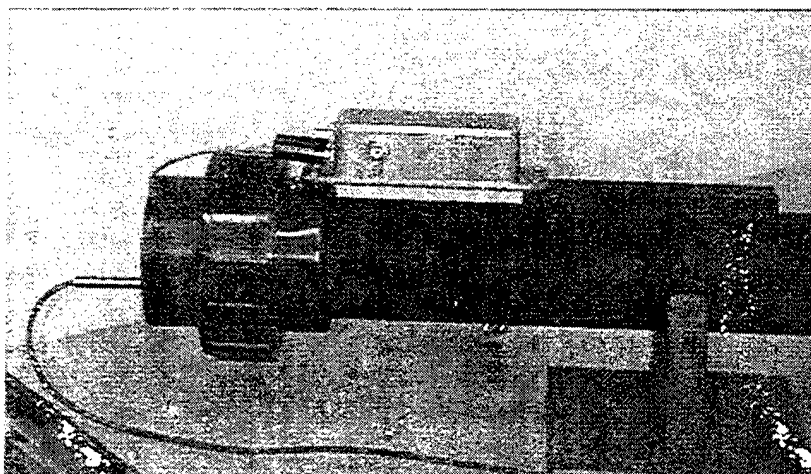
MICROPHONE CALIBRATION

1. a) Ensure the microphones at the sample end of the impedance tube are removed from their normal position at the top of the tube and screwed into the specially designed calibration cup holder similar to the picture shown below. Install the blank cover in the normal microphone position location:



(Note that the calibration microphone above with the white flange will not be used. A blank will be installed in its place)

b) When the microphones have been installed in the calibration cup holder, fasten the cup holder to the end of the tube. Ensure the microphone cord with the orange paint is plugged into the junction box holder marked with orange paint below the hole. The end of the assembly should look similar to the picture shown below:



c) The microphones are now in their calibration position. Ensure all equipment is installed per step 2a. The BNC connector on the junction box that must be attached to the SR-785 dynamic signal analyzer channel 2 is designated with an orange dot marked below. The other BNC connector (opposite side of the junction box) should go to channel 1.

d) Check to be sure that all joints are snugly sealed since air leaks can affect results significantly. Record the room temperature periodically during the experiment.

2. a) You are now ready to perform the two-microphone calibration. Using the SR-785 dynamic signal analyzer, depress the "disk" key on the panel. When the menu appears on the right side of the screen, depress the key next to the "file name"

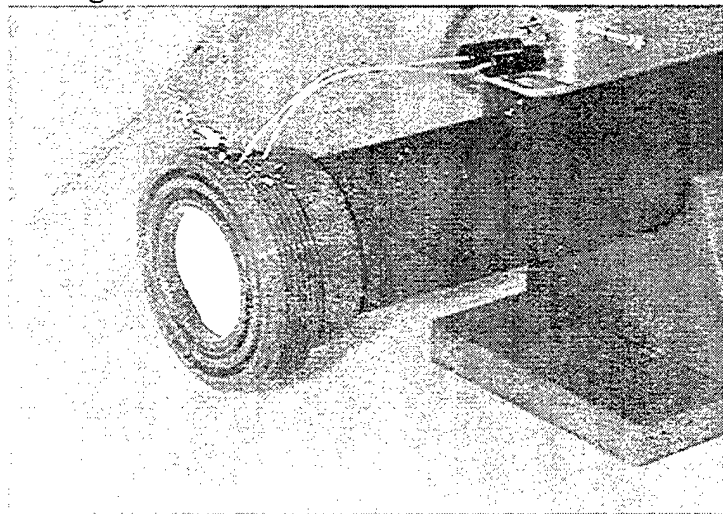
option on the right hand side of the screen. Moving the large circular knob slightly will cause a menu file to appear. Position the cursor on the file labeled "REIM.78S". Hit the enter key. Next hit the key next to the "recall settings" option on the screen menu. A new menu will appear. On the new menu, press the key next to the "recall from disk" option. A white noise signal will be applied. Carefully monitor your signal with the voltmeter to ensure you are not overdriving the speaker! **Signals in excess of 50mV may result in distorted measurements!**

b) Ensure the toggle switch on the junction box is in the "on" position marked with orange paint. **For best results, ensure microphone has been on for at least 15 minutes prior to measurements.**

c) Record the calibration data by depressing the "output" key on the SR-785 and noting the file start number indicated ie. 6. Ensure the active screen is channel A, the real part of the voltage ratio of the two microphones. Depress the "print screen" key and the data will be saved to the floppy disk. Next depress the "active display" toggle key. The active screen is now channel B, the imaginary part of the voltage ratio of the two microphones. Depress the "print screen" key and the data will be saved to the floppy disk under the next sequential file number. **Keep careful track of which data is saved under each file on your floppy disk. If you don't you will be unable to obtain acoustic impedance measurements from the MATLAB program.**

SAMPLE MEASUREMENT

1. a) After the calibration data are saved, remove the calibration cup from the end of the tube and unscrew the microphones from the holder. Reposition the microphones (and junction box) to their normal measurement position. **Again, ensure the BNC connector on the junction box that is attached to the dynamic signal analyzer on channel 2 is marked with an orange dot!** Ensure the microphone plate is bolted into the opening where the blank had been installed. The end of the assembly should now look like the figure shown below:



b) Install a cup containing a sample at the end of the tube.

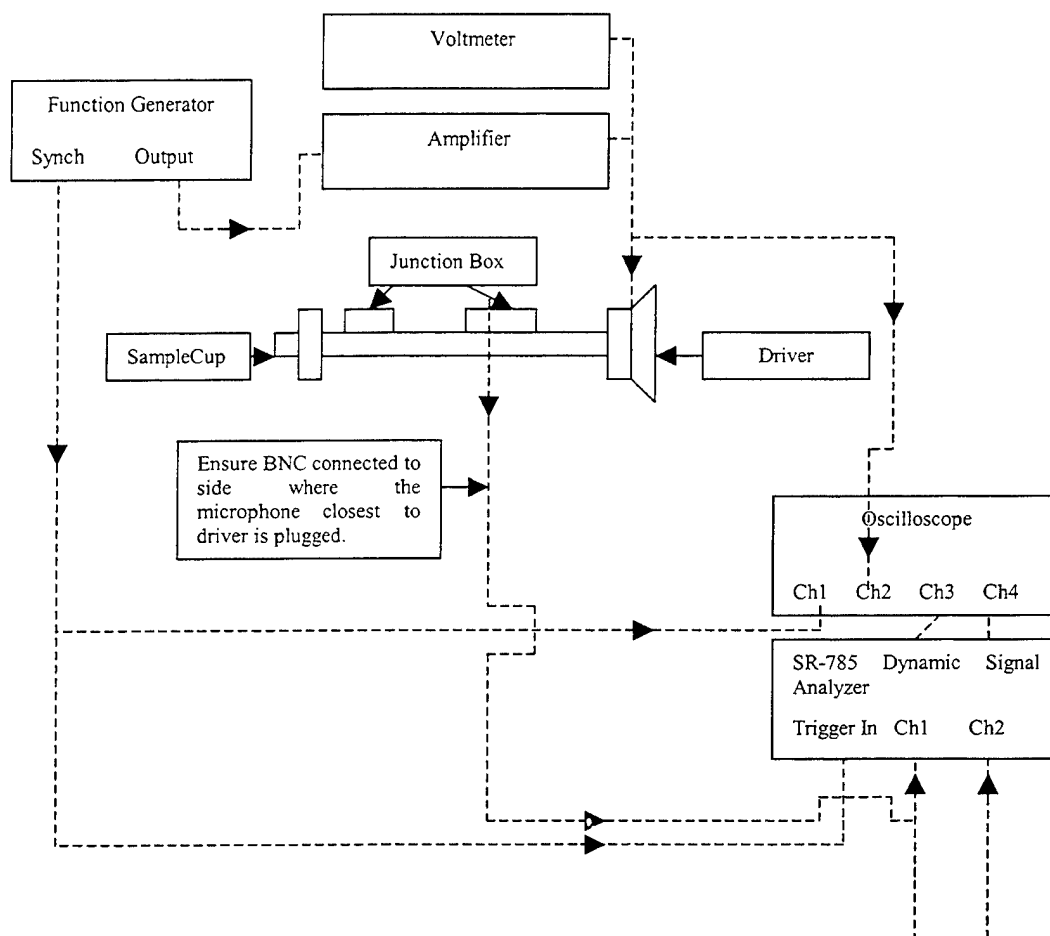
c) You are now ready to perform an acoustic impedance measurement. Repeat steps 3a through 3c as described above.

d) Repeat steps 3a through 3f for each sample provided and obtain a measurement with the end cup removed (ie. Open Tube). The sound radiated from the open end should not be dangerously loud, but ear-plugs are recommended.

ONE-MICROPHONE, TRANSIENT EXCITATION METHOD

SET UP:

1. a) Set up the apparatus according to the block diagram:



ABSORPTION COMPENSATION

1. a) Install a rigid boundary at the end of the tube. (Use a blanked sample holder).
2. a) You are now ready to perform the tube absorption compensation and a series of reflectivity measurements. Acoustic impedance may be derived from the complex reflectivity measurement (see KFCS eq. 6.3.18). Ensure the following

parameters are coming from the function generator to produce a half cycle burst mode pulse N=1 cycle: 1 volt amplitude; 4000Hz carrier frequency; 0 volt offset; 50% symmetry; negative 90 degrees phase; and N=1 cycle. You are now sending a pulsed signal into the impedance tube. Ensure the toggle switch on the junction box is in the "on" position marked with orange paint. **For best results, ensure microphone has been on for at least 15 minutes prior to measurements.**

b) Using the SR-785 dynamic signal analyzer, depress the "disk" key on the panel. When the menu appears on the right side of the screen, depress the key next to the "file name" option on the right hand side of the screen. Moving the large circular knob slightly will cause a menu file to appear. Position the cursor on the file labeled "REFLWTIM.78S". Hit the enter key. Next hit the key next to the "recall settings" option on the screen menu. A new menu will appear. On the new menu, press the key next to the "recall from disk" option. You will have two time delay windows where the signal will appear. The incident pulse will be set in the top window (channel A) and the reflected pulse will appear in the bottom window (channel B).

c) Depress the "trigger" key on the SR-785 and reset the time delays 1 and 2 to zero using the keys to the right of the screen and the dial. Next, depress the "window" key and reset the force length to zero as previously described.

d) Using the cursor, find the time where the pulse is zero (or very close) just prior to the rise of the peak of the first (incident) pulse. Note this time – it will be the value you will set for time delay 1. Using the cursor, find the time where the voltage is zero (or very close) just prior to the rise of the peak of the second (reflected) pulse. This time will be the value you will set for time delay 2. Subtract the second time from the first time and you will have the value for the force length. Using the "trigger" and "window" keys set these measured and calculated values.

e) Depress the "display setup" key. From the menu that appears to the right of the screen, select the "measurement option" and set it to "Freq. Resp.". Do this for the other channel using the "active screen" toggle button.

f) Hit the "start/reset" key to initiate reflectivity calibration measurement.

g) Record the calibration data by depressing the "output" key on the SR-785 and noting the file start number indicated ie. 6. Ensure the active screen is channel A, the real part of the voltage ratio of the two microphones. Depress the "print screen" key and the data will be saved to the floppy disk. Next depress the "active display" toggle key. The active screen is now channel B, the imaginary part of the voltage ratio of the two microphones. Depress the "print screen" key and the data will be saved to the floppy disk under the next sequential file number. **Keep careful track of which data are saved under each file on your floppy disk.**

SAMPLE MEASUREMENT

1. a) After the compensation data are saved, remove the blank cup from the end of the tube and install a cup containing a sample material. Repeat step g above for each sample provided and obtain a measurement with the end cup removed (ie. Open Tube). The sound radiated from the open end should not be dangerously loud, but earplugs are recommended.

DATA ANALYSIS WITH MATLAB

1. a) Using the floppy disk you have saved all files on, run the MATLAB programs "Impedance" and "Reflectivity". Ensure you follow all instructions very carefully. When it asks you to type in the file name under which a particular measurement is stored, be very careful to type it in exactly. Typically the SR-785 will save data under files beginning with the letters "Scrn" followed by four digits. Since the floppy disk will be installed in the MATLAB computer's "a" drive, you might type in the file as "a:Scrn0006". The computer will reproduce your SR-785 trace and ask you to confirm that it is your correct signal.

b) By following the instructions correctly, the programs will provide graphs of the acoustic impedance over the frequency range (the "Reflectivity" program will additionally provide the acoustic reflectivity for each material).

c) Print out each graph (real part, imaginary part, and both versus frequency as well as real versus imaginary) from both programs for each material and the open tube. Compare the acoustic impedance results obtained by the one and two microphone methods.

LIST OF REFERENCES

1. Kinsler, Lawrence E., Frey, Austin R., Coppens, Alan B., and Sanders, James V. *Fundamentals of Acoustics*, 4th ed., Chapters 8 and 10, John Wiley and Sons, Inc., 2000.
2. Song, Bryan H. and Bolton, Stuart J., "A Transfer-Matrix Approach For Estimating the Characteristic Impedance and Wave Numbers of Limp and Rigid Porous Materials," *Journal of Acoustical Society of America*, Vol. 107, No. 3, pp. 1131-1151, March 2000.
3. Stiede, Patricia E. and Jones, Michael G., "Comparison of Methods For Determining Specific Acoustic Impedance," *Journal of Acoustical Society of America*, Vol. 101, No.5, Pt. 1, pp. 2694-2704, May 1997.

THIS PAGE INTENTIONALLY LEFT BLANK

INITIAL DISTRIBUTION LIST

1. Defense Technical Information Center2
 8725 John J. Kingman Road, Suite 0944
 Ft. Belvoir, VA 22060-6218

2. Dudley Knox Library2
 Naval Postgraduate School
 411 Dyer Road
 Monterey, CA 93943-5101

3. Physics Department2
 Naval Postgraduate School
 833 Dyer Road
 Monterey, CA 93943-5002

4. Professor Steven R. Baker, Code PH/Ba3
 Department of Physics
 Naval Postgraduate School
 Monterey, CA 93943-5002

5. Professor Thomas J. Hofler, Code PH/Hf1
 Department of Physics
 Naval Postgraduate School
 Monterey, CA 93943-5002

6. David Grooms, Code PH/1
 Acoustics Teaching Laboratory
 Naval Postgraduate School
 Monterey, CA 93943-5002

7. Engineering and Technology Curricular Office, Code 341
 411 Dyer Road
 Naval Postgraduate School
 Monterey, CA 93943-5101

8. Sean O'Malley1
 463 Marlbridge Rd.
 Rosemont, PA 19010